Investigating Toxoplasma gondii peroxisome and the discovery of two Bisabolane Sesquiterpenes as anti-leshmanials.

MBEKEANI, ALISON,JULIA

Protozoa and Natural Products:

Investigating *Toxoplasma gondii* peroxisome and the discovery of two Bisabolane Sesquiterpenes as anti-leshmanials.

Alison Julia Mbekeani

A thesis presented for the degree of
Doctor of Philosophy

Department of Biosciences
University of Durham
England, UK
March 2019

Dedicated to

All the suffers of fatal infectious diseases globally, and the part that science will play in ensuring their future.

Abstract

The use of natural products for treating protozoan infections can be traced back to Rome in 1631, where cinchona tree bark was used to cure malaria. The discovery of novel naturally derived compounds for the treatment of cutaneous leishmaniasis and toxoplasmosis is vital for many vaccine deficient protozoan infections today. Here, the assessment of natural products against *Leishmania mexicana (L. mexicana)* was explored using a library of compounds screened against the mammalian stage of *L. mexicana* in *in vitro* assays. Two hit compounds from the screen were then used in metabolomic studies to determine mode of action. In addition, another natural compound, Aureobasidin A and its derivatives, and peroxisome inhibitors were screened against *Toxoplasma gondii* (*T. gondii).*

Peroxisomes are organelles involved in the metabolism of fatty acids and cholesterol. Other than lipid metabolism, peroxisomes contain many enzymes involved in several different metabolic processes. Catalase is involved in the neutralization of hydrogen peroxide thereby, preventing toxic build up within cells. This enzyme over time has become a key identifier of peroxisomes in many organisms. However, this is controversial when it comes to *T. gondii*. The use of catalase as a marker for peroxisomes in this parasite has been disputed, and in some cases led to the belief that the *T. gondii* does not possess these organelles. In this thesis, we take a different approach in to establishing the existence of peroxisomes. Through evolution *T. gondii* has maintained, within its genome, genes encoding peroxisomal proteins, named peroxins (Pex). Here we investigated the presence of peroxisomes within *T. gondii* using Pex proteins. Our experimental approach involved characterization of putative *Tg*Pex5 and protein ligand *Tg*SCP2. Using molecular biology, reverse genetics and protein characterization, we show that through pull-down assays, localisation and complementation of *Tg*Pex5 in yeast expression systems, we are able to provide evidence to prove the presence of peroxisomes within *T. gondii*.

Declaration

The work in this thesis is based on research carried out at the Department of Biosciences, Durham University, England, UK. No part of this thesis has been submitted elsewhere for any other degree or qualification and it all my own work unless referenced to the contrary in the text.

Acknowledgements

The journey to this PhD has been most enjoyable and I am thankful to God for seeing me through the four years which have seen; two deployments, one house move, one wedding, and one delightful baby.

To my scientific family, thanking all the Glasgow University, Bochum University and Durham University lab members for all their help and support. "Partners in protein purification crime" Emily Cardew and Becky Eno. A special thanks to my supervisors Paul Denny and Ehmke Pohl and Ian Edwards for all the support.

To all family, who are always there at the other end of the phone/WhatsApp/FaceTime and Facebook. Dad who may already have a PhD in parasitology and knows a lot about everything. My mother Rose and mother in-law Janet who spent the first half of 2018 looking after my daughter Ottilie as I visited various conferences and labs around the country. I am truly grateful.

To my aunt Kamana who has been checking up on my progress every month and steering me on! Such a great role model.

Lois and Anthea for the much needed distraction and suggestions of good sitcoms and dramas to keep me sane, not forgetting Kyla for instigating the write up process during my maternity "best advice ever."

Sheila and Richard Brucciani for all your moral support and encouragement throughout my educational career, could not have made it this far without you!

Last and certainly not least my husband Toby and my daughter who have been nothing but delightful in the past year(s). So grateful for all your support and love you both dearly.

Contents

List of Figures

List of Tables

Chapter 1

Introduction

1.1 Protozoan diseases

Protozoan diseases are one of the World's deadliest killers and present a severe threat to global health. The World Health Organisation (WHO), estimate that these diseases account for approximately 5 million deaths a year, predominately affecting the World's poorest nations. These unicellular eukaryotic organisms, include; malaria (caused by *Plasmodium falciparum, Plasmodium vivax, Plasmodium ovale, Plasmodium malaraie),* Chaga's disease (caused by *Trypanosoma cruzi*) /African sleeping sickness (caused by *Trypanosoma brucei rhodesiense, brucei gambiense*), amoebiasis (caused by *Enthamoeba histolytica*), leishmaniasis (caused by *Leishmania major, dovnvini, mexicana* etc), toxoplasmosis (caused by *Toxoplasma gondii)* to name a few.

These protozoan diseases have no available vaccines; malaria caused by *Plasmodium* and transmitted by mosquitos has many front-line drugs, but most of these are under a constant threat of developing drug resistance [1, 2]. To date there are no commercial available vaccines, and although there has been significant research into the malaria RTS-S vaccine, the vaccine has shown limited success in only providing 50% protection [3]. Currently this shows that there is no long-term immunization towards malaria. *T. brucei*, another well known protozoa, but transmitted by teste

fly and unlike malaria is classed as a neglected tropical disease and brings about African sleeping sickness but like other protozoan infections, lacks in drug therapeutics and has no known vaccine. There are few compounds used to treat African sleeping sickness, including pentamidine, suramin, melarsoprol, eflornithine, and nifurtimox [4, 5], and therefore, there is also a need to investigate the discovery of novel treatments. This lack of effective treatments for all of the above mentioned parasites has led many of these endemic areas to focus on other areas of disease prevention methods. For example; combined efforts of the use of bed nets and outdoor residual spraying, preventing vectors from spreading disease. Here a combination of insecticide usage (mainly DEET (N,N-diethylmetatoluamide)) together with the use of front-line treatments are both used to combat disease and have lead to many success stories as reported by the Center for Disease Control (CDC) and the WHO [6]. However, over many years the world has seen both increasing rates of insecticide and drug resistance, and many researchers have looked into the development of synthetic compounds [1, 2, 7–9]to tackle up coming resistance.

1.1.1 Protozoa: a global burden and need for new treatments and novel drug targets.

The research focus on drug discovery leading to novel anti-parasitic drug therapies, instead of parasitic vaccine development can be attributed mainly to cost. Vaccine trials require large cohorts of patients, volunteers, and staff which are costly in comparison to drug trials. However, more importantly, the complicated multistage life-cycles of these parasitic organisms makes the development of effective treatments very complex as shown in Figure 1.1. Many pathogenic protozoa have evolved complex life cycles in order to survive in their host(s). These sometimes involve a direct or monoxenous life cycle using a single host or an indirect or heteroxenous life cycle involving more than one host, therefore having more than one infected

reservoir to tackle when it comes to interventions of drug, vaccine or insecticide development.

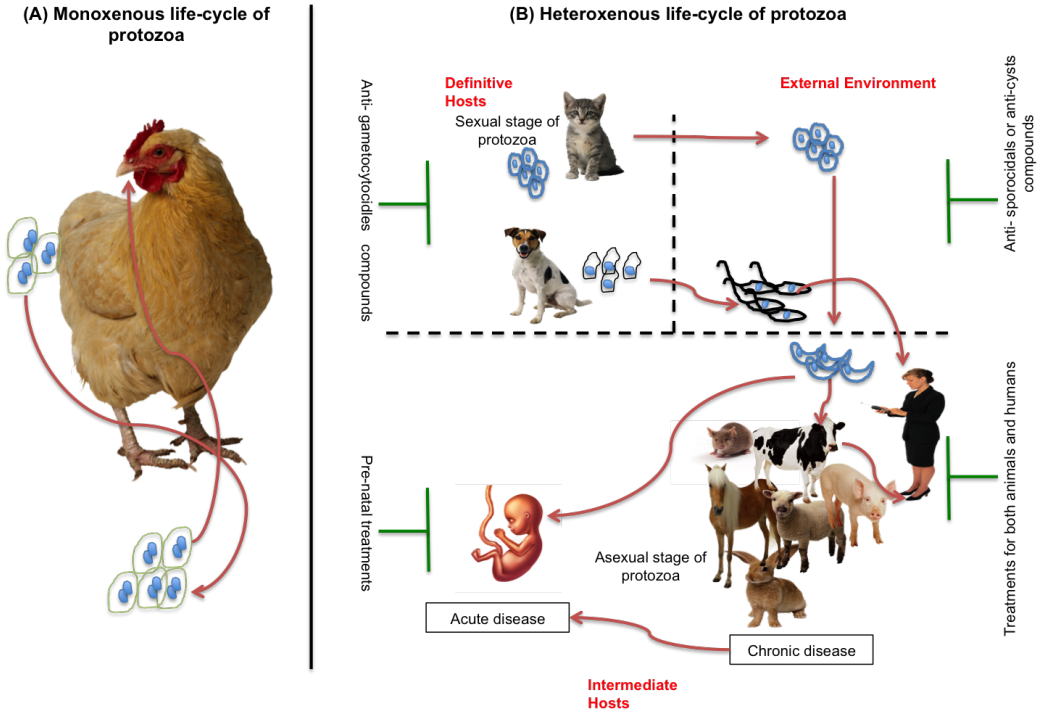

Figure 1.1: Drug-discovery programs targeting different stages of the protozoan life cycle: (A) Monoxenous or direct life cycle is where only one host is involved where the protozoa spends most of its mature adult life and where it reproduces. Whereas in a (B) heteroxenous or indirect life cycle two or more hosts are involved and therefore include an intermediate stage, making the life cycle more complex. Microsoft images and (https://www.dreamstime.com/stock-illustration-human-fetus-concept-illustration-as-prenatal-growing-baby-umbilical-cord-white-background-as-obstetric-medicine-image68323107)

All parasites following this general pattern of growth and development stage (maturation), reproduction (to include sexual and asexual) and transmission phases. It is these three different stages that drug discovery programs have exploited in the past, by developing stage specific compounds such as transmission blocking drugs, and compounds that affect the metabolism, mobility and protein expression [10]. Often over the past decades efficacious treatments showed toxicity with significant side effects as discussed in later. The emergence of drug resistance has meant that a search into novel compounds and new target identification and validation programs all over the world are even more vital. [11–13].

In this global fight against protozoan disease, two things have come into favour; one is increased funding; for example UK government in 2015 gave financial support for research in Neglected Tropical Diseases (NTDs) such as leishmaniasis. This has lead to collaborations between public and private institutions for example the 2012 London Declaration on NTD's (https://www.gov.uk/government/publications/2010-to-2015-government-policy-health-in-developing-countries/2010-to-2015-government-policy-health-in-developing-countries). The other is, the sequencing of protozoan genomes which has undoubtably helped in the discovery of many new molecular drug targets by focusing on parasite genetics. Research into these key areas, in addition to understanding of the different stages of the protozoan life cycles, are hoped to lead to the development or discovery of novel anti-parasitic compounds.

1.1.2 *Leishmania* and *Toxoplasma*

Why *Leishmania* and *Toxoplasma* ?

When it comes to leishmaniasis, the world has seen an increase in cases over the past decade in many areas where there had been a reduction of disease [14]. The reason for this can be attributed to an increase in poverty, which results in poorer healthcare and other social economic issues. Countries that have seen a rise in leishmaniasis include war-stricken zones like: Pakistan, Iraq, Saudi Arabia and Syria [15, 16]. Pre-conflict statistics in Syria show that there were approximately 23 000 cases per year in 1992, rising to 41 000 cases a year in 2012 [17]. In Pakistan, the displacement of people led to a 3.61% rise in the cases of leishmaniasis in war-affected Waziristan [14]. Also Kenya despite not being a war zone, experienced an outbreak in June 2017 as reported by WHO (WHO). This increase in leishmaniasis in regions affected by conflict (Figure 1.2) demonstrates the need for novel treatments and interventions in response to these outbreaks.

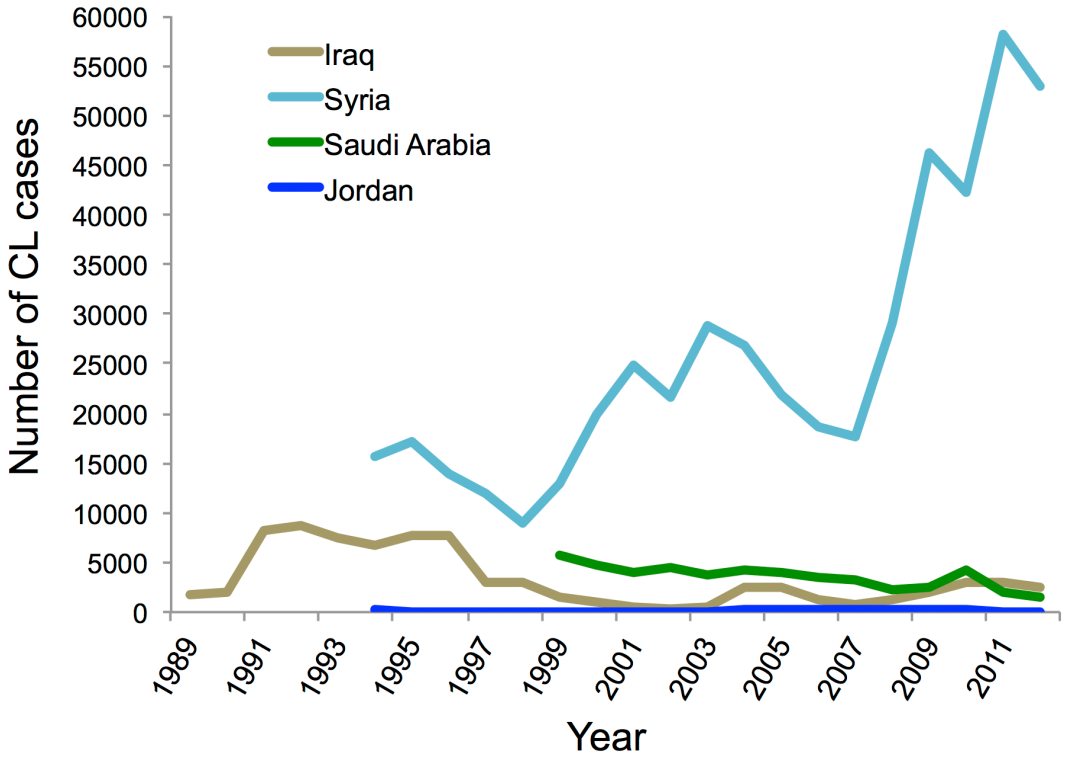

Figure 1.2: Number of cutaneous leishmaniasis (CL) cases from 1989 to 2011 in the Middle East. Taken from Salam *et al* 2014 [15]

Unlike leishmaniasis, toxoplasmosis is a significant threat to all unborn mammalian foetuses world-wide (WHO). Immunocompetent humans infected with *Toxoplasma* can live with the parasite symbiotically without showing any symptoms of disease. However, immunocompromised individuals including those with AIDS or cancer, when infected with the parasite do exhibit disease symptoms and require treatment [18]. Likewise, uninfected pregnant mothers are at risk of losing their unborn offspring, when infected by the parasite in their first trimester of pregnancy, which usually results in the loss of (infant) life [19]. Toxoplasmosis is also known to impact farms where livestock is a main source of income. This need to protect the unborn foetus highlights the importance of discovering new drug targets, target validation and also development and investigation into new therapies for animals and humans against *Toxoplasma.*

Research into the genetics of *Toxoplasma* by scanning through it's genome has previously helped identify key genes from *T. gondii* that have potential as putative

drug targets [20, 21]. In addition, other approaches for drug discovery include the use of screens, employing various *in vitro* drug assays with novel compounds, with the aim of identifying new treatments for toxoplasmosis [22, 23]. Additionally, the discovery of new drug targets within this parasite, such as the existence of an organelle within *T. gondii*, and assessing whether it has drug potential, could also lead to new treatments for toxoplasmosis [24].

1.2 *Toxoplasma gondii*

T. gondii is a protozoan parasite of the apicomplexcan family, that was discovered over 100 years ago in mammals by Nicolle and Manceaux [25].

1.2.1 *Toxoplasma gondii*

As an obligate intracellular pathogen *Toxoplasma* lives in host cells and has unique aspects to its cell biology and exists in various different cellular stages (Figure 1.3) as tachyzoites, bradyzoites, and sporozoites. [19, 25]. Tachyzoites are crescent shape and range in size from 2-6 μm, and typically have three membranes consiting of a plasmalemma and two other membranes that form an inner membrane complex. They also know to posses all the usual eukaryotic organelles such as endoplasmic reticulum, golgi bodies and a nucleus, the latter located towards the centre of the cell [26]. This form of the parasite multiplies rapidly in any cell of an intermediate host and within the intestinal cells of the definitive host. It enters these cells by actively penetrating through the host cell plasma membrane or by phagocytosis [26]. Once in the cell, tachyzoites asexually multiply by repeated endodyogeny in which two progeny form within the parent parasite. This ruptures the host cell as soon as it can no longer support the growth of the parasite and releases tachyzoites that subsequently infect other cells within the tissue [26]. Some of the tachyzoites in

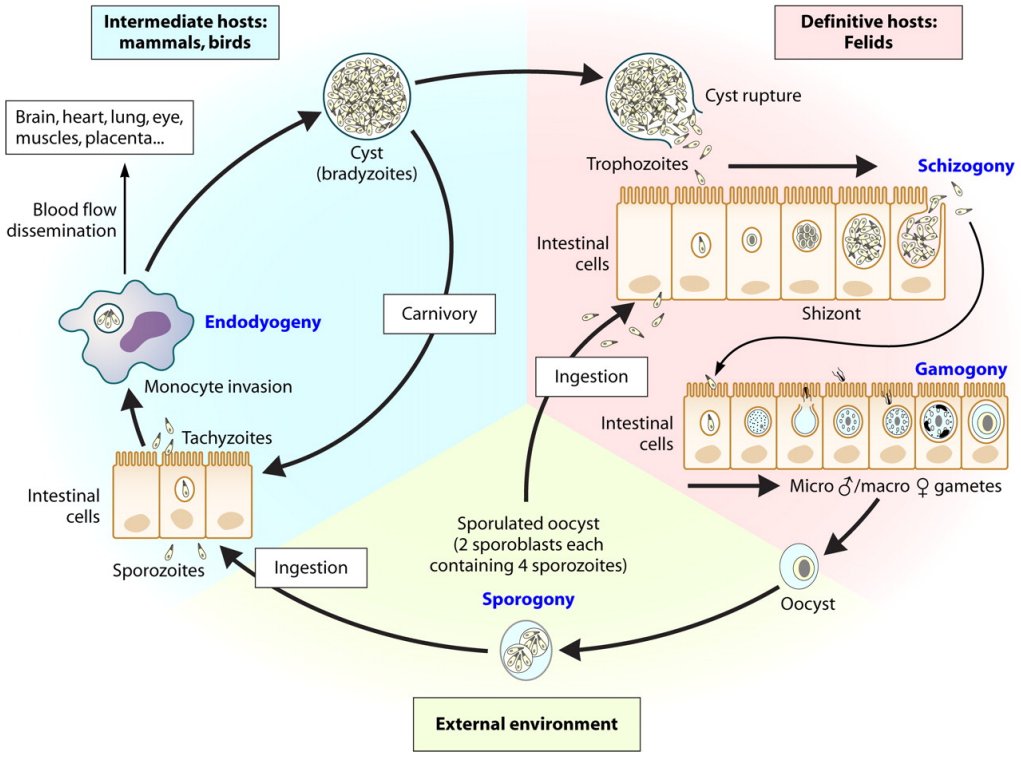

Figure 1.3: *Toxoplasma gondii* parasite sexual This cycle shows the various stages and forms of the parasite to including tachyzoites, bradyzoites and oocysts [27].

the infected host cells then develop into bradyzoites, which are contained within a tissue cyst. These cysts can be found in cells of the liver, lungs, brain, eyes and both skeletal and cardiac muscles and vary in size ranging from 5 -100 μM, enclosing hundreds of crescent-shaped bradyzoites [26]. Bradyzoites are similar to tachyzoites but are thinner in appearance, have the nucleus located towards the posterior end and are less susceptible to destruction by proteolytic enzymes when compared to tachyzoites. The other notable difference is in the pre-patent period (which is the time it takes to shed parasites within a cat host) such that, when a cat has had a meal with tachyzoites the period is longer, whereas if it has consumed bradyzoites the period is shorter. The ingestion of these two stages and sporozoites results in the infection of feline intestinal tissue [26, 27].

Once infected by either the tachyzoites or cyst, proteolyitic enzymes within the cat gut break down the cyst wall allowing the penetration of bradyzoites into the intestinal cells. These parasites first multiply asexually, followed by the sexual cycle

which occurs after approximately 2 days later. Here microgametes penetrate and fertilize mature macrogametes to form zygotes. After fertilization, an oocyst wall forms around the parasite giving it a spherical shape and size of approximately 10 μM. The cat then starts to shed unsporulated oocysts after approximately 10-18 days after the infection where the unsporulated oocyst, sporulate after 1-5 days in the external environment [26].

1.2.2 *Toxoplasma gondii* life cycle in indifinative and definitive host

The zoonotic nature of *Toxoplasma* has both a sexual and asexual stage within their life cycle. The tachyzoite form found in infected muscle tissues of mammals for example, pigs, cattle, humans and mice, are known as indifinative hosts. During the *T. gondii* life cycle, a *Toxoplasma* infected mouse known to be attracted to the urine of domestic cats, as a result of some alternation in their neurological pathways, renders the mouse fearless towards cats, making them easy prey. The cat is the definitive host and once infected by tachyzoites or bradyzoites travel to the intestinal tissue where they mature sexually from tachyzoites or bradyzoites into unsporolating oocysts. Unsporulating oocysts are then shed approximately two weeks after infection into soil or litter tray where after excretion depending upon aeration and temperature, the oocysts sporulate and spread into the environment. These oocysts can then contaminate other food and water sources, and thereby transmitted to other mammals, including humans. Contaminated food sources are often in the form of uncooked meat and raw vegetables that come into direct contact with infected cat faeces from soil but can also be transmitted directly between humans. Blood transfusions are also a source of *T. gondii* transmission in humans showing that there are four possible routes of infection resulting in toxoplasmosis Figure 1.4 [28].

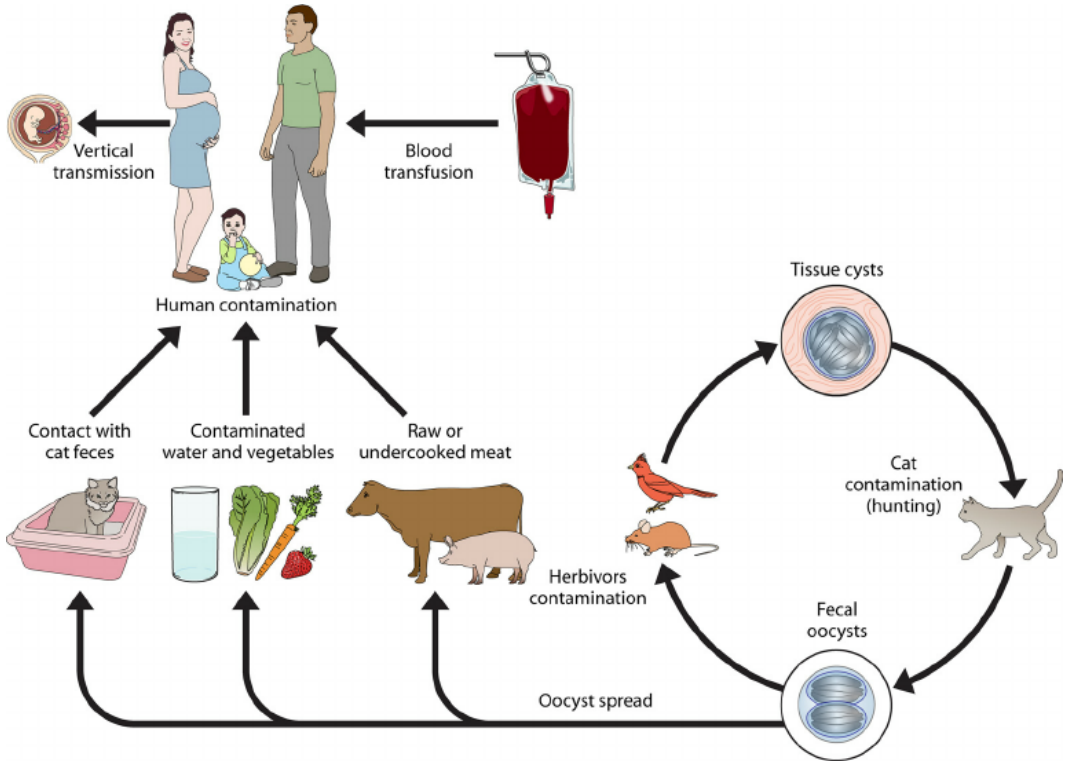

Figure 1.4: Life cycle of *Toxoplasma gondii* . The cycle starts from an infected intermediate host such as rodents, and other mammals including pigs, sheep and cattle. *T. gondii* at this stage in its life cycle is in its tachyzoite or bradyzoite stages and passes on to the definitive host through ingestion of an infected mouse. In the cat, the parasite completes its life cycle by shedding unsporelated faecal oocysts. Oocysts then develop into sporulated oocysts which, if they come into direct contact with human food sources are consumed, lead to *T. gondii* infection. [28]

1.2.3 Toxoplasmosis

Toxoplasmosis is caused by *T. gondii* was first identified as a disease in the tissues of a congenitally infected infant in 1939 and today affects a third of the world's population [19]. *T. gondii* is known to thrive in immunocompromised individuals and affects pregnant women, leading to either spontaneous abortion of the foetus or children born with toxoplasmosis as shown in Figure 1.5. If a woman becomes infected with *T. gondii* during pregnancy, this usually results in a miscarriage, a stillborn child, or a child born with congenital toxoplasmosis usually evident by an abnormally enlarged head [19]. Currently, there are few available drug treatments (Table 1.1) for pregnant women who become infected with *T. gondii* after conception. As

for immunocompromised individuals, the AIDS epidemic over the last three decades has resulted in an increase in *T. gondii* related infections (Figure 1.6), Reactivation of the parasite in HIV infected individuials leads to symptoms of fever, seizures and poor coordination, while those that acquire HIV first and subsequent *T. gondii* exposure develop a severe primary infection, leading to *Toxoplasma* encephalitis [18]. This opportunistic pathogen can cause similar symptoms in other immunocompromised individuals such as cancer patients (NHS). Today, toxoplasmosis as reported by the CDC infects 22.5% of the population in the USA, while in some countries like Brazil infection rates are reported to be as high as 95% (CDC). In the United Kingdom, 350 000 people in the population were estimated to be infected with this parasite (NHS, 2015). All of these infections together indicate an urgent need for the discovery of new therapies.

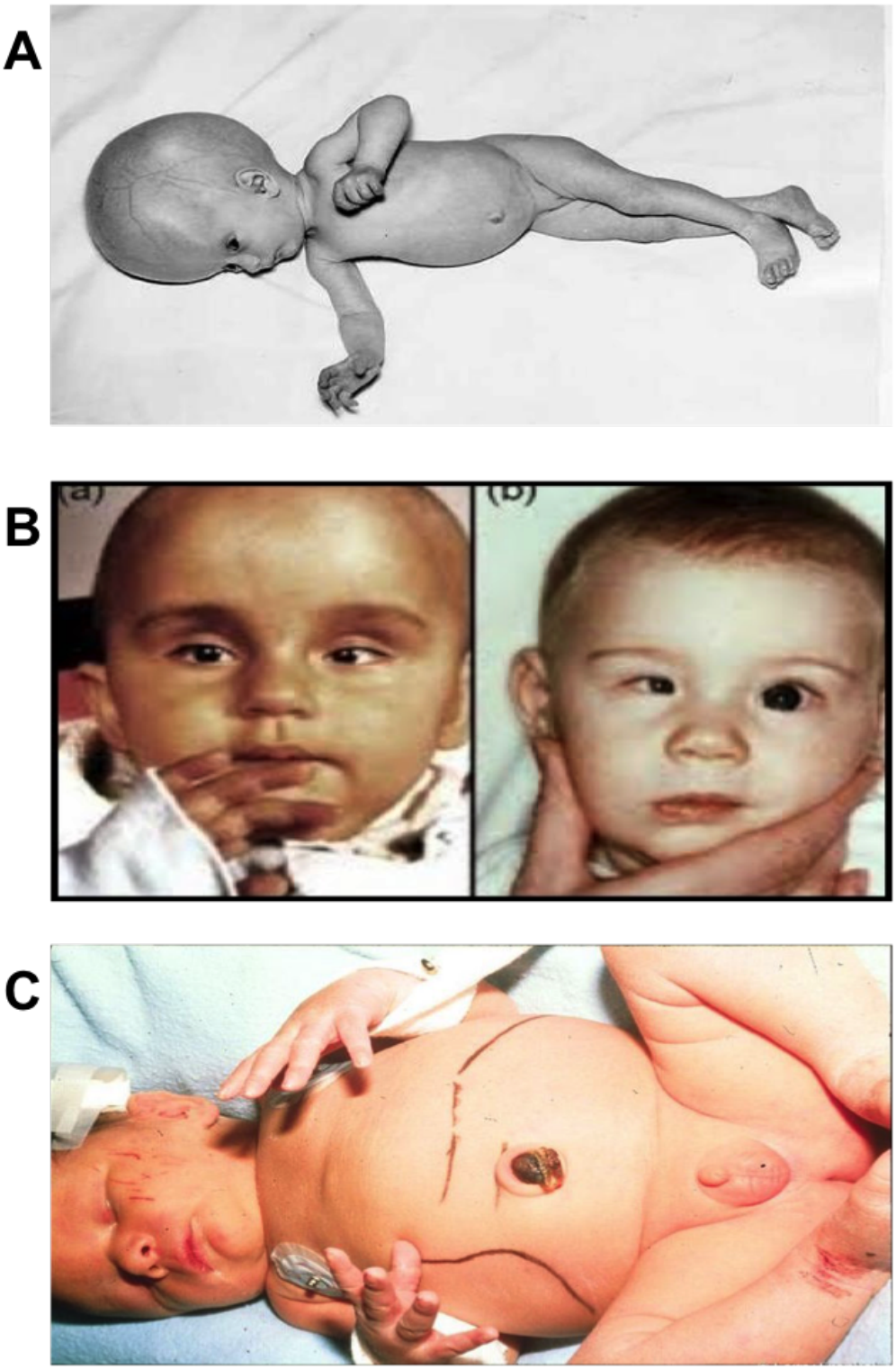

Figure 1.5: Children with various forms of toxoplasmosis; Fetus born with TORCH Syndrome or commonly known as Chronic Congenital Infection Syndrome has a range of complications to include damaged organs and Central Nervous System abnormalities and the fetus' chances of survival at this stage are quite reduced (A)(From Dubey JP, and Beattie CP. Toxoplasmosis of animals and Man. CRC Press, Baca Raton, Florida, 52, 1988). While a child with the ocular form of the disease and will suffer from blurred vision and photophobia and in some cases blindness (B) (http://www.infonet-biovision.org).Hepatosplenomegaly as shown in (C) is another type of fetal toxoplasmosis.

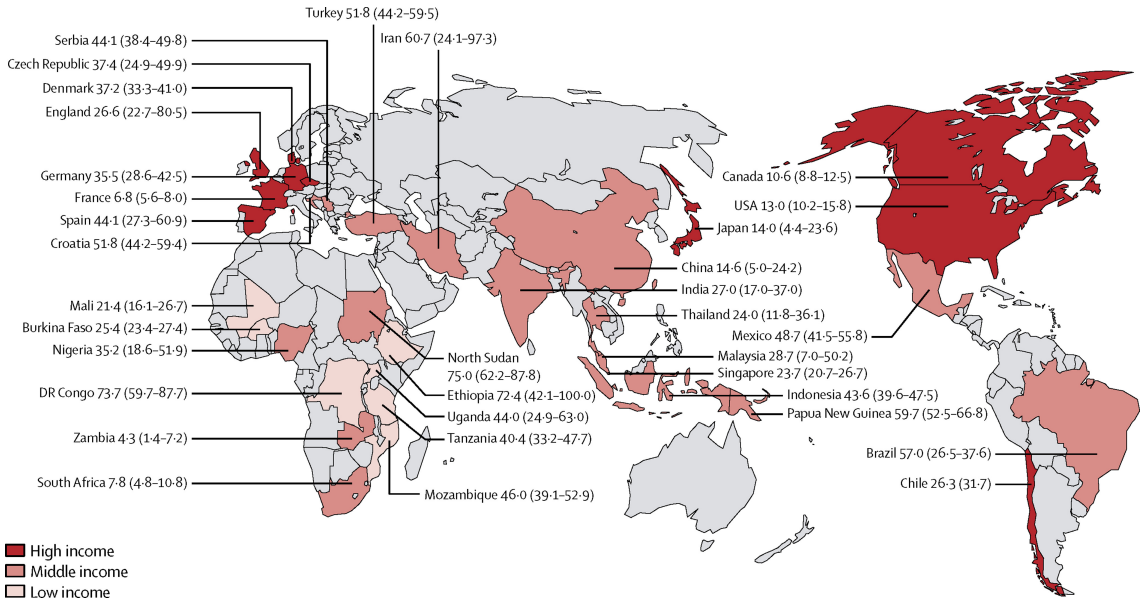

Figure 1.6: World map showing toxoplasmosis infections in association with increase in AIDS. The map clearly shows that the low income countries are the most affected and as a result of poor education, sanitary conditions lead to increases in toxoplasmosis mainly as a secondary infection [18]

1.2.4 Current treatments for toxoplasmosis

As shown in Table 1.1 current medicines for toxoplasmosis include a combination of therapies for different patients and consist mainly of pyrimethamine and sulfadiazine and leucovorin used in the prevention of haematologic toxicity. A review of 115 patients with *Toxoplasma* encephalitis found side effects of this combination therapy, leading to 44% of patients requiring a change of treatment [29]. The use of pyrimethanmine and sulfadiazine is also associated with severe liver necrosis, toxic epidermal necrolysis and agranulocytosis [30]. This highlights the importance of researching into discovery of new therapies that would be less toxic to patients. In addition to the high levels of toxicity associated with current modes of therapy, the problem of drug resistance is suspected to contribute to approximately 10% of treatment failures [13]. Clinical isolates with high levels of sulfonamide resistance have been found due to mutation in the dihydropterate synthase gene which includes

sulfadiazine, [13]. In addition to the toxicity and resistance presented by current drugs used to treat toxoplasmosis, the long treatment durations form several weeks to years are also problematic. The prolonged treatment regime is in part due to lack of drug efficacy against *T. gondii* tissue cysts during a treatment course. This again highlights the need and importance of new discoveries for treatments to be focused on compounds that would eliminate tissue cysts from the host cell, non-toxic and have a potential to be used in chronic infection as well as being safe to use during pregnancy [30].

NAME OF TREATMENT	DEMOGRAPHIC	MOLECULAR TARGET
Spiramycin (1st trimester) and pyrimethamine sulfadiazine and leucovorin (2nd and 3rd trimester)	Pregnant women, newborns and infants	Dihydrofolate reductase essential for DNA and RNA synthesis
Pyrimethamine and sulfadiazine plus folinic acid	People with ocular toxoplasmosis	Dihydrofolate reductase
Anti-retrovirals followed by pyrimethamine and sulfadiazine plus folinic acid	Immunocompromised individuals; AIDS usually in the form of toxoplasmic enchephalitis	Dihydrofolate reductase
Pyrimethamine and sulfadiazine plus folinic acid	Healthy non pregnant individuals	Dihydrofolate reductase

Table 1.1: Treatments for toxoplasmosis as reported by the CDC and WHO. [13, 30]

1.2.5 Drug discovery

As with all protozan research, drug discovery for toxoplasmosis poses many challenges primarily due to cost and the poorly understood biology, especially in the *Felidae* stages of the parasite but also in bradyzoites and tachyzoite forms. Some of the difficulties in therapy research can be attributed to two main causes. Firstly the

tough glycan-rich cyst wall of the bradyzoite is difficult to penetrate and has been a major hindrance in exploring this stage of the parasite. Secondly, the lack of an animal model that resembles *T.gondii* infection in humans. Despite these difficulties the development of rapid and reproducable *in vitro* drug assays makes the search for *T.gondii* therapeutics more achievable [30] [22]. *T. gondii* tachyzoite inhibition assays are often used and the RH strain of *Toxoplasma* is well adapted to *in vitro* culture. *T. gondii* bradyzoite inhibition assays, however, are not well established but are a crucial tool in research into encysted parasites. In addition, databases such as ToxoDB provide valuable information on genes that can be exploited to target specific proteins within organelles or the organelles themselves. *T. gondii* genome sequences are now available for ME49 (a Type II strain) and GT-1 (a Type I strain), and sequence alignments of these strains are available as genetic maps and single nucleotide polymorphisms (SNPs) alongside the commonly used Type I RH laboratory strain has allowed a better understanding of this obligate pathogen [31]. The ER and mitochondria of *Toxoplasma* offer excellent drug targets and some inhibitors have been identified that target these organelles and a similar approach would be to investigate an organelle [30]. The peroxisome is another organelle within *T. gondii* that offers significant potential as a target for novel.

1.2.6 Peroxisomes

Peroxisomes were first identified by Christian de Duve in the 1960s [32]. He first identified them in rat liver and later in protozoa, namely *Ancathamoeba* and *Tetrahymena pyriformis*. These early biochemical studies described peroxisomes as membrane-bound micro-bodies containing catalase and hydrogen-peroxide [32]. This well studied, functionally-diverse organelle, located in the cytosol of all eukaryotic cells has been linked to many catabolic functions (Figure 1.7). These include long chain fatty acids, branch fatty acids, D-amino acids, plasmogen synthesis, amino degradation

and purine metabolism [33,34]. Their functionality varies between organisms, for example, in animals, peroxisomes are involved in trafficking cholesterol, while in plants, as well as being involved in conversion of fatty acids to carbohydrates, they also play an important role in photorespiration (a process in plant photosynthesis) [33].

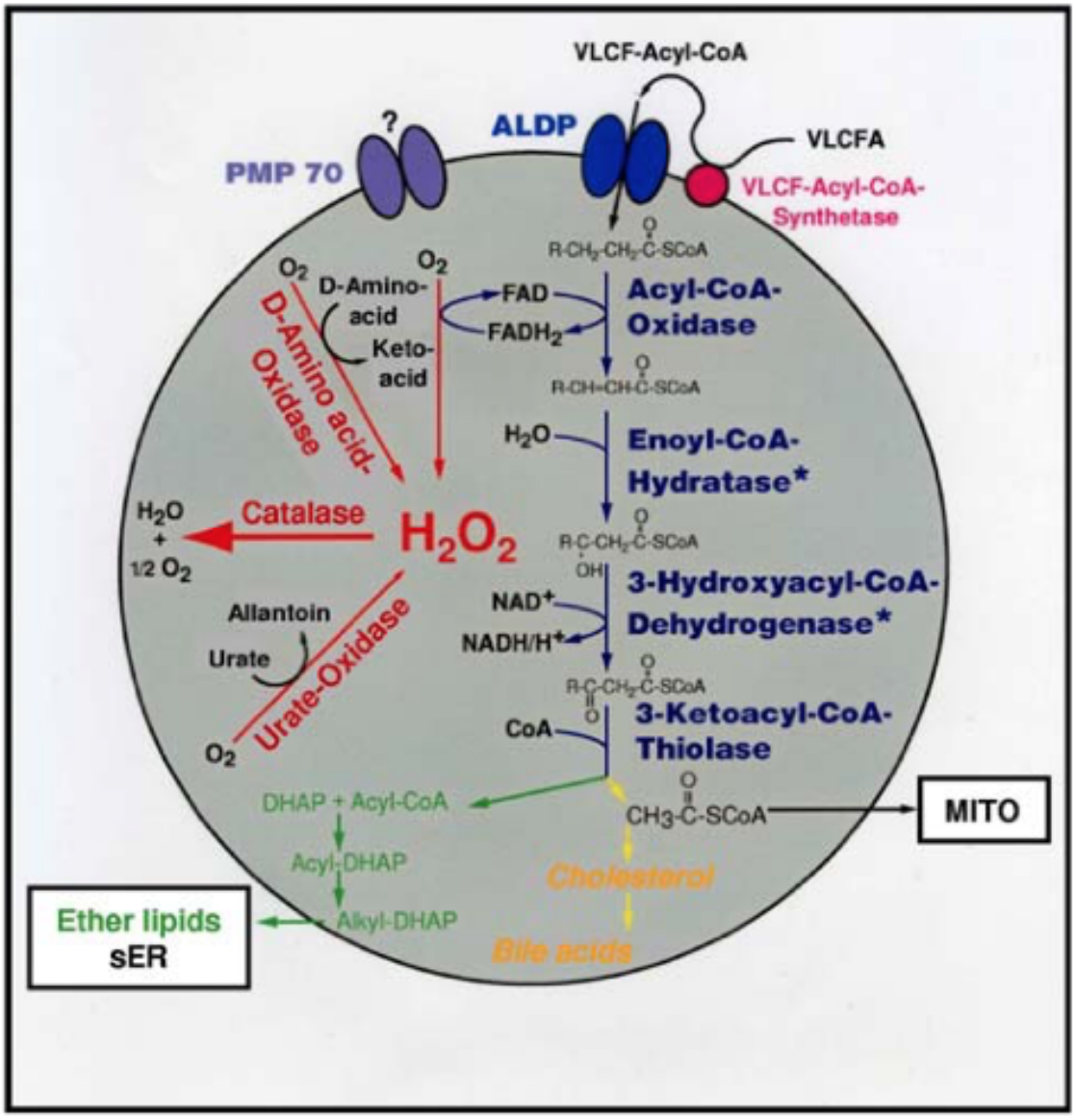

Figure 1.7: Biochemical processes in mammals adapted from Schrader *et al* [35]. The enzyme catalase breaks down hydrogen peroxide into water and oxygen

Peroxisome functionality is brought about by a group of proteins called peroxins (Pex). To date there are 32 known peroxins inculding; Pex1, Pex2, Pex3, PexMP3, Pex5, Pex6, Pex7, Pex10, Pex11A, Pex11B, Pex12, Pex13, Pex14, Pex16, Pex19,

Pex26, Pex28, Pex30 and Pex31. [36]. In most organisms peroxins are involved in trafficking post-translational proteins in the form of proteins bound to their co-factors and/or as protein complexes [37]. Proteins transported to the peroxisome via the peroxisomal matrix are recognised by two well known specific cytosolic receptors, Pex5 and Pex7. These receptors have been identified as the key players in cholesterol trafficking and lipid sorting. Transportation of lipids from the host cell cytosol to the peroxisome is shown in Figure 1.8. To do this, peroxisomes rely on a group of lipid carrying proteins also referred to as peroxisomal matrix proteins. There are two types of these proteins, uniquely identified by a Peroxisomal Targeting Signal (PTS). The first of these is PTS1 and is characterised by having these three amino acid residues (Serine-Lysine-Leucine) at the C-terminus of the matrix protein. The second, PTS2 has a sequence of R/K-L/V/I-X5-H/Q-L/A at the N-terminus. Research in yeast (*S.cerevisiae)* shows that Pex7 binds to thiolase via PTS2. PST1 proteins that on have been identified include Sterol Carrier Protein-2 (SCP2) [38] and catalase [24, 39]. SCP2, as its name suggests, moves sterol across membranes and also intracellularly. It is well established that in order to transport sterol and other cytosolic lipids, the PTS1 on SCP2 binds the C-terminus of Pex5 as a receptor during lipid transportation, while the N-terminus of Pex5 binds to Pex7 *[40–43].*

The Pex5 cycle in yeast (*Saccharomyces cerevisiae*) commences in the cytosol and involves the C-terminal end of Pex5 binding to the PTS1 of SCP2+(lipid) [41]. This Pex5-SCP2+(lipid) complex then interacts with other peroxins, such as Pex13 and Pex14 found in the peroxisomal membrane, allowing the SCP2+(lipid) to be released into the peroxisome. Pex5 then undergoes ubiquitination by either Pex2, Pex10 or Pex12 which allows Pex5 to be recycled into the cytoplasm by Pex1 and Pex6 [44]. The Pex5 cycle in yeast involves some hydrophobic protein complexes that are instead recognised by receptor Pex19 which binds to other peroxisomal membrane peroxins such as Pex3 [42, 45, 46]. Using Figure 1.8 to illustrate, the hypothetical *Tg*Pex5 (*T.gondii*Pex5) *Tg*Pex7 (*T.gondii*Pex7) cycle within *T.gondii* peroxisome

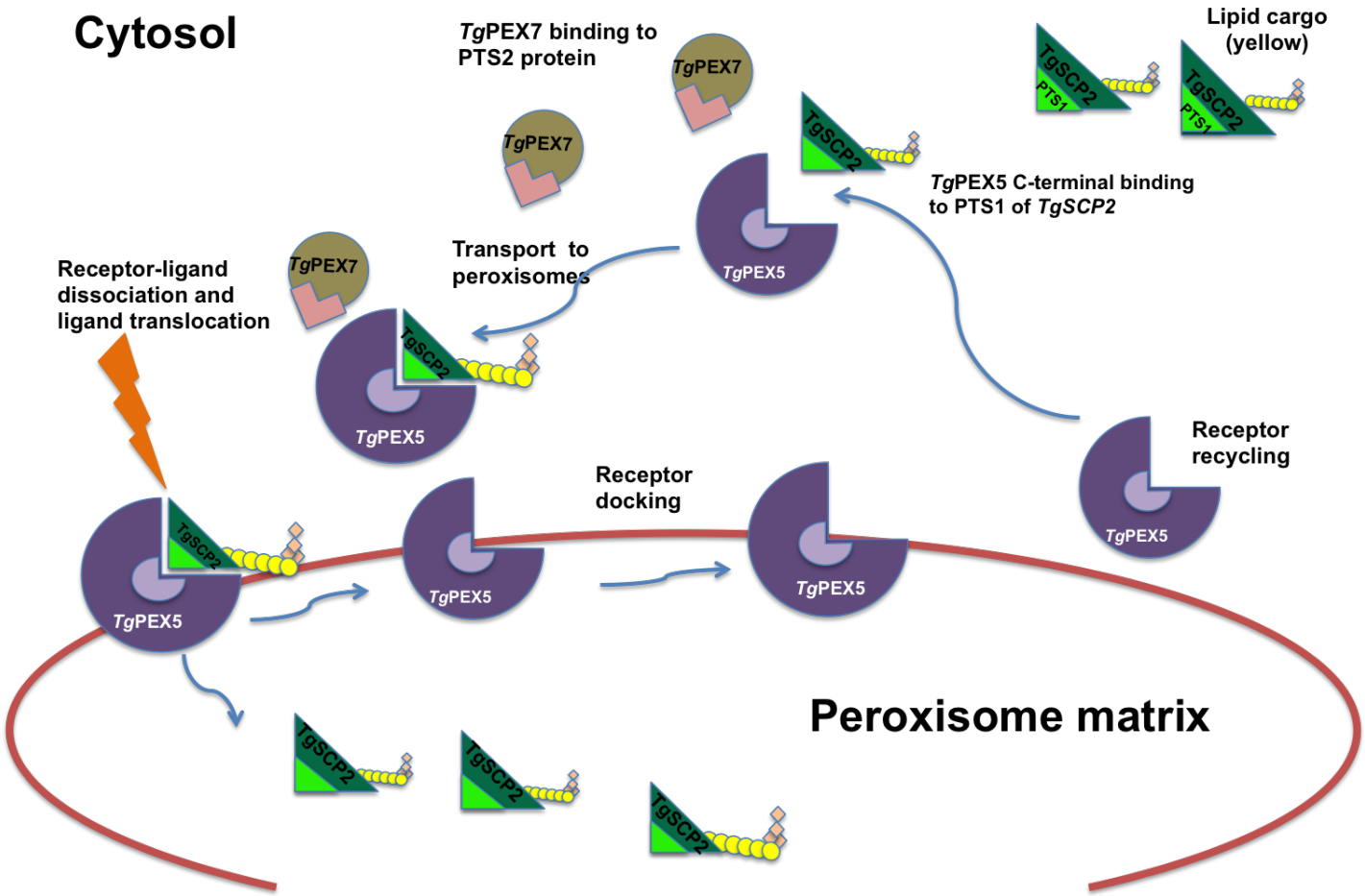

Figure 1.8: Model for transportation of lipids from cytosol to the peroxisome using Sterol Carrier Protein 2 (SCP2) and Pex5 receptor. SCP2 starts in the cytosol attached to its lipid cargo on its C-terminal end while the N-terminal of SCP2 has a PTS1 binding site which binds to the C-terminal of the Pex5 receptor. This Pex5-SCP2 complex attached to other peroxins like Pex7 then travels from the cytosol to the peroxisome and docks on the peroxisomal membrane. Once the Pex5-SCP2 complex is at the membrane the SCP2 with its lipid cargo are released into the peroxisomal matrix for various metabolic processes, while the Pex5 receptor is recycled for further transportation of lipids.

would involve the C-terminus of *Tg*Pex5 binding to the PTS1 of *Tg*SCP2+(sterol) to form a complex of *Tg*Pex5-*Tg*SCP2+ sterol which in turn would bind to the *Tg*Pex7 receptor. This complex when docked on the peroxisomal membrane, would allow the release of the sterol into the peroxisome matrix, while the *Tg*Pex5 receptor is recycled for further lipid transportation.

The ability of peroxins to transport both hydrophilic and hydrophobic proteins in most eukaryotes has been seen as essential. Mutations in the Pex genes (specifically in Pex5) in humans results in Zellweger-Syndrome, Neonatal Adrenoleucodystrophy or Infantile Refsum's disease, often leading to premature death [37]. These finding highlight the essential functionality of peroxins during peroxisomal biogenesis, and also their importance in the transportation and metabolism of lipids and other compounds such as hydrogen peroxide [35]. Despite the crucial role of peroxisomes in humans and other eukaryotes (especially eukaryotes living in oxygen poor environments), other protozoa have been reported to lack peroxisomes, including intestinal parasites such as *Giardia intestinalis* and *Enthamoeba histolytica.* Intracellular protozoan parasites such as the Microsporidia *Encephalitozoon cuniculi* and the Apicomplexans *Plasmodium falciparum,* and *Crptosporidium parvum* have also been reported to lack peroxisomes [47, 48]. In contrast, flagellate kineoplastids *Trypanosoma* and *Leishmania*, do have peroxisomes (glycosomes) and possess numerous glycolitic enzymes but lack catalase. [49]. In helminths, however, the genes found in peroxisomes seem to have been lost through evolution [34]. However, there is conflicting evidence for the existence of these organelles within toxoplasma and proof for peroxisomes is sparse, however unlike the helmiths, *T. gondii* does posses many peroxisomal genes (www.toxoDB.com). Here, we exploit information drived from the *Toxoplasma* genome to analyse and experiment on the key peroxin Pex5 and its associated protein SCP2. An interaction between this PTS protein and its respective protein partner has been demonstrated previously in studies of peroxisomes within *Toxoplasma* [50].

1.2.7 *Toxoplasma gondii* peroxisomes?

Obligate intracellular organisms such as *T.gondii* rely on the host for most of their nutritional requirements during infection, as they lack their own biological machinery to synthsise cholesterol. This inability of *T.gondii* to synthesize its own cholesterol makes it reliant on its mammalian host to provide these essential compounds. The uptake of lipids, as in all organisms, is important for post-translational modification of proteins as well as the building of membranes, making *T.gondii* heavily reliant on the exogenous uptake of lipids. Host lipoprotein-derived cholesterol is crucial for *T. gondii* replication. Nishikawa *et al* [21]showed that the absence and abundance of low-density lipoproteins (LDL) resulted in encystation and over-replication respectively [21]. These findings indicated that *T.gondii* evolved to allow trafficking of cholesterol in terms of storage, acquisition and transportation. There apppear to be various forms of cholesterol compartmentalization in *T. gondii* including unique mechanisms, which allow uptake and storage of LDL [24]. Databases searches using toxoDB have identified *T. gondii* genes encoding peroxins as well as their associated ligand binding proteins that carry PTS1 and PTS2 motifs (www.toxodb.org). Previous studies, used catalase in the protozoa *Ancanthaomoeba* and *Tetrahymena pyriformis* as as evidence for establishing the presence of these peroxisomes [32]. More recently, GFP fused to catalase was used to localise peroxisomes in *T. gondii*. The result of these experiments in tachyzoite and bradyzoite stages of *T. gondii,* showed that this fusion protein was mainly cytosolic and it was concluded that *T.gondii* harbored no peroxisomes *[51].* However, Kaasch and Joiner [52]also using catalase as a marker suggested that there are peroxisomes in *T. gondii* using experiments that showed the breakdown of H_2O_2 by catalase as an indicator of the presence of peroxisomes. They defend this argument by suggesting that cytosolic catalase would be insufficient to neutralise exogenous H_2O_2, whereas membrane-bound micro-bodies with a pool of catalase would be needed to scavenge the H_2 O_2 production [52]. More recently, evidence of the presence peroxisomes in *T. gondii*

has been supported by Lige *et al.* Their approach has been to use tagged GFP-*Tg*SCP2 in localisation studies [50].

In this project we adopted a similar approach to Lige *et al*, using a classical protein-centred approach. We functionally and structurally analysed two key targets *Tg*Pex5 and *Tg*SCP2 with the goal of proving that these proteins function like related Pex proteins from other organisms with peroxisomes in order to provide support for the existence of this organelle in *Toxoplasma.*

1.2.8 *Toxoplasma gondii* Aims and Objectives

1. To purify the Pex proteins *Tg*Pex5 and *Tg*SCP2, specifically the C-terminal end of *Tg*Pex5 ($TgPex5_{\text{C-TERMINAL}}$) and the PTS1 domain of *Tg*SCP2 ($TgSCP2_{\text{PTS1}}$).

2. To assess localisation through protein-protein interactions, using *Tg*PTS1 binding to *Tg*Pex5 in wild-type *T. gondii* .

3. To evaluate *Tg*Pex5 in complementation studies investigating its functionality in yeast and human Pex5 mutants.

4. Investigate the potential use of natural compounds and peroxin inhibitors against *Toxoplasma* both in the tachyzoite and bradyzoite stages, by optimising an *in vitro* assay and screening compounds against encysted *T. gondii* and non-encysted forms of *T. gondii.*

1.3 *Leishmania*

Leishmania like *Toxoplasma* is a protozoan zoonotic parasite, and has vertebrates as its primary host. [53].

1.3.1 *Leishmania* life cycle

All *Leishmania* species have two structural variants, the promastigote and amastigote as shown in Figure 1.9 . The mammalian life cycle of *Leishmania* begins with a bite from the parasite's vector the female *phlebotimine* sandfly which transfers the promastigote form of *Leishmania* from the proboscis into the skin of a human (anthroponotically), or through zoonosis. Here, while the sandfly vector is feeding, metacyclic promastigotes are phagocytosed by either macrophages or neutrophils and transformed into flagellated amastigotes [54]. Unlike other pathogens, the endosomal lysosomal enzymes within the macrophage have no effect on *Leishmania* allowing this parasite to grow and dividie through binary fission [28]. Ultimately, this causes the macrophage to burst, thereby releasing more *Leishmania* amastigotes into circulation infecting more macrophages and allowing the cycle to repeat until a sandfly takes its next blood meal. In the gut of the sandfly, the amastigotes transform into promastigotes, these form by simple division changing from procyclic to metacyclic promastigotes. These metacyclic promastigotes then migrate to the pharyngeal valve, ready for the next infection [28].

Leishmania promastigotes have are elongated with a flagellum, which is mainly used for migration from the sandfly gut to its probiscus, such that when cultured *in vitro*, insect like gut conditions such as a temperature of 26^{o}C and a pH of 7 are required. In contrast, the amastigote which is usually found in mononuclear phagocytes such as macrophages and the circulatory system of humans is oval or circular in shape with no visible flagellum and characteristically favours a temperature of 37^{o}C and a pH of 5.5 *in vitro*.

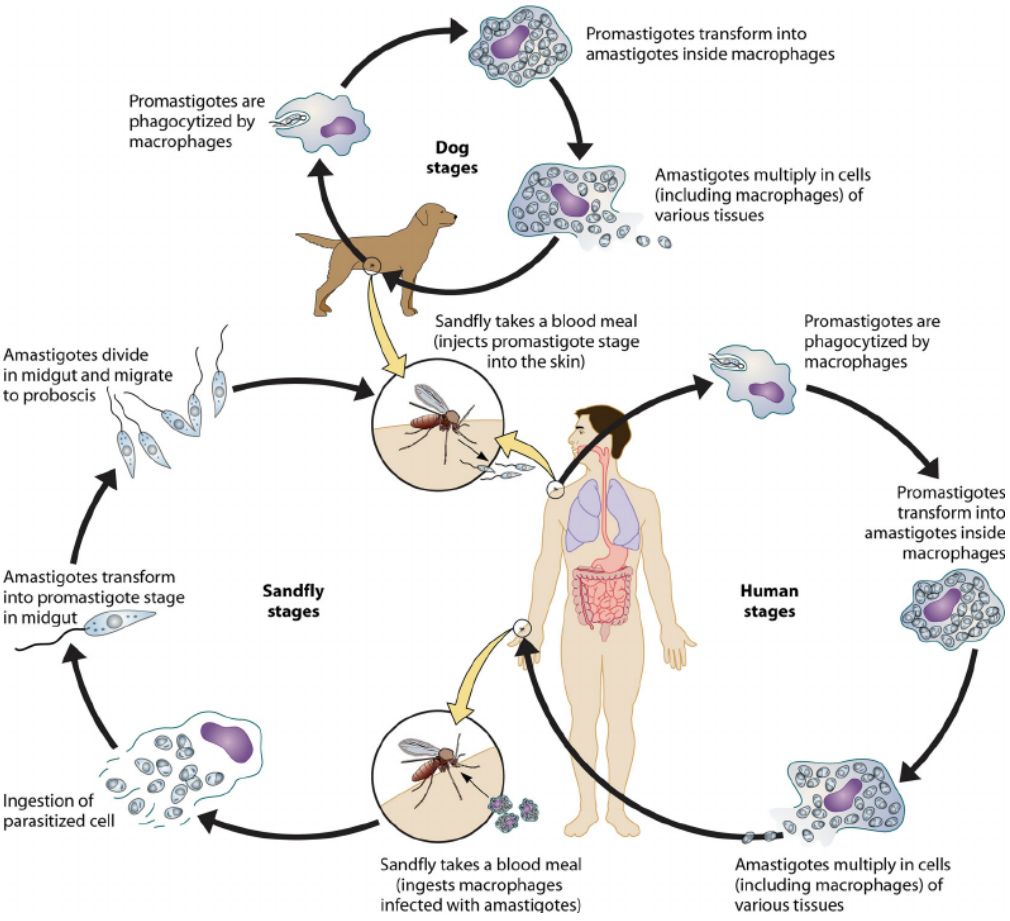

Figure 1.9: Life cycle of *Leishmania* in the human and dog stages starts with a bite from the sandfly , transferring the promastigote stage of *Leishmania* from the probiscus to the human or dog, where macrophages scavenge and engulf these promastigotes. While these promastigotes are in the macrophages they transform into amastigotes and replicates these are taken up by sandfly in it's next blood meal. In the sandfly stage the ingested amastigotes are transformed in the midgut of the vector back into promastigotes ready for another round of transmission. [28]

1.3.2 Leishmaniasis

Leishmania is comprised of many species (Table 1.2) including the *L. donovani* complex with two species, *L. donovani* and *L. infantum*, and the *L. mexicana* complex with three main species namely *L. mexicana, L. amazonensis,* and *L. venezuelensis* which also includes *L. tropica, L. major* and *L. aethiopica.* Subgenus *Viannia* has 4 primary species; *L. (V.) braziliensis, L. (V.) guyanensis, L. (V.) panamensis* and *L. (V.) peruviana.* Despite the large number of species, they are all morphologically

very similar and can only be distingusied by molecular techniques. Leishmaniasis is the disease that is caused by both old and new *Leishmania* species [55].

Old World Leishmania	New World Leishmania
L. tropica	*L. mexicana* (*L. mexicana, L. amazonensis, and L. venezuelensis)*
L. major	*L. [Viannia] braziliensis, L. [Viannia] guyanensis, L. [Viannia] panamensis, and L. [Viannia] peruviana*
L. aethiopica	-
L. infantum	-
L. donovani	*L. infantum or L. chagasi*

Table 1.2: Old and New World species of *Leishmania* [55]

There are to date 30 known species that infect mammals, of which 21 are known to infect humans and bring about three of clinical forms of disease: cutaneous, mucocutaneous and visceral leishmaniasis (Figure 1.11 and Figure 1.5).

1.3.2.1 Cutaneous leishmaniasis

Cutaneous Leishmaniasis (CL) is the most common form of the disease and arises from infection of epidermal tissue after promastigote host inoculation. Symptomatically it is distinguished by the appearance of skin lesions or skin sores, which develop within weeks of being bitten by the sandfly. These sores are known to change in size as well as appearance, after starting out as bumps they develop into nodules, which may be painless [28]. The lumps are predominately found under arms and on the hand as shown in Figure 1.10 (C). The ulcerated form usually develops on exposed parts of the body such as face, arms and legs and can cover these areas, bringing about serious disability to the infected individual (CDC and WHO). CL is caused by the, Old World species *L. major, L. tropica* and *L. aethiopica* and New World species *L. mexicana* and is most common in Afghanistan, Brazil, Iran, Peru, Saudi

Arabia and Syria (Figure 1.11).

1.3.2.2 Mucocutaneous leishmaniasis

Mucocutaneous leishmaniasis (MCL) also known as mucosal leishmaniasis and like cutaneous forms of the disease is physically debilitating, causing permanent damage of mucosal areas around the body. This can sometimes lead to partial or complete destruction of mucosal membranes such as those found in the nose, mouth and throat. The development of ML is a direct result of being infected by *L. braziliensis,* which can spread from the infected ulcer to various mucosal membranes around the body. The destruction of tissues in the surrounding mucosa (Figure 1.10 (A)) can lead to complete or partial destruction of mucous membranes of the nose and mouth. This disfigurement and resulting disability, exposes the sufferer to stigmatism and in some cases they are considered outcasts in countries like Bolivia, Brazil and Peru [15].

1.3.2.3 Visceral Leishmaniasis

Visceral Leishmaniasis (VL) also known as kala-azar (black fever) is the most severe form of leishmaniasis, like MCL and CL it typically develops after a few months, after being infected with VL specific *Leishmania: L. donovani* or *L. infantum.* In VL the parasite attacks internal organs such as the spleen, liver (Figure 1.10(B)) and bone marrow, leading to gastrointestinal bleeding, bouts of fever, severe anaemia and weight loss. Consequently, it is life threatening if not treated early, and fatality rates have been reported to be is as high as 100% within 2 years in countries such as Bangladesh, Brazil, India, Nepal and Sudan. In addition to these countries, increases in cases of VL also appear as a secondary infection in patients infected with HIV [56].

Figure 1.10: There are three clinical forms of leishmaniasis are caused by different species of *Leishmania*, and include clinical forms such as ; Mucocutaneous leishmaniasis mainly attacking mucosal membranes of the body (A), Visceral leishmaniasis infection which results in an enlarged spleen, liver and sever weight loss (B) and Cutaneous leishmaniasis found on the face arms and legs (C) [6].

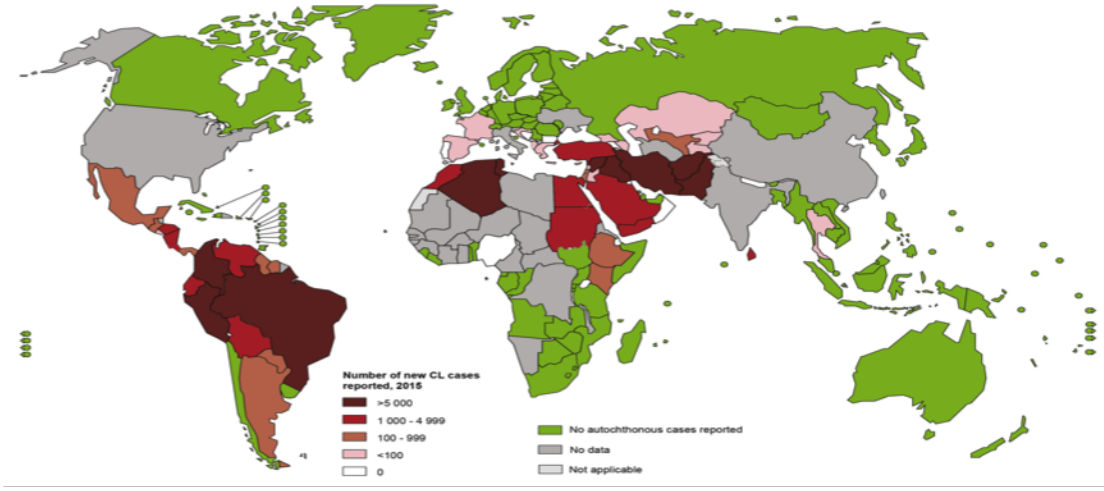

Visceral Leishmanisis

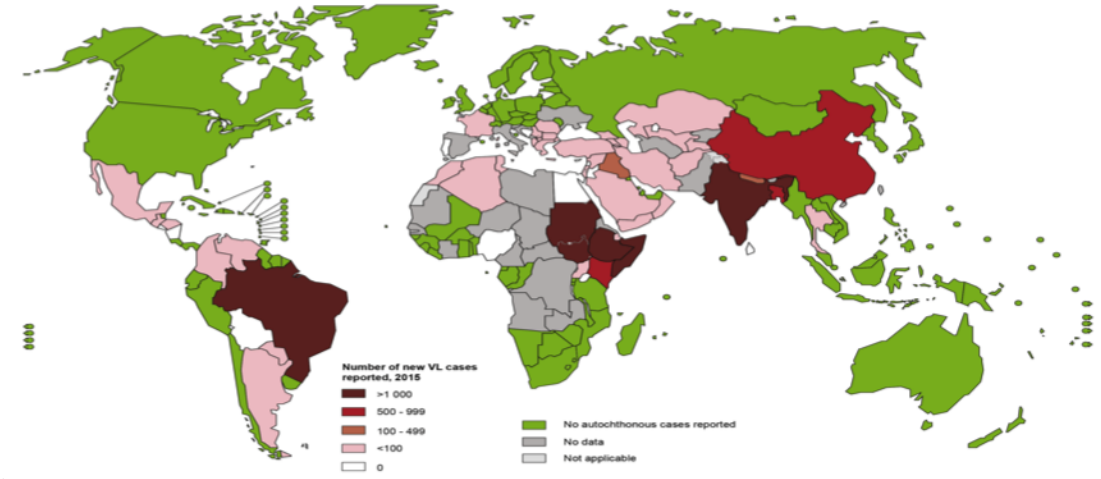

Cautaneous Leishmanisis

Figure 1.11: Global map of Cutaneous (CL) and Visceral Leishmaniasis (VL). As can be seen in both maps the number of VL cases was reported to be high in South America and the Middle East and parts of Eastern Africa. CL although the most common form of leishmaniasis seems to have reported lower cases in 2015 according to these WHO maps.https://www.dndi.org/diseases-projects/leishmaniasis/disease-background-vl/ accessed Nov 2018 and https://www.dndi.org/diseases-projects/leishmaniasis/disease-background-cl/ accessed Nov 2018

1.3.3 Current treatments for Leishmaniasis

Leishmaniasis is treatable when drugs are administered early during an infection [57]. Treatments for leishmaniasis are divided into three categories, namely; pentavalent antimonials including meglumine antimonate and sodium stibogluconate, Amphotericin B, an anti-fungal, and miltefosine. Pentavalent antimonials are the common front-line treatment and the drug of choice, although there have been reports of drug resistance against both antimonials. The development of resistance to pentavalent antimonials has encouraged their replacement by the alternate anti-leishmanials Amphotericin B and miltefosine, both of which are known to have good potentcy, but also have major side-effects [57].

1.3.4 Current front-line anti-leishmanials

There are three main compounds used as frontline anti-leishmanials

1.3.4.1 Pentavalent Antimonials

Pentavalent antimonials shown in Figure 1.12 (a) and (b) were the first chemotherapies to be used against leishmaniasis in 1930 and include meglumine antimonate and sodium stibogluconate. The mode of action of these antimonials is still unknown, although it has been suggested that they target several pathways in the amastigote stages including glycolysis, fatty acid beta-oxidation and inhibition of ADP phosphorylation [57]. These trivalent antimonials are the preferred drug of choice and are administered at about 20 mg/kg/day for 20 days and have a successful cure rate despite showing dangerous side-effects. A reduced safety profile after treatment has been reported with patients experiencing severe headaches, pancreatitis and cardiotoxicity, in 60% of leishmania sufferers in India known to be infected with antimonial resistant forms of leishmaniasis [57]. In addition, drug-resistance against these set of compounds has risen over the past 40 years, with the first drug resistant

isolates being reported as early as 1980 where patients in Guatemala and India saw the cure rate drop from 99%, to 86%, to 81% over a 4 year period [58].

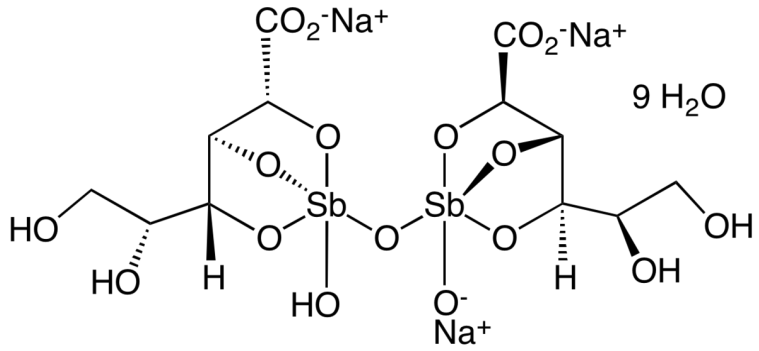

(a) Sodium stibogluconate

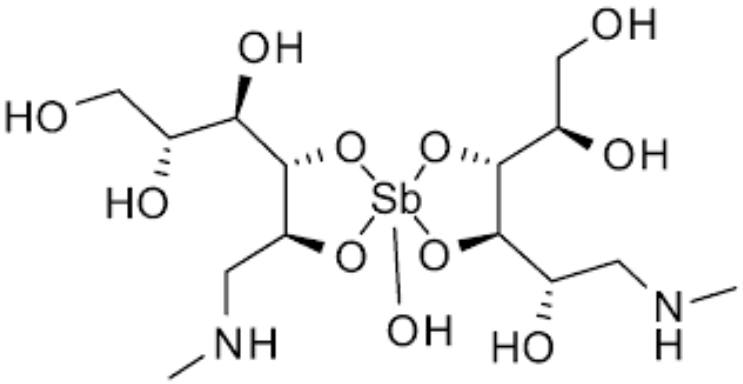

(b) Meglumine antimonate

Figure 1.12: Molecular structures of pentavalent antimonials, sodium stibogluconate (a) and meglumine antimonate (b) used in the treatment of leishmaniasis [57]

1.3.4.2 Amphotericin B

Amphotericin B (Figure 1.13) is a natural anti-fungal drug that was isolated from *Streptomyces nodosus* in the 1950's and used as an intravenous treatment for many fungal infections including candidiasis, coccidioidomycosis, cryptococcosis to name a few [59]. It is also used as a frontline treatment for leishmaniasis at 1 mg/kg/day for 20 days and has cure rates of up to 99%. The mode of action involves the development of pores within cellular membranes of the parasite, thereby causing an imbalance of ions causing inevitable osmotic lysis [57]. There has been little evidence of resistance developing against Amphotericin B, but the cost to the developing world in 2010 was between $162-$229 per course of treatment [59], which is a significant

cost and makes the drug unaffordable many parts of the world where leishmaniasis is rife.

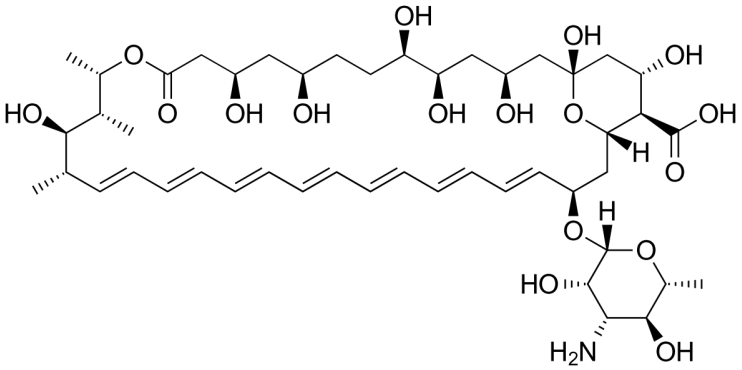

Figure 1.13: Molecular structure of amphotericin B [54]

1.3.4.3 Miltefosine

Miltefosine (Figure 1.14) sold under the trade name Impavido was first developed and manufactured as an anti-cancer drug in the 1980's [57]. It was subsequently approved as an anti-leishmanial for use in India in 2002 and is currently still undergoing clinical trials in other countries. Miltefosine is known to act on both the dimorphic (both promastigote and amastigote) forms of VL and CL and is reported to have a mode of action that involves inhibition of cytochrome c oxidase and may also affect lipid metabolism [57]. A 28 day treatment regime exists for miltefosine and ranges from 100 mg/kg/day for VL and 2.5 mg/kg/day in CL with cure rates at up to 94% in VL. Not many cases of resistance have been reported to date but side effects are reported 60% of the time in users and include nausea, vomiting, diarrheoa, headaches and dizziness [57].

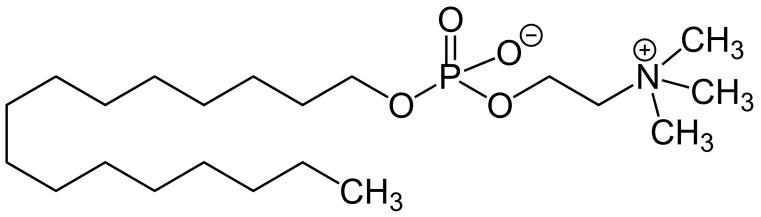

Figure 1.14: Molecular structure of miltefosine [57]

Growing resistance to anti-leishmanial drugs, prolonged treatment regimes, high toxicity and severe side effects has led to these treatments being reviewed. In addition, the current status of antilishemaninal drug discovery shows that the pipeline is empty, remeaning that a small inventory of anti-leishmanial drugs are used to treat all CL, MCL and VL cases. The increase in drug-resistant *Leishmania* as well as the rise of leishmaniasis cases, highlights the need for a new, affordable, larger library of compounds to treat *Leishmania*. The treatment of leishmaniasis over past decades involving front-line drugs is costly (Amphotericin B), and causes severe side-effects (Miltefosine) and in some cases, the emergence of drug resistance (pentavalent antimonials). As a consequence many research groups and endogenous people in both endemic and non-endemic areas have explored, investigated and tested the use of natural products, mainly plant derived in an effort to treat *Leishmania* (Tables 1.3 and 1.4) [60–63].

1.3.5 Natural products as anti-leishmanials

The use of natural products for treatment of protozoan disease dates back to 1631, where the bark of the cinchona tree was used as a treatment for malaria in Rome. This tree originated in Peru and was brought over to Europe by Jesuit priests and used to successfully treat King Charles II. Following this success, cinchona bark (also known as Peruvian bark) active componet in quinine, became popular in Europe and was deployed as the primary anti-malarial until the 1940's [64] where quinine was replaced by other antimalarials due to drug resistance. The rescue of quinine resistance in many endemic areas was by another natural compound called artmether. Today the search for new chemotherapies from natural products extends to many other protozoan diseases including the treatment of leishmaniasis [65].

1.3.5.1 Natural oil and wax extracts as anti-leishmanials

NAME	MODE OF ACTION	SPECIES OF LEISHMANIA	REFERENCE
Ferula galbaniflua oil	Not Known	Effective against *L. amazonensis* promastigotes	[63]
Tetradenia riparia oil	Not Known	Inhibits *L. amazonensis* promastigotes and *L. amazonensis* infected macrophages	[61]
Propolis tree resin, bioflavonids and waxes collected from *Apis mellifera* bees	Not Known	Inhibits *L. amazonensis* promastigotes and amastigotes	[62]

Table 1.3: Oil extracts from plants and trees used against *Leishmania*.

1.3.5.2 Plant extracts; fruit, leaves and barks as anti-leishmanials

NAME	MODE OF ACTION	SPECIES OF LEISHMANIA	REFERENCE
Coccina grandis leaf extract	Increases levels of IL-12 and TNF-α. *Leishmania* infection usually blocks IL-12, use of the drug restores normal immune function.	*L. donovani* infected macrophages	[66]
Euphorbia prostrata leaf extract	Cause necrosis of parasite.	Inhibits growth of both *L. donovani* promastigotes and amastigotes	[67]
Physalis pubescens fruit extract	Changes the morphology of the parasite.	Inhibits *L. amazonensis* promastigotes	[60]
Solanum lycocarpum fruit extract	Not Known.	Inhibits *L. amazonensis* promastigotes	[68]
Ginger extract	Not Known	Inhibits *L. amazonensis* promastigotes	[69]
Lacistema pubescens plant extract	Not Known	Inhibits *L. amazonensis* promastigotes and *L. amazonensis* infected macrophages	[70]

Table 1.4: Plant extracts from leaves, and barks used against *Leishmania*

As can be seen from the table above, there are many natural products which have been tested against *Leishmania* parasites. Success in the use of natural products as

anti-leishmanial agents *in vitro* is evident although the results mainly show success in blocking th promastigote stages and non-infected macrophages. In tackling the fight against leishmaniasis, all stages and disease causing species need to be targeted. Exploiting large libraries of natural compounds is one of the ways we could combat and develop new global treatments. Here the use of well established *Leishmania in vitro* assays [54, 71] could be used in drug screens against axenic amastigotes and *Leishmania* infected human macrophages for the discovery of novel effective compounds .

1.3.6 Inhibition of *Leishmania mexicana* by natural products Aims and Objectives

1. Investigative natural products as anti-leishmanials by fractionation
2. *In vitro* testing of natural compounds against axenic *L. mexicana* amastigotes, cytotoxicity testing against human macrophages and *L. mexicana* infected human macrophages.
3. Explore *L. mexicana* amastigote lipid metabolomics for hit compounds, and putative target validation.

Chapter 2

Materials and Methods

2.1 Sequence analysis

DNA and protein sequences for *T. gondii* were obtained from (www.toxodb.org) using the following reference numbers: ID TGGT1_234570, TGGT1_273740, TGGT1_201850, TGGT1_231870. Sequence alignments were carried out using ClusterW2 (ClusterW2 (http://www.ebi.ac.uk/Tools/msa/clustalw2/). Cloning strategies used ApE A plasmid Editor by M. Wayne Davis and Conversion Script by T.P. Breckon (see Appendix A)

2.2 Materials

2.2.1 Growth media, Culture media, antibiotics and inducer

For bacterial growth all liquid and solid Lysogay Broth, Miller's LB Broth (LB) media (Sigma-Aldrich, L3522) was made using distilled water and autoclaved at 121°C for 15 min. For broth, 25g LB powder per litre of water was used, while semi-solid LB for plates contained 25g LB and 15g Agar (Sigma-Aldrich, A9539). Both media were supplemented with relevant antibiotic where applicable. For long-term storage cultures were mixed to give 50% (v/v) glycerol and kept at -80%.

Mammalian cell line and *T. gondii*, were maintained in Dulbecco's Modified Eagle's Medium (DMEM) high glucose without L-glutamine (Sigma-Aldrich, D5671) supplemented with 10% Foetal Bovine Serum (FBS) (Gibco, 10270) 4 mM L-glutamine (Sigma-Aldrich, G7513) and 42 μM Gentamicin (Gibco 15710-049). 50% (v/v) FBS 20% (v/v) DMSO and 30% (v/v) DMEM was used to store cell lines and *T. gondii* infected cells at -150°C.

Antibiotics: 50 mg/mL stocks of Gentamicin (Gibco, 15710-049), Kanamycin (Sigma-Aldrich, K1377) and Ampicillin (Sigma-Aldrich, A0166) were made in distilled water, filter sterilised, aliquoted and stored at -20°C and used within a month.

Inducer, Isopropyl β-D-1-thiogalactopyranoside (IPTG) (Sigma-Aldrich, I5502) was made in distilled water to a 1 M concentration and stored at -20°C.

2.2.2 Buffers

Buffers used are listed below;

Buffer A: 100 mM KH_2PO_4(Sigma-Aldrich, RES20760-A7), 5 mM 2-mercaptoethanol (Sigma-Aldrich, M6250) pH 7.4

Glutathione-Buffer A: Glutathione column elution buffer consited of Buffer A with 20 mM reduced glutathione (Sigma-Aldrich, G4251) pH7.4

Storage buffer A: Buffer A and 50% (v/v) glycerol.

Nickel Elution-Buffer A: Nickel column elution buffer (Nickel Elution-Buffer A): Buffer A and 250 mM imidazole (Sigma-Aldrich, I5513) pH7.4

Buffer B: (SDS-PAGE running buffer): 10 X SDS-PAGE Running Buffer (1 L) contained 144 g glycine (Sigma-Aldrich, G8898) 30.2 g Tris (Sigma-Aldrich, T1503), then for 1 X running buffer 100 ml of 10 X to 900 ml distilled water was used. The buffer was used at concentration for gel electrophoresis.

Buffer C: For *T .gondii* transfection; Cytomix (Electroporation buffer): 120 mM KCl (Sigma-Aldrich, P9333) 0.15 mM $CaCl_2$ (Sigma-Aldrich, C1016) 10 mM

KH_2PO_4(Sigma-Aldrich, RES20760-A7), pH 7.6 25 mM HEPES (Sigma-Aldrich, H3375) pH 7.6, 2 mM EGTA , pH 7.6, 5 mM $MgCl_2$ (Sigma-Aldrich, M8266) adjusted with KOH (Sigma-Aldrich, P5958) to pH 7.6

LiT/PEG mix: 40% (w/v) PEG 3350 in LiT solution (LiT = 100 mM LiOAc and 10 mM Tris-HCL pH 7.4)

2.2.3 Bacterial strains, *Toxoplasma gondii* strain and cell lines

All plasmids, cell lines bacterial and parasitic strains are listed in Table 2.1, Table 2.2 and Table 2.3

Table 2.1: *E. coli* strains used in this study

Strain	Genotype	Source
DH5α (origin of strain was developed by D. Hanahan) [72]	*F- Φ80lacZΔM15 Δ(lacZYA-argF) U169 recA1 endA1 hsdR17(rk-, mk+) phoA supE44 thi-1 gyrA96 relA1* λ-	Invitrogen, 182163-012
BL21 (DE3) Rosetta (Brussels strain of *E. coli* by Delbrück and Luria) [73]	*huA2 [lon] ompT gal (λ DE3) [dcm] ΔhsdS λ DE3 = λ sBamHIo ΔEcoRI-B int::(lacI::PlacUV5::T7 gene1) i21 Δnin5*	NEB, C2527I
Stellar™ Competent Cells	*F–, endA1, supE44, thi-1, recA1, relA1, gyrA96, phoA, Φ80d lacZΔ M15, Δ (lacZYA - argF) U169, Δ (mrr - hsdRMS - mcrBC), ΔmcrA,* λ–	Clontech, 638909

Table 2.2: Parasite Strains and cell lines used in this study

Type	Description	Source
RH *T. gondii* (ATCC® 50174D™)	Organism: *T. gondii*	Prof. Markus Messiner
M379 L. mexicana (ATCC® 50156™)	Organism: *L. mexicana*	Dr. Paul Denny
HFF cells (ATCC® SCRC-1041™)	Organism: *Homo sapiens*, human , Cell Type: Fibroblast , Tissue: Skin; foreskin	Prof. Markus Meissner
Macrophage RAW 264.7 (ATCC® TIB-71™)	Organism: *Mus musculus*, mouse, Cell Type: Macrophage	Dr. Paul Denny
Fibroblast GM5756	Organism: *Homo sapiens*, human , Cell Type: Fibroblast , Tissue:	Prof. Ralf Ederman
Vero Cells	Organism: *Cercopithecus aethiops* ,Tissue: kidney	Dr. Paul Denny

Table 2.3: Plasmids for protein expression and localisation

Plasmid	Description	Source
*TgSCP2*pUC57	TGSCP2_TGGT1 _29097 1878 bp in pUC57 Amp^r	GenScript
TUB8 mycGFPmyoATy-HX	*T.gondii* transfection vector with GFP tag and TUB8 promoter Amp^r	Prof. M Meissner (Glasgow University)
pFA6a-GFP-eSKL	*T.gondii* transfection vector with GFP tag and TEF promoter Kan^r	Dr Lilach Sheiner (Glasgow University)
*TgSCP2*TUB8 mycGFPmyoATy-HX	TGSCP2_TGGT1 _29097 in *T.gondii* transfection vector with GFP tag and TUB8 promoter Amp^r	In House (A J Mbekeani)
pETM-30	Expression vector with His tag, GST tag, TEV protease cleavage site, Kan^r	Dr. Gunter Stier Heidelberg (www.embl.de)
pETM-30-*TgSCP2*	*TgSCP2* gene in expression vector with His tag, GST tag, TEV protease cleavage site, Kan^r	GenScript
pETM-30-*Tg*Pex*5*	*TgPEX5* gene in expression vector with His tag, GST tag, TEV protease cleavage site, Kan^r	GenScript

2.3 Protein Expression *Tg*Pex5$_{\text{C-TERMINAL}}$ and *Tg*SCP2$_{\text{PTS1}}$

Clones of *Tg*Pex5$_{\text{C-TERMINAL}}$ and *Tg*SCP2$_{\textbf{PTS1}}$ were obtained from pETM-30-*Tg*SCP*2* and pETM-30-*Tg*Pex*5* plasmids manufactured and supplied by GenScript. These plasmids were subsequently used in protein expression. When plasmid DNA was required, a mini-prep was performed using QIAprep Spin Mini-prep following manufactures guidelines (Qiagen, ID 27104).

2.3.1 Bacterial transformation

Transformation of BL21 with plasmid DNA allowed the expression of *Tg*Pex5$_{\text{C-TERMINAL}}$ and *Tg*SCP2$_{\text{PTS1}}$ proteins. Competent BL21 (DE3) cells were thawed on ice and 1-100 ng DNA added, then incubated at 42°C for 30 seconds, before returning to ice for 2 minutes. Growth media was then added followed by a further 1 hour incubation at 37°C. A porportion of the culture was then spread onto agar plate, carrying the relevant selective antibiotic. Transformed colonies were chosen and used to inoculate LB broth supplemented with antibiotic and used to make glycerol stocks. Both DH5α glycerol stocks for future cloning experiments and BL21 stocks for large scale protein expression were generated.

2.3.2 *Tg*Pex5$_{\text{C-TERMINAL}}$ and *Tg*SCP2$_{\text{PTS1}}$ expression & purification

Expression of *Tg*Pex5$_{\text{C-TERMINAL}}$ and *Tg*SCP2$_{\text{PTS1}}$ recombinant proteins in BL21 cells was scaled up starting form a single colony streaked from glycerol stocks. 20ml of starting culture of BL21 pETM-30-*Tg*SCP*2* or pETM-30-*Tg*Pex*5* was used to inoculate 1 litre of LB containing 50mM Tris-hydrochloride (Sigma-Aldrich, 10812846001 ROCHE), supplemented with 1% (w/v) glucose (Sigma-Aldrich, G8270) and 50

µg/ml kanamycin (Sigma-Aldrich, K1377) at pH 7.5. Culture flasks were placed at 37°C in a shaking incubator at 150 rpm. When an OD600nm˜0.5-0.8, was achieved, the temperature was reduced to 20°C for 1 hour, then protein expression induced with 0.5 mM IPTG (Sigma-Aldrich, I5502) and grown overnight at 30°C. Cultures were then centrifuged at 4000 rpm for 35 min at 4°C and re-suspend in 35 ml of Buffer A. Cell pellets were flash frozen in liquid nitrogen and stored at -80°C until needed.

For protein purification the process, $Tg\text{Pex5}_{\text{C-TERMINAL}}$and $Tg\text{SCP2}_{\text{PTS1}}$ Stored frozen pellets from overexpressed cultures of $Tg\text{Pex5}_{\text{C-TERMINAL}}$and $Tg\text{SCP2}_{\text{PTS1}}$ were thawed and re-suspended in 15 mL Nickel Elution-Buffer A supplemented with an EDTA-free complete protease inhibitor cocktail tablet (Sigma-Aldrich, 04693159001 ROCHE) and 1 mg/mL lysozyme (Sigma-Aldrich, L1667) 1 mg DNase I and 1 mg RNase A. Cells were then sonicated using a Bandelin Electronic UW2200 sonicator for 5 x 1 min with 15 second pulses. The lysate was kept on ice during and after sonication and centrifuged at 40 000 rpm (JLA 8.100) for 45 min, at 4°C. The supernatant was filtered through a 0.45 µm filter [40, 74]and the soluble fractions containing fusion protein were subjected to digestion by TEV protease at 4°C overnight. This solution was passed through a GSTrap column and bound proteins eluted in Buffer A and glutathione. The products at each stage of the purification were analysed by SDS-PAGE [40].

2.3.3 Glutathione affinity chromatography

The filtered supernatant was applied to a 1 mL glutathione Sepharose 4B resin column (GSTrap) using a peristaltic pump (GE, 17-5130-01), pre- equilibrated in Nickel Elution-Buffer A. This GSTrap column was washed with Nickel Elution-Buffer A and eluted with Glutathione-Buffer A [40].

2.3.4 Tag Cleavage, dialysis and protein concentration

The eluted products containing fusion protein were then cleaved with TEV protease (Sigma-Aldrich, T4455) in accordance with the manufacture's instructions. In pilot studies protein precipitation occurred upon cleavage with TEV at 30°C for 1 hour. Further studies found that precipitation was prevented by cleavage at 4°C overnight. Dialysis from Nickel Elution-Buffer A supplemented with 20 mM reduced glutathione into Nickel Elution-Buffer A was performed after samples had been cleaved with TEV. The buffer exchange was through dialysis tubing (10 kDa molecular weight cut-off (MWCO), and was carried out for 3 hours at 4°C to remove the cleaved tag. Following dialysis, samples *Tg*Pex5$_{\text{C-TERMINAL}}$ and TgSCP2$_{\text{PTS1}}$were concentrated using Merck Millipore filters, 10kDa MWCO) [40].

2.3.5 Nickel affinity chromatography

TEV-cleaved products were next applied to a column Ni-NTA column, pre-equilibrated in Buffer A. The flow-through was retained proteins which contained the cleaved *Tg*Pex5$_{\text{C-TERMINAL}}$ and *Tg*SCP2$_{\text{PTS1}}$while His$_6$-TEV and His$_6$-GST remained bound to the Ni-NTA column (GE Healthcare). Nickel Elution-Buffer A was then used to remove the His-tagged peptides [40]. Following manufactuers guidelines SDS-PAGE equipment and protocols were adopted during protein expression and purification stages. For the polyacrylamide gel; 30% acrylamide, resolving buffer, stacking buffer, Ammonium persulfate (APS) 10% w/v (Sigma-Aldrich A3678) and TEMED (Sigma-Aldrich T9281) were used and electrophoresed in Buffer B at 200 V for 60 minutes [74].

2.4 *In vitro* localisation of *Tg*SCP2 and enhanced PTS1-Tagged GFP in *Toxoplasma gondii*

*Tg*SCP2 and enhanced PTS1-Tagged GFP cDNA was cloned into independent plasmid vector and later transfected into *T. gondii* and used to infect confluent HFF-1 cells, prior to fixation and antibody staining [24].

2.4.1 Cloning *Tg*SCP2$_{\text{COMPLETE}}$ into TUB8mycGFPmyoATy-HX and GFP-enhanced(e)PTS1 into pFA6a-GFP-eSKL

Cloning of respective PCR fragments was carried out using two different cloning methods. For *Tg*SCP2$_{\text{COMPLETE}}$ into TUB8mycGFPmyoATy-HX, The Clontech® Laboratories, Inc. In-Fusion® HD Cloning Kit was used, while the GFP-enhanced(e)PTS1 into pFA6a-GFP-eSKL used standard cloning techniques as described below.

2.4.1.1 Cloning *Tg*SCP2$_{\text{COMPLETE}}$ into TUB8mycGFPmyoATy-HX

As previously described [24]the complete cDNA of *Tg*SCP2 was cloned into the plasmid vector using the entire sequence of *Tg*SCP2 (TGSCP2_TGGT1_29097 Length: 1878 bp), using InFusion™ and following the manufactuers guidelines . This technique allowed directional cloning of PCR fragment into our linearized vector with >95% cloning efficiency. Here, *Tg*SCP2 was amplified from cDNA purchased from Genscript *Tg*SCP2pUC57 by the primer pair FW primer SCP2 TUB8 and RV primer SCP2 TUB8 (Table 2.4). Amplified fragments of ~1.9 KDa for *Tg*SCP2 were cloned into TUB8mycGFPmyoATy-HX. Sucessful insertion of *Tg*SCP2 was confirmed by restriction site mapping using *EcoRI* and *BamHI* in *Tg*SCP2 and DNA sequenced by Eurofins show in Appendix A. The new construct TUB8mycGFPmyoATy-HX-*Tg*SCP2 was introduced into Stellar™ competent cells by transformation . Trans-

formant colonies were selected and used to inoculate liquid LB supplemented with appropriate antibiotic and used to make glycerol stocks. Mini-prep plasmid DNA made using QIAprep Spin Mini-prep method was subsequently used in transient transfection.

2.4.1.2 Cloning GFP-enhanced(e)PTS1 into pFA6a-GFP-eSKL

The GFP-enhanced(e)PTS1 cassette was amplified from the vector pFA6a-GFP-eSKL [75] using the primer pair FW primer (e)PTS1 pFA6a and RV primer (e)PTS1 pFA6a (Table 2.4). The PCR product was inserted into pTUB8-myc-GFP to form pTUB8-GFP-ePTS1.

2.4.2 Maintenance and culture of HFF-1 and *T. gondii*

The maintenance and culture of a variety of *T. gondii* strains on HFF-1 cells for the various experiments used in this project followed perviously described protocols as described and detailed below [76, 77].

2.4.2.1 Maintenance and culture of HFF-1 and *T. gondii* Type I (*RH* and RH-HX-KO-YFP2-DHFR)

RH T. gondii wild-type and RH-HX-KO-YFP2-DHFR parasites were grown on human foreskin fibroblasts HFF-1 (ATCC SCRC, 1041) in an incubator at 37 ℃. HFF-cells were thawed at 37 ℃, 5%,CO_2 HFF-1 in DMEM (Sigma-Aldrich, D5671) supplemented with 10% FBS (Gibco, 10270) 4 mM L-glutamine, 42 µM Gentamicin HFFs and incubated overnight. After the addition on trypsin, cells were seeded into other flasks and reached confluency in 2-3 days. Thereafter, 1:4 split was carried out every week to maintain the HFF-1 culture. *RH T. gondii* or RH-HX-KO-YFP2-

DHFR parasites were then used to infect confluent HFF-1 cells. These tachyzoite cultures were grown continuously at 37 ℃ until HFF-1 cells lysed and extracellular parasites were present. Extracellular *T.gondii* were then subcultured onto fresh HFF-1 for a repeat cycle [76, 77].

2.4.2.2 Maintenance and culture of HFF-1 and *Toxoplasma gondii* Type II (*Pru*-GRA2-GFP-DHFR)

Pru-GRA2-GFP-DHFR *T. gondii* parasites were also grown on human foreskin fibroblasts HFF-1 using the same conditions as the *RH* strain. Once tachyzoite culture had been established, parasites were grown continuously under the same conditions. If encysted bradyzoites were required then once tachyzoites had formed plaques, media DMEM supplemented with 10% FBS 4 mM L-glutamine 42 µM Gentamicin at pH8 was used to allow the transformation of tachyzoites to encysted bradyzoites over a 24 hour period as described by [78].

2.4.3 *Toxoplasma gondii* transient transfections

Transient transfection followed the protocols described by Soldati and Boothroyd [39].

2.4.3.1 TUB8mycGFPmyoATy-HX-*Tg*SCP2 transfection of *Toxoplasma*

DNA TUB8mycGFPmyoATy-HX-*Tg*SCP2 plasmid DNA for transfection was prepared using ice cold 100% EtOH 1% NaAceate and incubated at -20ºC overnight, then centrifuged at 14 000 rpm for 30 min followed by two washes with 70% ethanol. The supernatant was removed and the pellet left to dry for 15 min. Between 30-60 µg of DNA was then used for *T. gondii* transfection. Freshly lysed extracellular *T.*

gondii approximately 10^7 extracellular parasites from HFF's, were centrifuged at 1000 rpm at 4^{o}C for 10 min. The supernatant was discarded and cells washed with Cytomix and centrifuged for 5 min at 1200 rpm. Plasmid DNA (approximately 60 µg) mixed with the resuspended parasite cell pellet in cytomix containing 100 mM ATP and 100 mM GSH, before adding to an electroporation cuvette. For electroporation, in a Bio-Rad, Gene Pulser Xcell™ Electroporation Systems, settings were "square wave protocol #3 Voltage : 1700 V Pulse Length: 0.2 ms # of pulses: 2 interval: 5 sec 4 mm cuvette gap." Transfected parasites were used to inoculate a dish containing confluent HFF cells grown on coverslips..

2.4.3.2 ePTS1-GFP transfection into *Toxoplasma*

For the ePTS1-GFP transfection, after the amplicon was purified, the PCR product was cloned into pTUB8-myc-GFP to form pTUB8-GFP-ePTS1. The *Toxoplasma* RH strain were transfected with pTUB8-GFP-ePTS1 and used to infect HFF cells cultured on glass coverslips as described above.

2.4.4 Immunofluorescence assay for *Toxoplasma gondii* transfection

For the immunofluorescence assay (IFA), HFF cells grown on coverslips were inoculated with TUB8mycGFPmyoATy-HX-*TgSCP2* transfected *T. gondii* and Enhanced PTS1-Tagged GFP transformed *Toxoplasma* parasites [77, 79].

2.4.4.1 TUB8mycGFPmyoATy-HX-*TgSCP2* in *Toxoplasma*

For TUB8mycGFPmyoATy-HX-*TgSCP2* in *Toxoplasma,* cells were fixed with 4% (w/v) paraformaldehyde (Sigma-Aldrich, P6148) in phosphate buffered saline (PBS)

(Sigma-Aldrich, P5493) for 20 min at room temperature at 24 hrs and 48 hrs. Fixed cells were permeabilized and blocked using 0.2% Triton-X100 (Sigma-Aldrich X100), 2% bovine serum albumein (BSA) (Sigma-Aldrich, 05470) in PBS and stained. DAPI (ThermoFisher Scientific) and primary antibodies (anti-IMC1 and anti-GFP; Roche) diluted 1:1000, were used in study. Cells were incubated for 1 hour at room temperature then washed three times, and incubated with Alexa488 goat anti-mouse and Alexa594 goat anti-rabbit (ThermoFisher Scientific) for 45 min at room temperature, in a mixture of PBS with 0.02% Triton-X-100 and 2% BSA.

2.4.4.2 Enhanced PTS1-Tagged GFP in *Toxoplasma*

Similarly enhanced PTS1-Tagged GFP in *Toxoplasma*, after 24 h, cells were also fixed with 4% paraformaldehyde at room temperature for 20 minutes and washed in PBS, before permeabilization and blocking in PBS 0.02% Triton-X-100/2% BSA for a further 20 min. Cells were then incubated for 1 hour at room temperature with the primary antibodies anti-IMC1 and anti-GFP diluted 1:1000, washed three times, and incubated with Alexa488 goat anti-mouse and Alexa594 goat anti-rabbit for 45 min, also at room temperature and in PBS 0.02%, Triton-X-100 and 2% BSA [80].

2.4.5 Microscopy for transfected *Toxoplasma gondii* parasites.

Super-resolution microscopy was used to visualise antibody stained parasites. Using an ELYRA S.1 microscope (Zeiss) equipped with a plan apochromat 63×, 1.4 NA oil immersion lens. Coverslips with transfected parasites were used for imaging and photographs recorded with a CoolSNAP HQ camera (Photometrics) and processed using ZEN Black software (Zeiss) and analysed using Fiji [81].

2.5 *Tg*Pex5 yeast complementation

Various yeast complementation strategies that allowed quantitative and qualitative analysis are described below and were used in determining the functionality of *Tg*Pex5 and *Tg*Pex7.

2.5.1 Cloning of *Tg*Pex5 into yeast plasmid vector pIRES2-EGFP-SKL

For cloning, complete cDNA of *Tg*Pex5 into plasmid vector, we used the entire sequence of *Tg*Pex5 (TGGT1_231870 Length: 2679 bp). Using the Infusion cloning kit and following manufactuers guidelines (Clontech® Laboratories, Inc. In-Fusion® HD Cloning Kit User Manual), *Tg*Pex5 was amplified from genomic DNA by primer pairs as shown in Table 2.4. An amplified fragments of approximately 2.7 Kbp for *Tg*Pex5 was cloned into the yeast plasmid vector pIRES2-EGFP-SKL using infusion cloning. pIRES2-EGFP-SKL-*Tg*Pex5 plasmids introduced transformed into Stellar^{TM} competent cells . Transformed colonies were selected and used to inoculate liquid LB supplemented with appropriate antibiotic and used to make glycerol stocks.

2.5.2 Culture and maintenance of yeast strains

The *Saccharomyces cerevisiae* strains used were UTL-7 (wild-type), and UTL-7ΔPex5 all grown at 30°C in YPD medium or YPD plates containing 2% glucose (Sigma-Aldrich, G7021), 2% peptone (Sigma-Aldrich, 19942) and 1% yeast extract (Sigma-Aldrich, 70161) as previously described [82].

2.5.3 Transfection of pIRES2-EGFP-SKL-*Tg*Pex5 into WT and mutant yeast

The transfection of pIRES2-EGFP-SKL-*Tg*Pex5 into UTL-7, and UTL-7ΔPex5 (null mutant) involved several stages as described [83]. First, *Tg*Pex5-pIRES2-EGFP-SKL DNA was isolated using a QIAprep Spin Mini-prep kit. For transfection all strains were grown as described in subsection 2.5.2 and harvested in 1.5 mL microcentrifuge tubes. 1-10 µg plasmid DNA was then added to Herring/salmon sperm DNA (already denatured at 95℃ for 5 minutes) and LiT/PEG mix (2.2.2) and placed on a shaker for 15 minutes at room temperature. Samples were incubated for 12 minutes at 42℃ and centrifuged at 14 000 rpm for 5-10 seconds, supernatant removed and cells resuspended in 50 µl of sterile water before plating onto -URA plates to be used in spot test, immunoflorecence assay and oleate yeast growth assays.

2.5.4 Spot test for transfected *Tg*Pex5

Transfected colonies were picked from -URA plates (section 2.5.3) and were used to inoculate 10 mL of 0.3% glucose medium and grown overnight. 1 mL of culture was then spun, supernatant removed, and the pellet re-suspended in 1 mL sterile water. The pellet was washed 3 times with sterile water before OD_{600}nm measurement. Optical density measurements involved 100 µl cells + 900 µL sterile water. Once an OD_{600}nm between 0.2 - 0.5 was achieved, serial dilutions of transfected yeast and control yeast cultures were made using a 1:10 dilution. 1.0 µl of each of the serial dilutions was pipetted onto glucose-URA and olate-URA plates. Controls on the plates were also added and included serial dilutions of 1.0 µl of UTL-7ΔPex5 and the empty plasmid vector. Plates were incubated at 30°C for 3 to 4 days before image capture by DSLR (Digital Single Lens Reflex) as described [84].

2.5.5 Oleate liquid culture growth assay of transfected *Tg*Pex5

The culture from subsection 2.5.4 was used to inoculate 10 mL of 0.3% glucose medium and grown overnight. 1 mL of culture was then centrifuged, and the pellet re-suspended in 1 mL sterile water. The 100 µL pellet was washed 3 times with sterile water to remove glucose before being resuspended in 900 µL of sterile water. Once an OD_{600} nm of less than 0.1 was achieved, the 1 ml volume was used to inoculate 10 ml of oleate media and incubated at 30℃ for 24 hours.

2.5.6 Yeast immunoflorecence assay of transfected UTL-7, and UTL-7ΔPex5

For the immunofluorescence assay (IFA), cells from the remaining serial dilutions (2.5.4) were fixed with 4% w/v paraformaldehyde (Sigma-Aldrich, P6148) in phosphate buffered saline (PBS) for 20 min at room temperature. Cells were then permeabilized and blocked using 0.2% Triton-X100 , 2% bovine serum albumen in PBS. Cells were DAPI stained and visualised using a wide-field fluorescence microscope (Zeiss Axiovision (version 4.6.3) microscope and 1300Y digital camera (Roper Scientific RTE) . The GFP signal was visualized using a 450-490 nm band pass excitation filter, a 510 nm dichromatic mirror and a 515-565 nm band pass emission filter.

2.6 *Tg*Pex5 complementation of human fibroblasts

The experiments described below used in determining the functionality of *Tg*Pex5 in human fibroblasts.

2.6.1 Cloning of *Tg*Pex5 into human plasmid vector pRS416-WT

The cloning of complete cDNA of *Tg*Pex5 into pRS416-WT using the entire sequence of *Tg*Pex5 (TGGT1_231870 Length: 2679 bp) we used InFusion^{TM}. Both *Tg*Pex5 was amplified from genomic DNA by primers pairs as shown in Table 2.4. Amplified fragments of ~ 2.7 Kbp for *Tg*Pex5 was cloned into human plasmid pRS416-WT. Following manufacturers guidelines pRS416-WT-*Tg*Pex5 was transformed into Stellar^{TM} Competent Cells . Transformant colonies were selected and used to inoculate liquid LB supplemented with appropriate antibiotic and when required, a plasmid mini-prep prepared as stated previously.

2.6.2 Maintenance and culture of wild-type and mutant fibroblasts

GM5756 (wild-type) and, ΔPex5 GM5756 (mutant), were cultured and maintained at 37 ℃, in a 5% CO_2 incubator. Cryo-preserved WT-human and mutant fibroblasts containing DMSO, were thawed at 37 ℃ and added to DMEM supplemented with 10% FBS 4 mM L-Glutamine, 1% penicillin/streptomycin (Sigma-Aldrich, P4333) and incubated overnight. The following day cells are washed once to remove DMSO and reached 70% confluency between 3 to 4 days. Trypsin (Sigma-Aldrich, T1426) was used to detach cells which were then seeded into other flasks, until they reached 70% confluency over a 2-3 day period. Thereafter, a 1:3 split was carried out every week to continue fibroblast culture. These were then used in transformations.

Table 2.4: Oligonucleotides for Infusion cloning and sequencing

Name	Sequence (5' → 3')	Use
FW primer *Tg*Pex5-pRS416-WT	CAA TAT ATC ATA ACA CGT CGA CTG ATG GCT TTC CGT GCG	Infusion cloning into pRS416-WT
RV primer *Tg*Pex5-pRS416-WT	CTT AGC GGC CGC ACT AGT AGA TCT TTA GAC GTT CTT GAT CAT CCC	Infusion cloning into pRS416-WT
FW primer *Tg*Pex5	TCG ACT GAT GGC TTT CCG TG	Sequencing
RV primer *Tg*Pex5	GCA CTA GTA GAT CTT TAG ACG TTC	Sequencing
FW primer *Tg*Pex5-pIRES2-EGFP-SKL	CTC AAG CTT CGA ATT CTG ATG GCT TTC CGT GCG	Infusion cloning into pIRES2-EGFP-SKL
RV primer *Tg*Pex5-pIRES2-EGFP-SKL	GAG GGA GAG GGG CGG ATC CGG TTA GAC GTT CTT GAT C	Infusion cloning into pIRES2-EGFP-SKL
FW primer *Tg*Pex5	GGG ATT TCC AAG TCT CCA CC	Sequencing
RV primer *Tg*Pex5	TTG CAT TCC TTT GGC GAG AG	Sequencing
FW primer SCP2 TUB8	CTA TAC AAA GCT GCA GAA ATG CCC GTG CGA TTC GAC	Infusion cloning into TUB8 mycGFPmyoATy-HX
RV primer SCP2 TUB8	GC ACA ACG GTG ATT AAT TAA CTA TAG TCG ACT GGT TTT GGG	Infusion cloning into TUB8 mycGFPmyoATy-HX
FW primer SCP2	GCG CAG AAG ACA TCC ACC AAA C	Sequencing
RV primer SCP2	TTT GGT GGA TGT CTT CTG CG	Sequencing

2.6.3 Transfection of *Tg*Pex5-pRS416-WT into fibroblasts

Plasmid DNA *Tg*Pex5-pRS416-WT and control plasmids were used in the transfection of wild-type and null mutant fibroblasts. WT-GM5756, and ΔPex5 GM5756, and fibroblasts were grown to 70% confluency, and 1.5 x 10^4cells dispensed onto coverslips. After 24 hrs, fibroblasts at 70% confluency were transfected following the X-tremeGENE 9 DNA transfection Reagent protocol (Roche) and incubated for 72 hrs ·

2.6.4 Transfected GM5756 and ΔPex5GM5756 immunofluorecence assay

For the immunofluorescence assay (IFA), cells were washed 3 times with PBS and fixed with formaldehyde (Sigma-Aldrich, F8775) for 20 min at room temperature. Fixed cells were permeabilized and blocked using 0.2% Triton-X100, 2% BSA (Sigma-Aldrich, 05470) in PBS and stained accordingly as before with, DAPI, antibodies and anti-GFP. For imaging wide-field fluorescence microscopy was used, (Zeiss Axiovision (version 4.6.3)) and a 1300Y digital camera (Roper Scientific RTE) and the GFP. GFP signal was visualized as before.

2.7 Screen of natural compounds against *Leishmania mexicana*

The *in vitro* screen of test compounds from Hypha Drug Discovery Ltd, against *L. mexicana* M379 amastigotes used three assays: an axenic assay, cytotoxicity involving a RAW 264.7 human macrophages and *L. mexicana* M379 amastigotes and RAW 264.7 macrophage infection assay.

2.7.1 HDLSX library generation and format

This was carried out by Hypha Discovery

HDLSX library generation and format Scale-up fermentations of fungi selected for inclusion in the HDLSX library were obtained in multiple shake flasks (each 250 mL Erlenmeyer flask containing 100 mL Leatham's medium, contents per litre of water: D-Glucose (25.00 g), L(+)-glutamic acid monosodium salt monohydrate (3.20 g), KH_2PO_4 (2.00 g), $MgSO_4.7H_2O$ (2.00 g), mineral solution (10 mL), trace element solution (1.0 mL), vitamin solution (1.0 mL) and 1% aqueous salicylic acid (0.10 mL)) to a total volume of 1-5 L. The fermentations were harvested after the same period of time that yielded the original activity of interest and this could vary from as little as 3 to as many as 100 hundred days. Aqueous broth actives were harvested by various methods depending on the polarities of the components of interest including extraction with ethyl acetate or capture using Diaion HP20 resin and elution with methanol/acetonitrile. Biomass actives were extracted using methanol-acetone (1:1). The extracts were concentrated to dryness for storage. The extracts were weighed and portions stored in 96-well blocks as 10 mg/mL solutions in DMSO.

2.7.2 Assay-guided Purification

This was carried out by Hypha Discovery

Preliminary small-scale activity-guided purification studies on hits from 12 organisms that showed promising antiparasitic activity profiles (EC_{50}< 1mg/mL; therapeutic index >100) were conducted using semi-preparative HPLC approaches as follows: extract aliquots (0.9 mL) were chromatographed by reversed phase HPLC on an Xbridge Prep Phenyl 5 μm OBD column (19 mm x 100 mm) with a guard column (19 mm x 10 mm), using gradient elution of 10-100% acetonitrile in water in the presence of 0.1% formic acid over 8 min, held at 100% acetonitrile for 3 min before

returning to starting conditions over 1 min at a flow rate of 17 mL/min. 24 fractions were collected for each fractionation and concentrated to dryness in a Genevac HT12 centrifugal evaporator. The resulting dried fractions were re-dissolved in DMSO-MeOH (3:1, 0.45 mL) and aliquots (25 µL) transferred to 96 well microtitre plates, lyophilised for shipping. Analysis of active fractions by HPLC-mass spectrometry employing an orthogonal reversed phase HPLC-MS method was conducted on a SymmetryShield RP8 column (3.5 µm; 4.6 mm x 75 mm) eluted with a linear gradient of 10-95% MeCN in water, containing 10 mM ammonium formate + 0.1% formic acid, at a flow rate of 1 mL/min, held at 95% MeCN for 1.0 min before returning to initial conditions over 0.5min; total run time 12 min. UV-visible spectra were acquired using a Waters 2996 photodiode array detector and positive and negative ion electrospray mass spectra were acquired using a Waters Acquity SQ detector. Putative molecular weights, UV-Visible maxima and producing organism taxonomic data were used to search two natural products databases to identify known compounds, namely Antibase and the Chapman and Hall Dictionary of Natural Products. Specific chromatographic methods were then developed for the most promising active primary fractions to separate and resolve their constituent components/HPLC peaks using a reversed phase column chemistry orthogonal to that used for the primary fractionation step (usually SymmetryShield RP8). The primary fraction was then fractionated on the semi-preparative scale and individual HPLC peaks collected into secondary fractions that were concentrated to dryness, re-dissolved and shipped for assay as described above.

2.7.3 Scale-up Purification and Structure Elucidation

This was carried out by Hypha Discovery

The target compounds were purified by preparative HPLC methods scaled-up from the purification methods developed from the small-scale assay guided purifi-

cation investigations. HD871-1 was purified from the Diaion HP20 extract of a 5 L fermentation of *Marasmius sp.* HFN871. The extract was first chromatographed by preparative HPLC on a Waters Nova-Pak C18 column (40 x 100 mm with a 40 x 10 mm guard column) eluted with a gradient increasing linearly from 10-95% acetonitrile in water containing 0.1% formic acid over a period of eight minutes at a flow rate of 50 mL/minute. HPLC was used to check for the presence of the target metabolite with MH+ at m/z 263 and this was present in fractions eluting between 4.5 and 5.5 minutes. These were combined and further purified by semi-preparative HPLC on a Waters Atlantis T3 ODS column (10 x 250 mm) eluted isocratically with 45% aqueous acetonitrile containing 0.1% formic acid at a flow rate of 4.6 mL/minute. HPLC-MS analysis showed that the compound of interest was present in fractions eluting from 8-9 minutes. A final purification step was achieved by semi-preparative HPLC on a Waters X-Select C18 column (19 x 100 mm with a 19 x 10 mm guard column) eluted with a linear gradient increasing from 25-30% aqueous acetonitrile containing 0.1% formic acid over a period of fourteen minutes at a flow rate of 20 mL/minute. The peak eluting at 10 minutes was collected and concentrated to dryness to yield pure HD871-1 (6.9 mg) as a colorless residue. 1H and 13C NMR spectra were acquired at 500 MHz and 125 MHz, respectively, at 298K in DMSO-d6, on a Bruker AVANCE III 500 MHz NMR spectrometer at the University of Surrey, Guildford, UK. Datasets for structure elucidation included COSY, HSQC, HMBC and NOESY spectra, which were interpreted at Hypha Discovery using Mestrenova software. High resolution mass spectrometry was conducted on a Bruker micrOTOF-Q instrument.

2.7.4 Maintenance and cell culture of *Leishmania mexicana M379* amastigotes

L. mexicana M379 amastigotes parasites were maintained, in Schneider's Insect medium (Sigma-Aldrich, S0146) supplemented with 15% FBS and 1% penicillin/streptomycin pH 7 (SIM_{15}) and incubated at 26 ℃. After 3 days procyclic promastigotes were centrifuged at 2000 rpm for 10 mins and re-suspended in Schneider's Insect medium supplemented with 20% FBS and 1% penicillin/streptomycin at pH 5.5 (SIM_{20}) to a concentration of 5 x 10^5 parasites/mL. After 6 days incubation at 26℃ the metacyclic forms were then inoculated into fresh SIM_{20} at 5 x 10^7 parasites/mL and incubated at 32℃ for a further 5 to 7 minutes for transformation into amastigotes to be used in axenic assays (subsection 2.7.6) and infection assays (subsection 2.7.8) [85, 86].

2.7.5 Maintenance and culture of *RAW 264.7* murine macrophages

Murine macrophages *(Mus musculus* leukaemia virus transformed macrophage (RAW267.4) cells (ATCC TIB-71) are an immortal cell line frequently used because it is robust and gives high differentiation and reproducible proliferation. *RAW 264.7* macrophages were cultured and maintained at 37℃ at 5% CO_2 . Cryo-preserved RAW 264.7 were thawed at 37℃ and added to DMEM supplemented with 10% FBS and 1% penicillin/streptomycin and grown overnight as previously described [85] . DMSO was removed the following day and cells reached 80% confluency between 3 to 4 days. For sub-culture cells were scraped and seeded into other flasks and reach confluency in 2-3 days. A 1:4 split was carried out every week to continue macrophage culture and counted using a Neubauer Improved Haemocytometer. These were used in cytotoxicity (subsection 2.7.7) and infection assays (subsection 2.7.8) when required.

2.7.6 Axenic *Leishmania mexicana M379* amastigotes screening assay

Axenic amastigotes were cultured as described [85] (subsection 2.7.4) and used in subsequent axenic *L. mexicana M379* EC_{50} and single point amastigote assays .100 µL of 1 x 10^6 amastigotes from an axenic culture were seeded onto 96-well flat bottom plates (Fisher-Scientific 10792552). For EC_{50} assay serial compound dilutions of eight 3-fold dilution steps covering a range from 100 - 0.04 mg/mL were prepared in culture media SIM_{20}. For the single point assays 1 µL (unknown conc) of compound/extract was added to 99 µL of SIM_{20} culture media. 100 µL of each of these compound preparations were then added to the parasites to give a final parasite concentration of 5 x 10^5 per ml and total volume of 200 µL. 10 µM Amphotericin B was used as a positive control and 2% DMSO as negative control all prepared in CM. After a 24 hour incubation 10 µL of alamarBlue (Invitrogen, DAL1025) was added and incubated for a further 4 hours before obtaining a fluorescent readout (λ_{ex} 560 nm, λ_{em} 600 nm) using a plate reader Synergy^{TM} HTX Multi-Mode Microplate Reader (Biotek 560EX nm/600EM nm) [86, 87]. All experiments were carried out a minimum of three times on separate occasions and in triplicate to ensure a robust data set.

For the initial screening of the HDLSX library (313 extracts) a dose response approach was taken, testing was in duplicate against both axenic amastigote *L. mexicana* and mammalian cells. The Selectivity Index (SI) was calculated from these data (EC_{50} mammalian cells / EC_{50} *L. mexicana*). Subsequent fractions were screened at single concentrations in triplicate against the parasite. Determination of the EC_{50} of the identified novel antileishmanials against axenic amastigote *L. mexicana* was carried out using the same assay in triplicate on three separate occasions.

2.7.7 Cytotoxicity screen using *RAW 264.7* macrophages

Cytotoxicity assays were carried out using *RAW 264.7* cultured in culture media (CM_{10})composed of DMEM supplemented with 10% FBS , and 1% penicillin/streptomycin (Sigma-Aldrich, P4333) and incubated at 37℃ at 5% CO_2 until they reached 80% confluency as previously optimised [54]. Once confluency was achieved, macrophages were seeded at 2.5 x 10^5 cells mL^{-1} in culture media (CM) in 96-well flat bottom plates (Fisher-Scientific 10792552) on day 1. On day 2 CM_2 made up of DMEM (Sigma-Aldrich, D5671) supplemented with 2% FBS (Gibco, 10270), and 1% penicillin/streptomycin (Sigma-Aldrich, P4333) was used to wash macrophages, followed by the addition of 200 µL/mL of CM_2 to each well and incubated for 24 hours. On day 3, all macrophages were washed 5 times with CM_2, before addition of 100 µL of test compounds/extract (10 mM DMSO stock solutions, serial compound dilutions of eight 3-fold dilution steps covering a range from 100 - 0.04 mg/mL) and control solutions (1 µM Cyclohexamide used as a positive control and 2% DMSO as negative control) all prepared in CM_2, then incubated at 37℃ in 5% CO_2 . After 24 hour incubation on day 4, 10 µL of alamarBlue was added to each well. A 4 hour incubation at 37℃, 5% CO_2 with alamarBlue (Invitrogen, DAL1025) was followed by fluorescent (λ_{ex} 560 nm, λ_{em} 600 nm) using a plate reader to determine cell viability [87]. All experiments were carried out independently a minimum of three times and in triplicate data and the raw data used in statistical analysis explained later.

2.7.8 *Leishmania mexicana* M_{379} amastigotes and *RAW 264.7* macrophage infection assay

For the infection assay as previously described by [54, 86, 87], on day 1, well maintained *RAW 264.7* macrophages (2.7.5) were seeded at 2.5 x 10^5 cells/mL in CM_{10} and added to 96-well flat bottom plates (Fisher-Scientific 10792552) incubated for 24 hours at 37ºC, 5% CO_2 . On day 2, macrophages were washed with

CM_2 followed by the addition of 1 x 10^6cells/mL axenic *L. mexicana* M_{379} amastigotes in CM_2 and incubated overnight for 24 hours at 37^{o}C, 5% CO_2 . On day 3, infected macrophages were inspected under the microscope to ensure infection. Test compounds in CM_2solution from 10 mM DMSO stock solutions were used for serial compound dilutions of eight 3-fold dilution steps covering a range from 100 - 0.04 mg/mL. Control solutions of 1 µM Cyclohexamide and 10 µM Amphotericin B for uninfected *RAW 264.7* macrophages and infected *RAW 264.7* macrophages respectively and 2% DMSO as negative controls were added and plates incubated for 24 hours at 37^{o}C, 5% CO_2 . On day 4, infected *RAW 264.7* macrophages were washed 5 times with Schneider's Insect medium (Sigma-Aldrich, S0146) pH 7 (SIM) and inspected under the microscope to ensure the removal of all extracellular amastigotes. This was then followed by cell lysis using 0.05% *v/v* for 30 seconds to lyse *RAW 264.7* macrophages before the addition rapid addition of neutralising solution SIM_{15}. Plates were then incubated at 26 ^{o}C for 48 hours. On day 6, 10 µL of alamarBlue (Invitrogen, DAL1025) was added to each well followed by a 4 hour incubation at 26 ^{o}C and fluorescent readout (λ_{ex} 560 nm, λ_{em} 600 nm) using plate reader (Biotek 560EX nm / 600EM nm). All experiments were carried out on three different occasions and in triplicate to ensure a robust data set then raw data used in statistical analysis to determine EC_{50} values. The Selectivity Index (SI) was calculated from these data (EC50 *RAW 267.4* / EC50 intracellular *L. mexicana*).

2.7.9 Statistical analysis

Data were analysed using a macro programmed Excel spreadsheet (Appendix B) and Graphpad Prism (V 7.0). Sigmoidal curves were plotted to show growth inhibition against compound concentration and produce EC_{50} values, Z' values and standard deviation were all produced from the dose-response plots.

2.8 Effect of HD871-1 and HDL871-2 on *Leishmania mexicana* amastigotes metabolome

Experiments described in this section involved the two hit compounds identified after the entire screen of 313 natural compounds from Hypha. These two compounds were used for the metabolomics study.

2.8.1 Half time to cell death assay

The aim of the half time to death assay was to determine the correct concentrations to be used in the experiment examining the effect of HD871-1 and HD871-2 on *L. mexicana* M_{379} amastigotes metabolome. For this 10 mM stocks of both HD871-1 and HD871-2 were diluted in SIM_{20} and plated out in triplicate onto sterile 24 well plates (Nunc) to final concentrations of 10, 5, 2.5, and 1.25 µM. 1 x 10^7 parasites/mL final concentration were then added to theses serial dilutions to give a final volume of 1 mL/well. Plates were then incubated at 32^{o}C and the number of parasites examined at four time points 12, 24, 36 and 48 hours by microscopic observation

2.8.2 Cell extraction for *Leishmania mexicana* M_{379} amastigotes

The optimum time point for cell extraction of the *L. mexicana* M_{379} amastigotes metabolome as determined by the half time to cell death assay (subsection 2.8.1) for HD871-1 and HD871-2 was at 10 µM for 36 hours. After 36 hours compound exposure amastigotes started to die.

2.8.2.1 Seeding *Leishmania mexicana* M_{379} amastigotes

L. mexicana M_{379} amastigotes were cultured as detailed in subsection 2.7.4 to concentration of 1 x 10^8 parasites/mL and were seeded into T75 tissue culture flasks

(Starsted, 83.3911) at a concentration of 5 x 10^7parasites/mL in SIM_{20}. Compounds HD871-1 and HD871-2 and negative control DMSO were added to flasks. Each sample and control were seeded and inoculated with compound or control in quadruplicate. Flasks were then incubated at 32ºC for 36 hours and amastigotes counted for metabolic extraction.

2.8.2.2 *Leishmania mexicana* M_{379} amastigotes metabolome post-exposure to HD871-1, HD871-2 and DMSO

For the cell extraction of *L. mexicana* M_{379} amastigote metabolome post-exposure to HD871-1, HD871-2 and DMSO, 5 x 10^7parasites/mL of each sample in quadruplicate was harvested by a 15 minute centrifugation at 1430 g and temperature rapidly reduced by placing samples on dry ice, with intermittent vigorous mixing to avoid cell lysis. Samples were then maintained at a temperature of 4℃ for the rest of the protocol. Samples were centrifuged at 1250 g for 10 minutes before supernatants were removed and pellets resuspended in 1 mL of their residual media. These 1 mL of suspensions were then transferred to 1.5 mL centrifuge tubes and further centrifuged at 2260 g for a further 10 minutes. Supernatants were removed and pellets resuspended in PBS for a 10 minute wash at 2260 g. After the PBS wash, extraction media (chloroform (Sigma-Aldrich, 288306):Methanol (Sigma-Aldrich, 322415) : Water) (CMW in a ratio of 1:3:1 v/v/v) was added to the pellets, mixed and left on a shaker at maximum speed for 1 hour. After incubation, samples were centrifuged at 18890 g for 10 minutes and the supernatant removed placed in a vial and sealed with Argon before storing at -80℃ until analysis by mass spectrometry. [86, 88].

2.8.3 Metabolome analysis

All twelve samples were analysed by liquid chromatography-mass spectrometry (by Erin Manson, Glasgow Polyomics Research Centre) and evaluated by IDEOM in an excel template.

Metabolites were extracted and analysed as follows: For LC-MS metabolomic analyses, samples were first separated using HPLC with a 150 x 4.6 mm ZIC-pHILIC (Merck) column on UltiMate 3000 RSLC (Thermo Scientific). Mass detection used an Orbitrap Q-Exactive mass spectrometer (Thermo Fisher) at Glasgow Polyomics, using positive and negative polarity switching mode, with a 10 µL injection volume and flow rate of 300 µL/min. 249 authentic standards were included to assist compound identification. Data were processed and analyzed using mzMatch [89] and IDEOM software [90]. All the MS analyses were performed in at least triplicate. Exact mass is measured and this is converted, where possible to a formula corresponding to that mass. Screening of a database of metabolites with that formula then yields a putative identity. Where an authentic standard has a matching mass and retention time this is taken as a likely hit. Other annotations are tentative (metabolomics standards initiative level 2, [91] with this data.

2.9 *In vitro* screen of natural compounds against *Toxoplasma gondii*

Two approaches were used for compound screening and involved a screen against 5 compounds and some peroxisome specific inhibitors. The 5 compounds were screened against both Type I and II *T. gondii* while the Pex inhibitors were screened against Type I *T. gondii.*

2.9.1 *In vitro* screen of natural compounds against *Toxoplasma* Type I

As described in subsection 2.4.2.1 cultured HFF cells and extracellular RH-HX-KO-YFP2 tachyzoites were used in a *Toxoplasma* susceptibility assay. 1 x 10^4 cells per well were seeded onto 96 well microtitre plates (Nunc). HFF cells after an 18 hour incubation at 37℃, 5% CO_2 , had the addition of isolated RH-HX-KO-YFP2 tachyzoites at 6250 parasites per well and incubated at under the same conditions for a further 20 hours. Following incubation test compounds with eight serial dilutions of 2-fold dilution steps covering a range from 0.04 -10 μg/mL were added.

2.9.2 Optimised *in vitro* screen of natural compounds against *Toxoplasma* Type II

Experiments were previously described [78, 92] in subsection 2.4.2.2 with cultured HFF cells and extracellular *Pru*-GRA2-GFP-DHFR tachyzoites used in a *Toxoplasma* bradyzoite susceptibility assay. 1 x 10^4 cells per well were seeded onto 96 well microtitre plates (Nunc). After an 18 hour incubation at 37℃, 5% CO_2 ,HFF cells had the addition of isolated *Pru*-GRA2-GFP-DHFR tachyzoites at 6250 parasites per well and incubated at 37℃, 5% CO_2 for a further 48 hours to allow encysted bradyzoites to develop. Tachyzoites differentiated to the bradyzoite-like form in HFF cells via an alkaline shift to pH8. Following incubation, test compounds with eight serial dilutions of 2-fold dilution steps covering a range from 10 - 0.04 μg/mL were added.

2.9.3 *In vitro* screen of Pex5 and Pex14 inhibitors against *Toxoplasma* Type II

HFF cells were seeded at 104 cells per well in a 96 well plate and maintained in fluorobrite medium. After 18 hours at 37°C, isolated *T. gondii* tachyzoites were inoculated into the host cells at 6250 parasites per well, compounds were added after a further 20 h incubation period, with concentrations starting at 50 μM and terminating at 0.21 μM via a 3-fold serial dilution. Pyrimethamine at 40 μM acted as the positive control and DMSO 2.5μM the negative control. Plates were analysed every 24 hrs post addition of the compounds from 48 to 144 hours, with an excitation and emission wavelength of 510 nm and 540 nm, respectively. Data was analysed using GraphPad Prism.

2.9.4 Analysis for both *Toxoplasma* Type I and Type II

All plates for natural compounds were then read after 3 or 6 days using a Biotek Synergy H4 plate reader (Excitation 510 nm; Emission 540 nm). While, the plates for the Pex inhibitors were read every 24 hours post addition of compounds from 48 to 144 hours, with an excitation and emission wavelength of 510 nm and 540 nm respectively. All graphs plotted in Graphpad Prism V7 to generate IC_{50} , CI and R squared values.

Chapter 3

Results: Exploring natural products as potential anti-leishmanials

This chapter examined the results of a number of anti-leishmania assays used in the screening of a MycoDiverse^{TM} HDLSX 313 Fungal Extracts library of natural compounds provided by Hypha DiscoveryLtd. The library consists of approximately 10 000 refined fractions from fermentations of higher fungi which were made using Hypha's proprietary technology producing undescribed compounds with very high structural novelty and low molecular weight (MW <500). In order to assess the potential use of natural products against cutaneous leishmaniasis (CL), the library of natural compounds was screened against the mammalian stage of *Leishmania mexicana.* This followed a fractionation and scale up of selected hit compounds and dereplication. From this a novel compound which demonstrated activity in an infected cell model was discovered.

The research contained in Chapters 3 nd 4 has been published in the International Journal of Parasitology

Mbekeani, A.J., Jones R.S., Llorens, M.B., Elliot, J., Barrett, M.P., Steele, J., Kebede, B., Wrigley, S.K., Evans, L., and Denny, P.W. Mining for natural product antileishmanials in a fungal extract library.

3.1 Previous work

Amphotericin B, is a well known natural product used in the treatment of leishmaniasis, and has paved the way for the research and discovery of new natural products for the treatment of this disease. Hypha Discovery (http://www.hyphadiscovery.co.uk) have exploited the wide availability of higher fungal strains by creating a large-scale extract (HDLSX) library of 1-5 litre volume fermentation extracts from these fungi. These mushroom-producing basidiomycetes and ascomycetes, have been under- explored in the field of antiprotozoal drug discovery, including work for anti-leishmanials. This unique resource has previously been screened against each other microbial pathogens and human tumour cell lines, showing biological activity against [93,94]. A total of 313 compounds were screened and followed by a primary, secondary and tertiary screens carried out by myself and other members within our lab.

3.2 Primary Screen

A primary screen was carried out on 313 fungal extracts from the HDLSX library against the mammalian stage of *Leishmania mexicana* axenic amastigotes using a protocol for antileishmanial testing from Chadbourne *et al.* [95]. Extracts with an Effective Concentration eliciting 50% inhibition of proliferation) (EC_{50}) < 0.025 mg/mL were selected. From the 313 extracts, 38 passed the criteria with a selectivity index (SI) >48 and after the cytotoxicity screening against mammalian cells and for other intellectual property reasons, there were a final 17 compounds. Replicated compounds from the Hypha database were removed to leave 12 hits (HDLEX-9, 18, 79, 14, 21, 22, 159, 171, 33, 35, 67, 127) from the primary screen as shown in Table 3.1.

Compound number	Amastigote EC50 mg/ml	Vero EC_{50} mg/mL	Selectivity index (SI)	SI >48	Selection
HDLSX-171	3.37E-16	>1.33E+00	>3.95E+15	Y	Y
HDLSX-106	2.45E-02	1.07E-02	4.38E-01	N	N
HDLSX-67	1.31E-04	6.35E-03	4.84E+01	Y	Y
HDLSX-33	5.22E-04	>1.33E+00	>2.55E+03	Y	Y
HDLSX-134	6.66E-04	3.28E-04	4.92E-01	N	N
HDLSX-14	6.84E-04	>1.33E+00	>1.94E+03	Y	Y
HDLSX-159	7.94E-04	3.96E-01	4.99E+02	Y	Y
HDLSX-127	9.26E-04	>1.33E+00	>1.44E+03	Y	Y
HDLSX-21	2.72E-03	1.34E-01	4.92E+01	Y	Y
HDLSX-208	2.77E-03	>1.33E+00	>4.80E+02	Y	N
HDLSX-79	3.26E-03	1.83E+00	5.61E+02	Y	Y
HDLSX-27	3.36E-03	9.97E-03	2.97E+00	N	N
HDLSX-177	3.56E-03	>1.33E+00	>3.73E+02	Y	N
HDLSX-84	4.84E-03	1.07E-01	2.21E+01	N	N
HDLSX-23	5.09E-03	2.29E-01	4.50E+01	N	N
HDLSX-179	5.94E-03	1.37E-01	2.31E+01	N	N
HDLSX-130	6.75E-03	>1.33E+00	>1.97E+02	Y	N
HDLSX-209	6.86E-03	4.40E-02	6.41E+00	N	N
HDLSX-18	7.15E-03	>1.33E+00	>1.86E+02	Y	Y
HDLSX-22	7.42E-03	>1.33E+00	>1.79E+02	Y	Y
HDLSX-39	7.55E-03	6.92E-02	9.17E+00	N	N
HDLSX-213	9.05E-03	>1.33E+00	>1.47E+02	Y	N
HDLSX-13	9.24E-03	>1.33E+00	>1.44E+02	Y	N
HDLSX-72	9.53E-03	1.69E-01	1.77E+01	N	N
HDLSX-126	1.02E-02	>1.33E+00	>1.30E+02	Y	N
HDLSX-114	1.03E-02	5.92E-03	5.73E-01	N	N
HDLSX-37	1.18E-02	9.93E-02	8.42E+00	N	N
HDLSX-180	1.47E-02	>1.33E+00	>9.06E+01	Y	N
HDLSX-9	1.47E-02	>1.33E+00	>9.03E+01	Y	Y
HDLSX-8	1.48E-02	7.26E-02	4.92E+00	N	N
HDLSX-40	1.61E-02	9.71E-02	6.05E+00	N	N
HDLSX-44	1.74E-02	>1.33E+00	>7.63E+01	Y	N
HDLSX-28	1.78E-02	1.32E-01	7.45E+00	N	N
HDLSX-85	1.89E-02	>1.33E+00	>7.04E+01	Y	N
HDLSX-211	1.90E-02	>1.33E+00	>7.00E+01	Y	N
HDLSX-145	2.06E-02	7.91E-01	3.85E+01	N	N

Table 3.1: The 38 potent hits (EC_{50} < 0.025 mg/ml against axenic amastigote *L. mexicana*) were counter screened against mammalian vero cells. Those with a selectivity index (SI) >48 were initially selected. Final selection (12 hits, Y= Yes, N = No) was made after subtracting those with known cytotoxicity and intellectual property issues, and de-replication.

3.3 Primary Fractionation and Secondary Screening

The 12 hit compounds then underwent fractionation, yielding 24 fractions per sample. 10 of theses compounds had components demonstrating activity against axenic amastigotes at 1 mg/ml (HDLEX-9, 18, 79, 21, 22, 159, 171, 35, 67, 127; Figure 3.1). Initial mass spectrometry analysis (Figure 3.2) indicated the complexity and, in some cases, content of the active fractions. For example, striatals (including striatal B (Sub-figure 3.2) were present in HDLEX-21 (from 2007.20 HFN65 *Cyathus cf. crassimurus*). This group of compounds has previously been shown to have antileishmanial activity [96]. A pure sample of the related compound striatal B (XR562) was tested and found to have an EC_{50} of < 0.8 µM, but was toxic to mammalian cells. Other compounds identified at this stage and deprioritised were a glycolipid from HDLSX-18 (HFN67, *Dacryopinax* sp.), which had low potency with an $EC_{50} > 100$ µM and the known metabolite nitidon from HDLSX-67 (HFN528 *Junghuhnia nitida*), which is cytotoxic against other cell lines [97].

3.4 Secondary Fractionation

Secondary fractionation was carried out on the 8 remaining active compounds (HDLEX-9, 21, 22, 159, 171, 35, 127) of the primary screen as they demonstrated chemical novelty (Figure 3.3). Fractions were screened against axenic amastigotes at 1 mg/mL. HDLSX-9, 22, and 127 derived fractions had components demonstrating activity against axenic amastigotes, although further fractionation of the 5 other primary fractions (including from HDLSX-21 not containing striatal B) did not yield samples with high level activity. Initial analyses by mass spectrometry indicated the complexity and, in some cases, content of the active fractions. Informed by these analyses, secondary fractions were screened against axenic amastigotes if pure (HDLSX9Fr9+10F7 and HDLSX127Fr11Fr9; Figure 3.3 A and G) or further

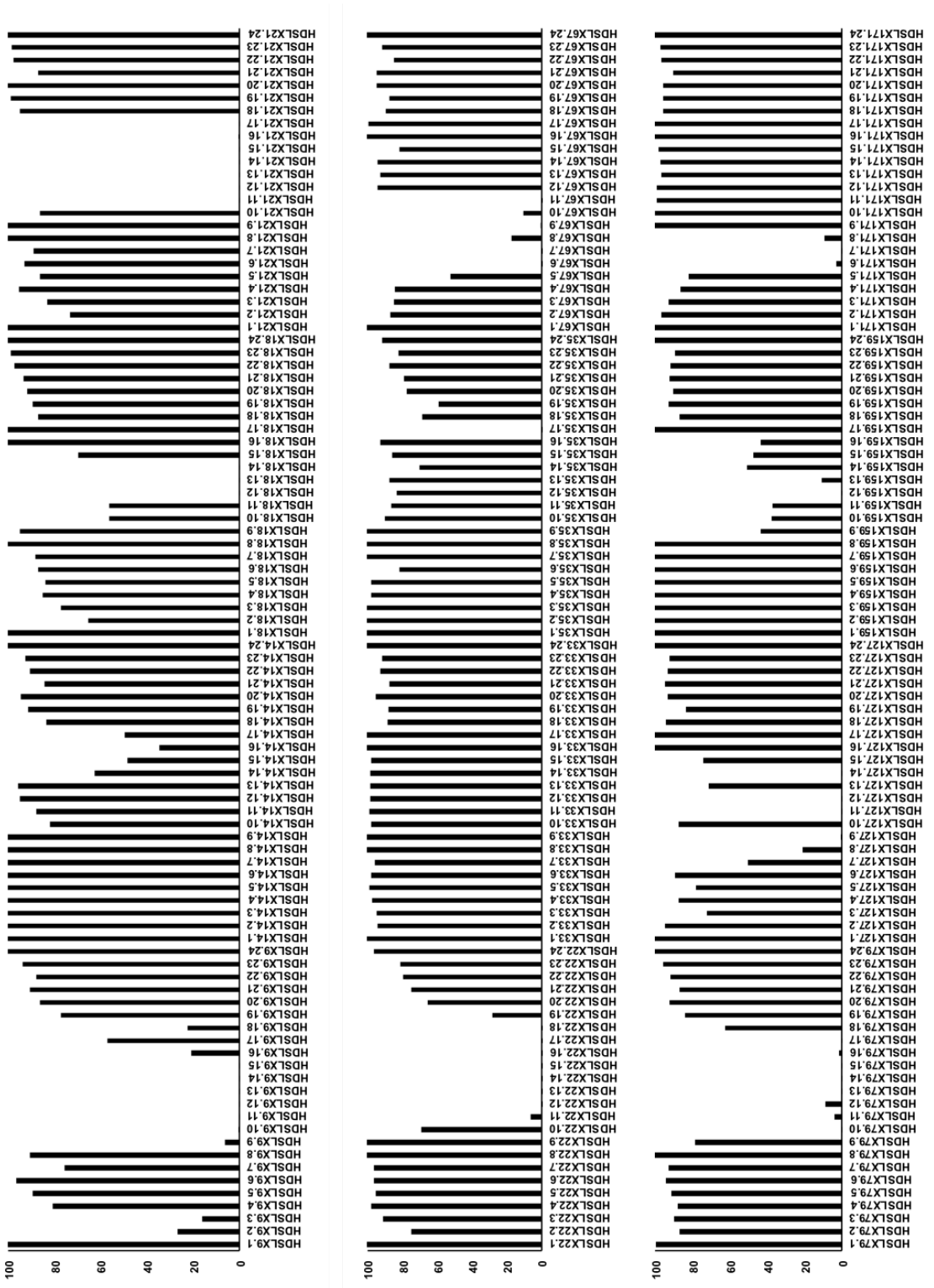

Figure 3.1: List of extracts that were part of the primary fractionation process. 10 fractions from this procedure were chosen for secondary fractionation and screening. Y-axis shows proliferation (%) relative to vehicle (DMSO) treated control and x-axis shows the ID of the primary fractions

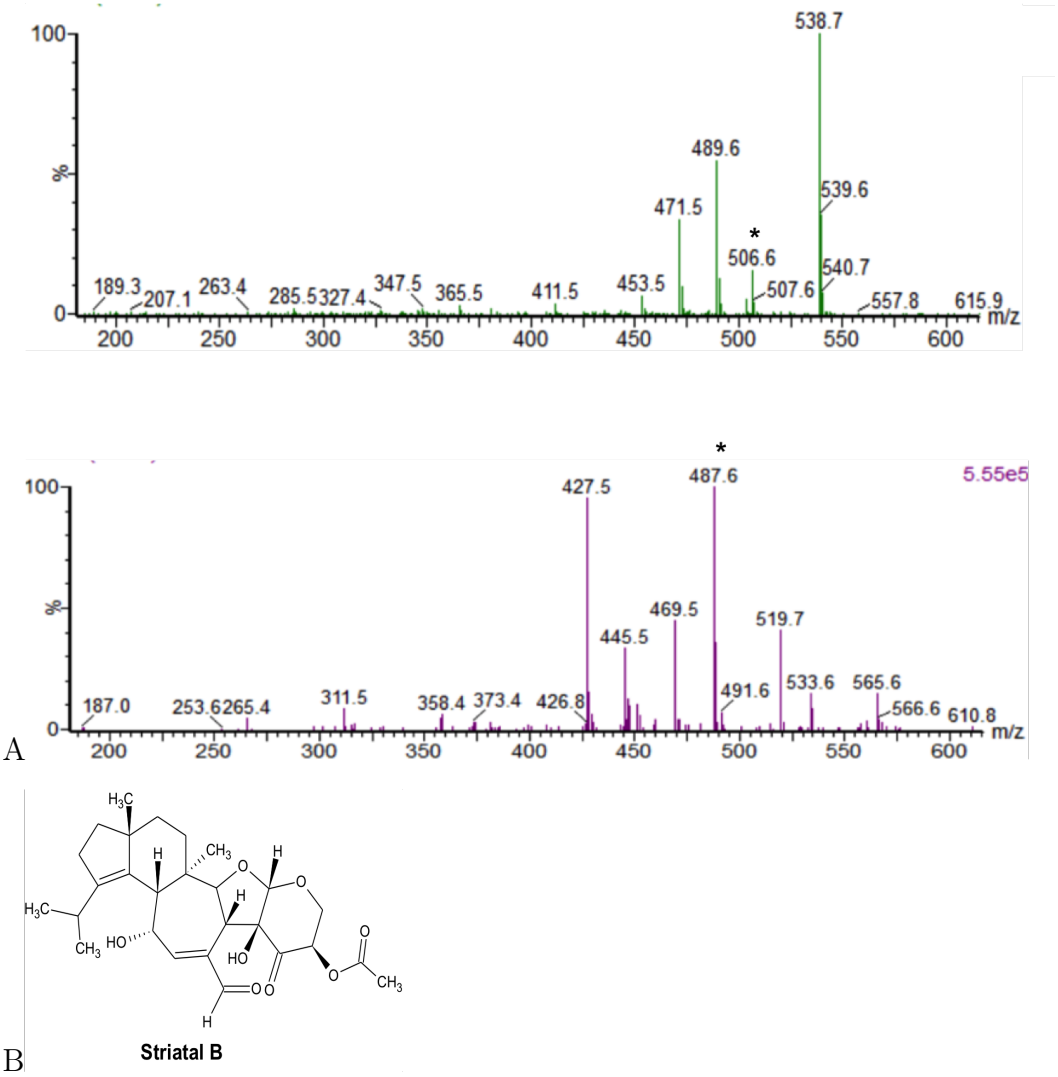

Figure 3.2: Spectrum of compounds. A peak (6.5 min) in fraction 14 of HDLSX-21 had a product MH+ m/z 489.6, MNH4+ m/z 506.6 in the positive ion spectrum green peaks) and [M-H]- m/z 487.6 in the negative ion spectrum (purple peak). This corresponds to known antimicrobial striatal B.

fractionated (from HDLSX-22; Figure 3.3 D) before screening. The pure HDLSX-9 (HDLSX9Fr9+10F7) secondary fraction had minimal activity against the *L. mexicana* amastigotes with an $EC_{50} > 100$ μM.

3.5 Tertiary Screening

For the tertiary screen, fractions (11-24 fractions) and other extracts provided by Hypha shown in Table 3.2 were then screened at 1 mg/mL in a M_{379} *L. mexicana* in a high throughput AlamarBlue® single point assay.

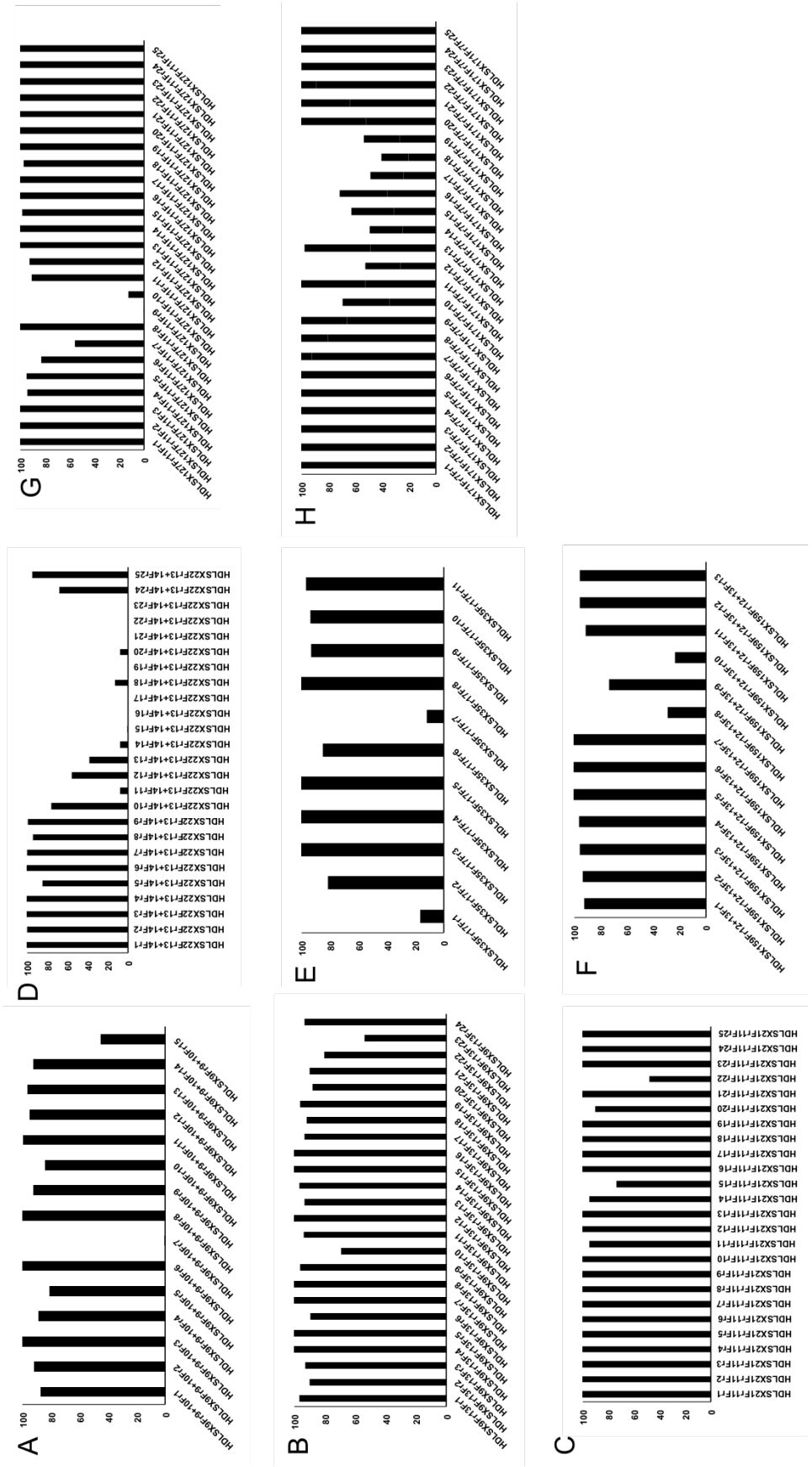

Figure 3.3: Screening of secondary fractions of the 8 active primary fractions against against axenic amastigote *L. mexicana* at 1 mg/ml. The x-axis shows the secondary fractions from A, HDLSX9 fractions 9 and 10; B HDLSX9 fraction 13; C HDLSX21 fraction 1; D HDLSX22 fractions 13 and 14; E HDLSX35 fraction 17; F, HDLSX159 fractions 12 and 13; G HDLSX127 fraction 11; H, HDLSX171 fraction 7. The y-axis shows proliferation (%) relative to vehicle (DMSO) treated control.

Name	Active/Not Active	Name	Active/Not Active
HDSLX-35 (Fr 14) Fr 1-10	Not active	HDSLX-35 (Fr 15) Fr 1-3	Not active
HDSLX-35 (Fr 14) Fr 11	Not active	HDSLX-35 (Fr 15) Fr 4	Not active
HDSLX-35 (Fr 14) Fr 12-19	Not active	HDSLX-35 (Fr 15) Fr 5-7	Not active
HDSLX-35 (Fr 14) Fr 20-21	Not active	HDSLX-35 (Fr 15) Fr 8	Not active
HDSLX-35 (Fr 14) Fr 22	Not active	HDSLX-35 (Fr 15) Fr 9-11	Not active
HDSLX-35 (Fr 14) Fr 23-24	Not active	HDSLX-35 (Fr 15) Fr 12	Not active
HDSLX-35 (Fr 14) Fr 25	Not active	HDSLX-35 (Fr 15) Fr 13-16	Not active
HDSLX-35 (Fr 14) Fr 26	Not active	HDSLX-35 (Fr 15) Fr 17	Not active
HDSLX-35 (Fr 14) Fr 27-28	Not active	HDSLX-35 (Fr 15) Fr 18-19	Not active
HDSLX-35 (Fr 14) Fr 29	Not active	HDSLX-35 (Fr 15) Fr 20	Not active
HDSLX-35 (Fr 14) Fr 30-31	Not active	HDSLX-35 (Fr 15) Fr 21	Not active
HDSLX-35 (Fr 14) Fr 32-33	Not active	HDSLX-35 (Fr 15) Fr 22	Not active
HDSLX-35 (Fr 14) Fr 34-48	Not active	HDSLX-35 (Fr 15) Fr 23	Not active
HD871-1	Active	HDSLX-35 (Fr 15) Fr 24-48	Not active
HD871-2	Active	2007.117.3 EtOAc EXTRACT	Not active
HDSLX-171 (2007.117.3) Fr 7	Not active	HDSLX-171 (2007.117.3) Fr 21	Not active
HDSLX-171 (2007.117.3) Fr 8	Not active	HDSLX-171 (2007.117.3) Fr 22	Not active
HDSLX-171 (2007.117.3) Fr 9	Not active	HDSLX-171 (2007.117.3) Fr 23	Not active
HDSLX-171 (2007.117.3) Fr 10	Not active	HDSLX-171 (2007.117.3) Fr 24	Not active
HDSLX-171 (2007.117.3) Fr 11	Not active	HDSLX-171 (2007.117.3) Fr 25	Not active
HDSLX-171 (2007.117.3) Fr 12	Not active	HDSLX-171 (2007.117.3) Fr 26	Not active
HDSLX-171 (2007.117.3) Fr 13	Not active	HDSLX-171 (2007.117.3) Fr 27	Not active
HDSLX-171 (2007.117.3) Fr 14	Not active	HDSLX-171 (2007.117.3) Fr 28	Active
HDSLX-171 (2007.117.3) Fr 15	Not active	HDSLX-171 (2007.117.3) Fr 29	Not active
HDSLX-171 (2007.117.3) Fr 16	Not active	HDSLX-171 (2007.117.3) Fr 30	Not active
HDSLX-171 (2007.117.3) Fr 17	Not active	HDSLX-171 (2007.117.3) Fr 31	Not active
HDSLX-171 (2007.117.3) Fr 18	Not active	HDSLX-171 (2007.117.3) Fr 32	Not active
HDSLX-171 (2007.117.3) Fr 19	Not active	HDSLX-171 (2007.117.3) Fr 33	Not active
HDSLX-171 (2007.117.3) Fr 20	Not active	HDSLX-171 (2007.117.3) Fr 34	Not active
2007.117.3 BM EXTRACT	Active	XR562	Active

Table 3.2: Fractions and some other extracts provided by Hypha were screened at 1 mg/mL in M_{379} *L. mexicana.*

From this first tertiary screen, pure HDLSX-127 secondary fraction (HD871-1; HDLSX-127Fr11Fr9 in Figure 3.3) and three other compounds (2007.117.3 BM EXTRACT, XR562 and HD871-2) were used in various assays. Utilising a previously established assay [54, 71], compounds were tested against infected macrophages and for macrophage cytotoxicity, as shown in Figure 3.4 and Table 3.3. For the axenic *L. mexicana* amastigote dose-response assay, Amphotericin B and DMSO controls

gave expected results in each instance. Compounds HD871-1, HD871-2, XR562, and 2007.117.3 BM EXTRACT all gave EC_{50} value of $\leq$10 μM. Likewise for the macrophage assays Cyclohexamide and DMSO controls also gave expected results and these four compounds gave high EC_{50} values of HD871-1 at 23.80 μM, HD871-2 at 16.49 μM, and 2007.117.3 BM EXTRACT at 250 μM showing non-toxic effects against the macrophages, these were then used in the *L. mexicana* intramacrophage assays. XR562 at 0.84 μM showed toxicity towards the macrophages. The three selected compounds having passed the toxicity assay were then used in the *L. mexicana* intramacrophage assay . This *ex vivo* assay is known to mimic *in vivo* amastigotes during clinical forms of cutaneous leishmaniasis, was used [95]. For *L. mexicana* intramacrophage assay, both controls were within expected ranges and four compounds tested gave respectable EC_{50} values (HD871-1 at 4.32 μM, HD871-2 at 5.32 μM, XR562 at 2.14 μM and 2007.117.3 BM EXTRACT at 700 μM). The two compounds demonstrating a promising profile with respect to efficacy HD871-1 at 4.32 μM, HD871-2 at 5.32 μM with a selectivity of 5.51 and 6.23 respectively were then used in metabolic studies.

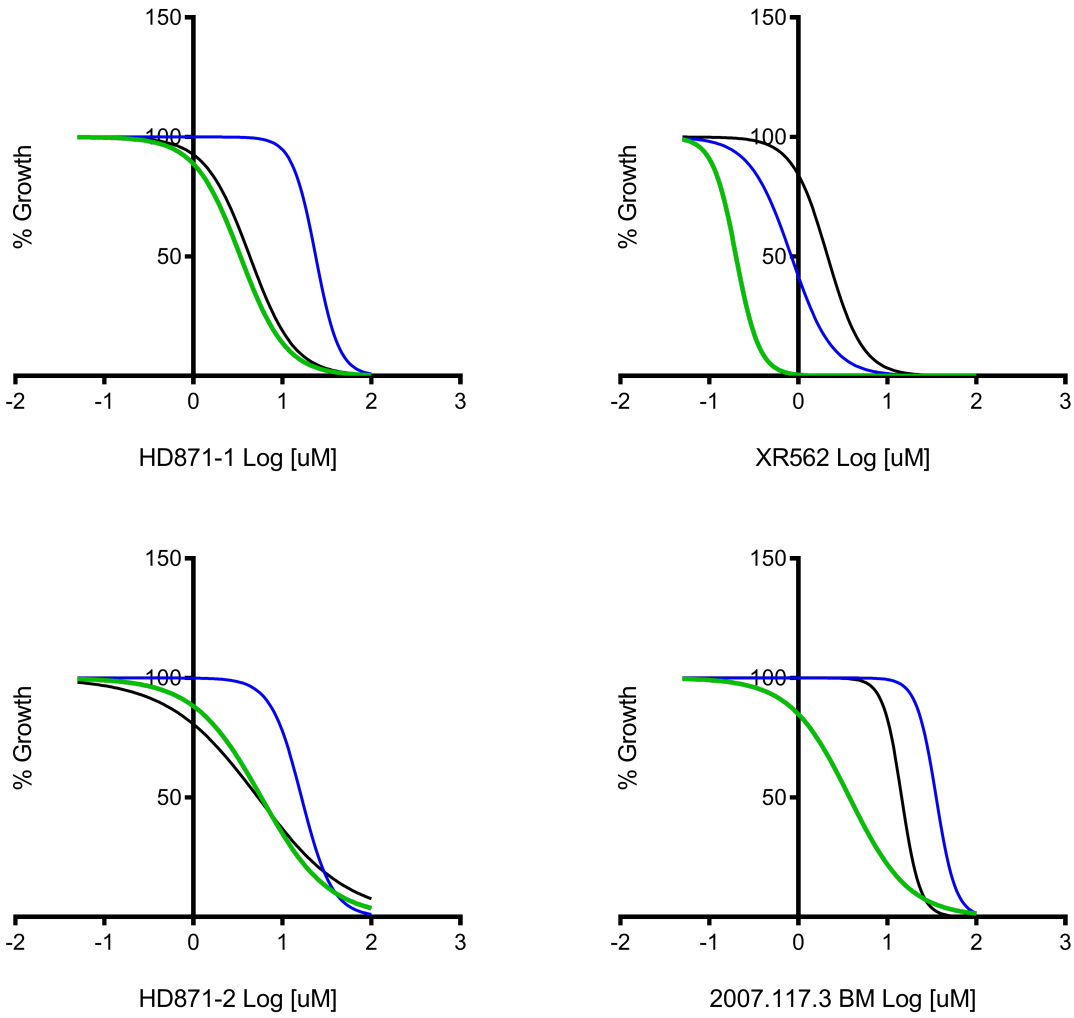

Figure 3.4: Dose-response curves for four compounds tested in the macrophage cytoxicity assay indicate that HD871-1, and HD871-2 gave high EC_{50}values (blue line.) Dose-response curves for HD871-1, HD871-2 and XR562 compounds tested in the *L. mexicana* intramacrophage assays in black plot line gave low EC_{50}, while all four compounds tested in the *L. mexicana* axenic assays in green line gave an EC_{50}value of $>$ 10 µM.

Compounds	Axenic (black plot line)	95%CI	SD	Cytoxicity (blue line)	95%CI	SD	Infection (green line)	95%CI	SD
HD871-1	3.39 µM	1.32	4.35	23.80 µM	2.531	5.63	4.32 µM	2.39	4.42
HD871-2	5.81µM	2.81	5.33	16.49 µM	2.13	4.23	5.32 µM	2.72	3.92
XR562	0.20 µM	2.17	5.68	0.84 µM	2.51	4.28	2.14 µM	3.33	4.37
2007.117.3 BM EXTRACT	0.5 µM	1.72	6.15	200 µM	1.53	3.98	700 µM	3.0	4.33

Table 3.3: EC_{50} of compounds tested in axenic, macrophages (toxicity) and intramacrophage (infection) assays, that correspond to Figure 3.4

The 313 compounds in the primary and secondary screens were tested and 64 selected compounds into a third single point assay screen, from which 10 showed an inhibition of greater than 80%. The level of activity of 6 of the compounds that showed <50% inhibition in the dose-response axenic assay, and were not effective enough to pass through to the next round of anti-leishmanial screening. Therefore, 4 compounds with EC_{50}values of under 10 μM went through to macrophage and intra-macrophage assay testing. A concentration range of 100 μM was used in Figure 3.4. HD871-1, HD871-2, XR562, and 2007.117.3 BM EXTRACT displayed the lowest EC_{50} in the axenic assay, while also maintaining a low EC_{50} in the intramacrophage assay but high EC_{50} in the toxicity macrophage assay (Figure 3.4).

The results were promising, and while 60 of the compounds did not meet the experimental threshold, 4 of the compounds were efficacious against *L. mexicana* amastigotes. The macrophage assay eliminated XR562 from the hit list as it gave a low EC_{50} of 0.84 μM and is therefore toxic to mammalian cells, while HD871-1 and HD871-2, and 2007.117.3 BM EXTRACT gave an EC_{50}value < 10 μM in the same assay. HD871-1 and HD871-2 yielded excellent results giving an $EC_{50}$of 3.39 μM and 5.81 μM in the axenic assay respectively, and high EC_{50}values of 23.80 μM (HD871-1) and 16.49 μM (HD871-2) for the toxicity assay, while maintaining low EC_{50} in the intramacrophage assays. The inhibition against *L. mexicana* shown by these two compounds when compared to the $EC_{50}(> 10$ μM) of the current frontline and second-line anti-leishmanial drugs, like miltefosine and amphotericin B, warranted further exploration. The two hit compounds one of which is shown (Figure 3.5) were therefore used in metabolomic analysis in the search for their targets.

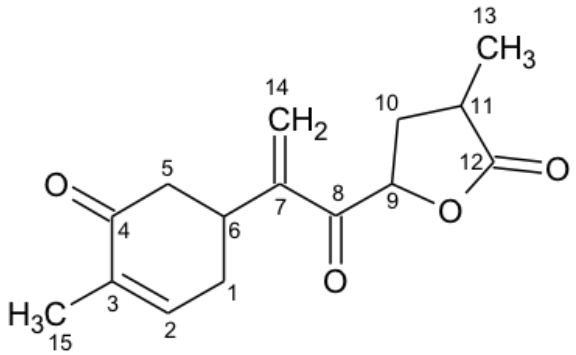

Figure 3.5: Molecular structure of HD871-1

3.6 Anti-leishmanial conclusions

This chapter, describes the screening of 313 extracts from the Hypha Discovery compound library against *L. mexicana.* Four compounds with anti-leishmanial properties (EC_{50} of less than 10 μM) in the axenic and *L. mexicana* intramacrophage assays were identified although only two of the compounds showed low mammalian cytotoxicity. These two hit compounds, HD871-1 and HD871-2, were selected for further analyses.

Chapter 4

Results: Metabolomic analyses

In this chapter we examine the two hit compounds HD871-1 and HD871-2 identified from the assays in chapter 3. The aim was to explore effects on metabolism of compounds HD871-1 and HD871-2 in *L. mexicana* axenic amastigotes.

4.1 Preliminary work on metabolomics in *Leishmania*

Previous studies examined the metabolic effects of miltefosine, the first approved oral drug for the treatment of leishmaniasis [88]. These studies showed that after exposure to miltefosine the known metabolites including sterols and other lipid pathways are affected within *Leishmania* species.

4.1.1 Half-time to death assay

A half time to death assay was carried out to identify the optimum concentration to be used in examining the effect of HD871-1 and HD871-2 on the *L. mexicana* amastigote metabolome. The optimum conditions for cell extraction of *L. mexicana* amastigotes metabolome as determined by the half time to cell death assay for

HD871-1 and HD871-2 exposure, was determined as 10 μM with a 36 hour compound exposure, as disscused below.

4.2 Metabolomic determination of *Leishmania* response to HD871-1 and HD871-2

Analyses were carried out on treated and untreated *L. mexicana* axenic amastigotes using DMSO as a control. The effect on metabolites associated with samples treated with HD871-1 or HD871-2 and without compound was then determined. Approximately 500 were detectable and a selected few shown in Table 4.1. Identification of metabolites took place when the metabolome in question increased or decreased following exposure of either HD871-1 and HD871-2 in a 36 hour time period. Significant changes were evaluated as these with a P value of < 0.05 and a fold change of $\pm$ 3-4 for at least one of the comparisons made.

4.3 Effect on nucleotide metabolism post-exposure to HD871-1 and HD871-2

Treated samples experienced an increase in deoxynucleotide monophosphates and a decrease in deoxynucleotide diphosphates (Figure 4.1). These changes point to alterations in DNA metabolism, but the impact on cell viability is not certain. Profound decreases in orotate and dihydroorotate also point to an alteration of pyrimidine biosynthesis, but pyrimidines themselves were not diminished, presumably due to the parasite's ability to transport and interconvert pyrimidines [98].

Identification	Mass of metabolite	RT (Retention Time)	Untreated	HD871_1	HD871_2	All increased significantly p<0.05 t-test
L-Cystine	240.02	12.74	0.00	166.45	184.30	Increased
Cystine	240.02	12.74	0.00	166.45	184.30	Increased
S-glutathionyl-L-cysteine	426.09	12.89	0.00	145.81	137.28	Increased
dAMP	331.07	10.44	1.00	3.20	3.77	Increased
dTMP	322.06	10.7	1.00	4.00	4.73	Increased
dCMP	307.06	11.71	1.00	3.07	3.94	Increased
dGMP	347.06	12.19	1.00	4.60	6.12	Increased
Trypanothione	361.65	12.49	1.00	0.02	0.02	All decreased significantly p<0.05 t-test
Glutathione	307.08	11.63	1.00	0.37	0.33	Decreased
dADP	411.03	11.27	1.00	0.48	0.50	Decreased
dTDP	402.02	11.58	1.00	0.37	0.34	Decreased
Orotate	156.02	9.62	1.00	0.13	0.08	Decreased
Dihydroorotate	158.03	10.15	1.00	0.06	0.04	Decreased
trypanothione-disulfide	360.64	14.17	1.00	0.41	0.28	Decreased
NADPH	372.55	12.82	1.00	0.36	0.28	Decreased

Table 4.1: Selected metabolites affected by exposure to HD871-1 and HD871-2.These metabolites all showed a significant decrease and increase.

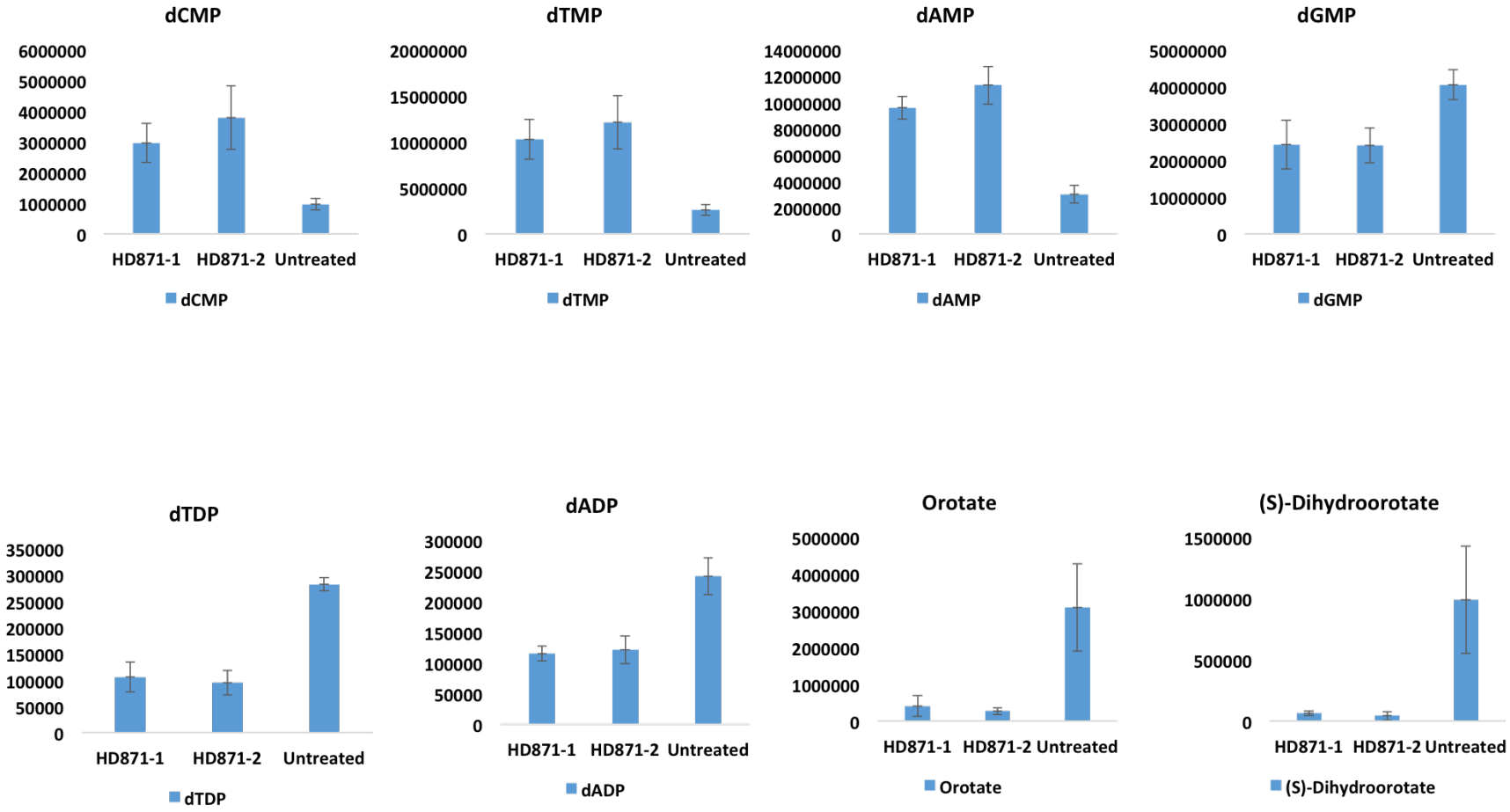

Figure 4.1: Effect of HD871-1 and HD871-2 treatment on nucleotide metabolism in *Leishmania mexicana* axenic amastigotes. Compared with untreated samples, levels of dAMP, dTMP, dCMP and dGMP all increased significantly during the course of treatment while the deoxydinucleotides dADP and dTDP diminished (dGDP and dCDP were not identified). Orotate and dihydroorotate were both significantly diminished by treatment. The y-axis shows arbitrary units (AU).

4.4 Effect on trypanothione metabolism post-exposure to HD871-1 and HD871-2

Trypanothione, the bis(glutathionyl) spermidine adduct that performs key redox roles in *Leishmania* spp and other trypanosomatids, was greatly diminished in treated cells. The peak of this compound (Table 4.1) ($m/z = 361.6527$ corresponding to the doubly positively charged trypanothione) was poorly resolved by chromatography, hence quantitative comparison is not possible, but treated cells contained profoundly less signal for this mass than untreated cells (Figure 4.2) In addition to reduced trypanothione, its oxidised disulphide derivative, (m/z = 361.6441), was also 3-4 fold less abundant in treated cells, and its thiol precursor glutathione (m/z = 307.0837) also diminished in abundance by >60% in the treated cells. Another poorly resolved peak consistent with oxidised cysteine derivative, cystine (m/z = 240.0238) was identified in treated, but not untreated cells. In summary; NADPH, trypanothione, trypanothione disulfide, spermine, glutathione, L-cysteine and S-glutathionyl-L-cysteine all linked to the trypanothione pathway, were identified in the metabolic analyses of *L. mexicana*.

4.5 Possible modes of action HD871-1 and HD871-2

As observed, in both the *L. mexicana* HD871-1 and HD871-2 treated parasites, the metabolome affected, either by an increase or decrease, pointed towards the trypanothione and nucleotide metabolism pathways. Trypanothione in kinteoplatids has been well studied [99] and a complex formed between spermidine and glutathione is used in the maintenance of thiol–redox balance during defence against reactive oxygen species. This thiol redox system is essential for all trypanosomatids living in the human host, and it is the importance of thiol–redox metabolism that has been exploited, by identifying key enzymes involved in this pathway, leading to the development of anti-kinetoplastidal compounds [99].

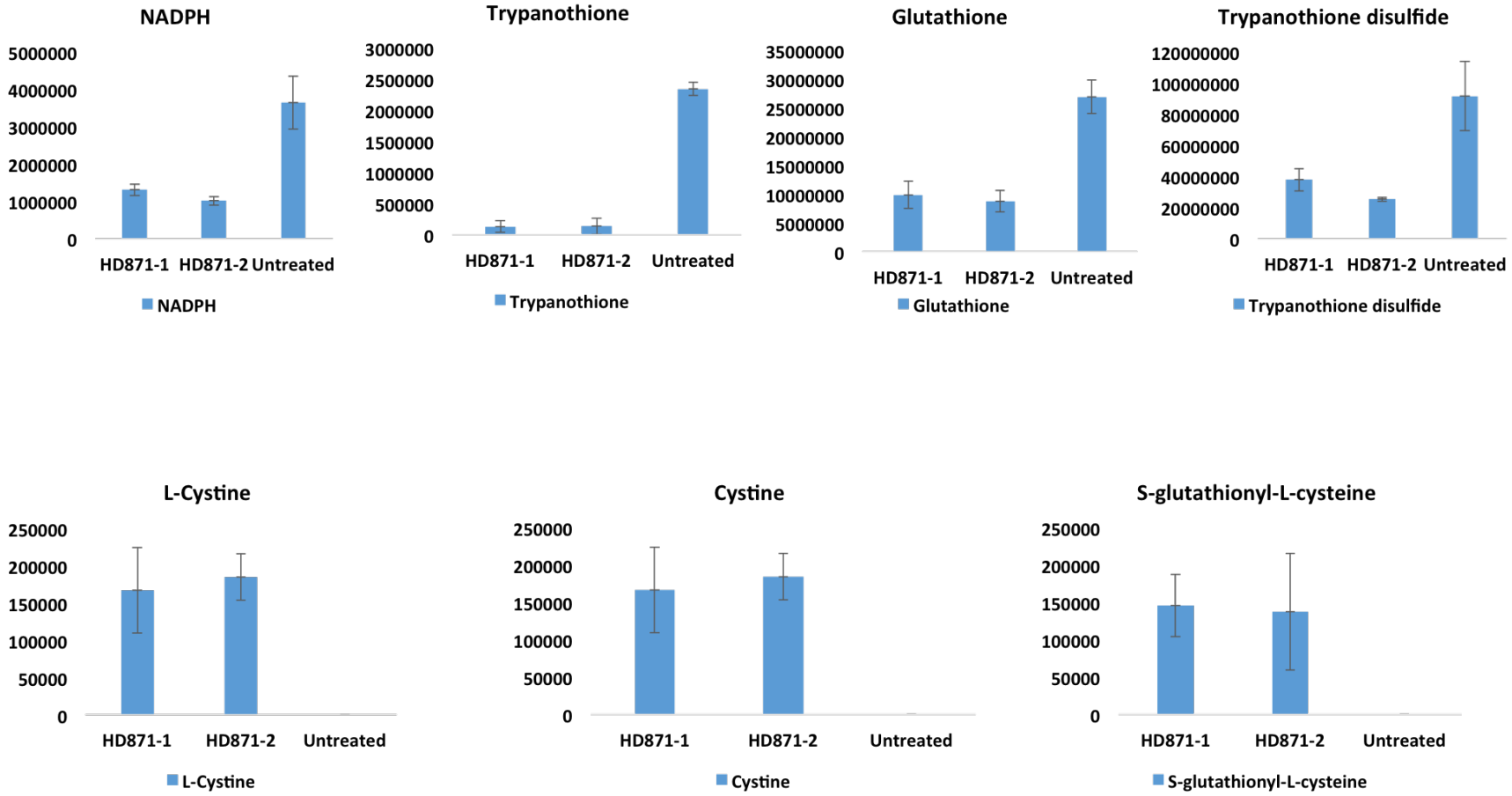

Figure 4.2: Effect of HD871-1 and HD871-2 on trypanothione metabolism in *Leishmania mexicana* axenic amastigotes when compared with untreated samples, shows levels of L-cystine, Cystine and S-glutathionyl-L-cysteine increase significantly during the course of treatment while trypanothione, trypanothione-disulfide, NADPH and glutathione were significantly diminished by treatment. y-axis is arbitrary units (AU).

For the untreated *L. mexicana,* the metabolism of trypanothione (Figure 4.3) in this parasite can be divided into three parts; synthesis, regeneration and utilization [99]. During synthesis, trypanothione synthatase (TS) ligates two glutathione molecules to a single molecule of spermidine (or spermine) using ATP as an energy cofactor, this trypanothione compound is then used in various processes of detoxification (for example xenobiotics), cell proliferation, protein thiol-redox homeostasis and protection against oxidants. The regeneration process involves trypanothione reductase (TR) and the recycling of NADPH and NADP to produce more trypanothione, this trypanothione also interchanges to trypanothione disulphide using tryparedoxin.

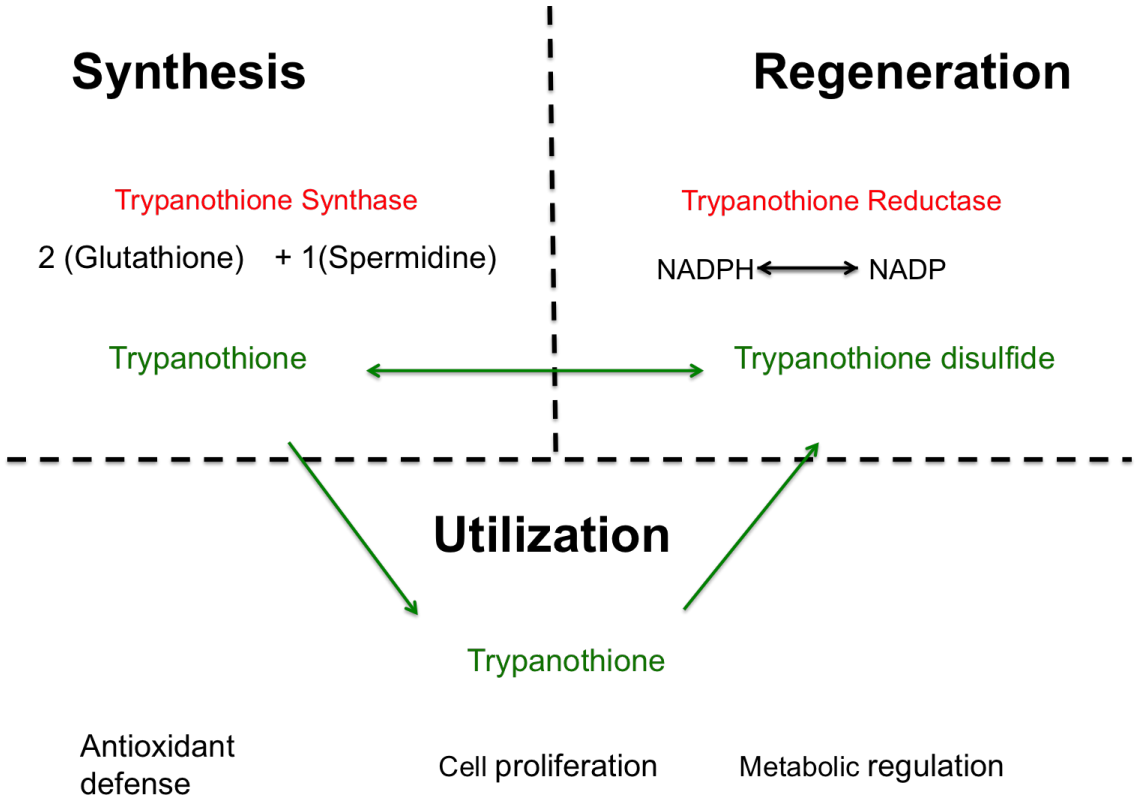

Figure 4.3: Untreated *L. mexicana* trypanothione metabolism, involving trypanothione synthase catalysing 2 gluthatione + 1 spermidine + 2 ATP molecules during synthesis to generate one trypanothione molecule and regenerating trypanothione through trypanothione reductase using NADPH, which can be supplied by the oxidative phase of the pentose phosphate pathway via glucose 6-phosphate dehydrogenase [99].

However, in the HD871-1 and HD871-2 treated samples the key metabolites,

starting with trypanothione were reduced relative to the untreated samples Figure 4.4, this was also a likely result of there being a lower amount of glutathione during the synthesis process. The regeneration process which involved the use of NADPH, was also lower in these treated parasites, which may also have lead to the reduced amount of trypanothione disulfide. As expected, and seen in most pathways, the decrease in one area of metabolism, can increase of metabolism in another. Hence, the decrease in the trypanothione metabolome pathway resulted in an increase in upstream metabolomes. Activation of cysteine metabolism pathway, fits in with the increased amount of glutathione available, causing increased amounts of L-cysteine, cysteine and S-Glutathionyl-L-cysteine. The reduced amount of trypanothione of the treated *L. mexicana* could have been a result in the compounds inhibiting enzymes involved in this pathway, leading to an imbalance of the thiol-redox system, and increase in reactive oxygen species, and reduced cell proliferation.

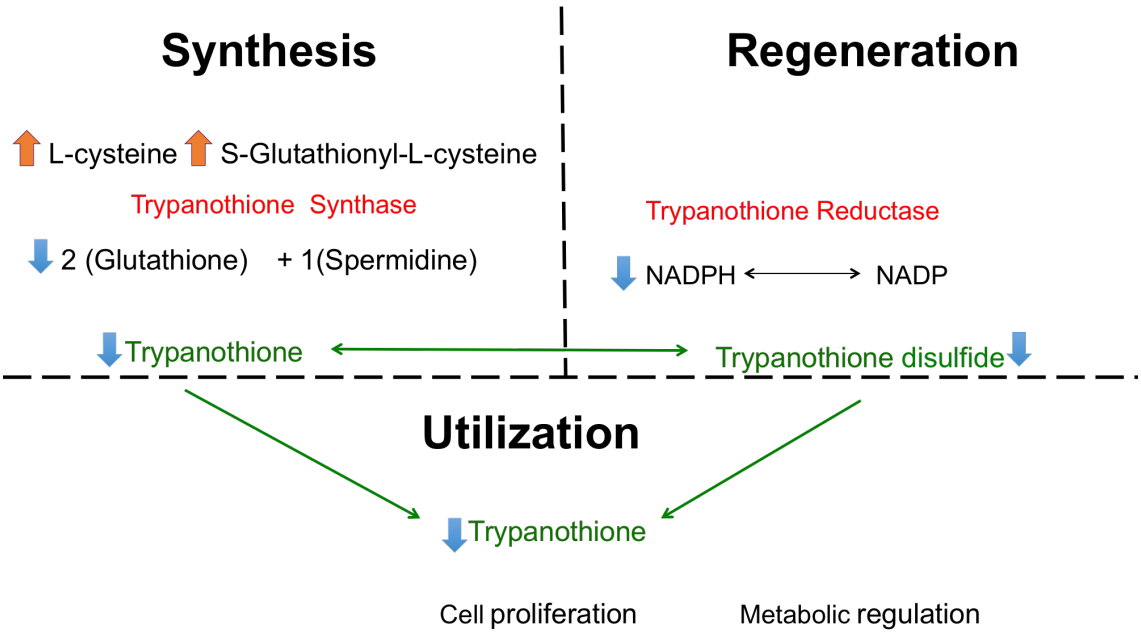

Figure 4.4: HD871-1 and HD871-2 treated *L. mexicana* trypanothione metabolism shows a lack of activity in trypanothione synthase catalysis in the combination of 2 glutathione + 1 spermidine + 2 ATP molecules during synthesis and lack of regeneration of trypanothione disulfide through trypanothione reductase using NADPH. This may have lead to oxidative stress and resulted in parasite death.

4.6 Putative drug targets

The comparison between treated and untreated samples highlighted the likely importance that trypanothione and nucleotides play in terms of parasite survival. With respect to nucleotide metabolism changes in the deoxynucleotide pool indicated possible changes in DNA metabolism, although whether this is a cause of cell death is unclear and secondary effect due to other changes is not clear and make it difficult to identify a target. For trypanothione metabolism however, trypanothione reductase and trypanothione synthase may well be the target of the two hit compounds, as the levels of trypanothione were reduced. The lack of trypanothione disulfide and NADPH also pointed towards inhibition of trypanothione reductase. Further investigation into which enzyme is affected by the compound would be the next step to define the precise target.

4.7 Metabolomic analysis conclusions

The experiments described in this chapter, illustrate the use of a robust platform offering broad coverage of *Leishmania* metabolites in addition to identifying the effects on the trypanothione pathway as a result of the treatment of HD871-1 and HD871-2. Many other pathways were also shown to be perturbed by theses two compounds. HD871-1 and/or HD871-2 which may inhibit trypanothione biosnthesis (synthase/reductase) in *L. mexicana* coupled to the non-toxic effects shown in the macrophage assays. The low EC_{50} values from the intramacrophage drug screens shown in the previous chapter make these natural compounds ideal candidates for drug target validation and further *in vivo* studies.

Chapter 5

Results: An investigation into natural compounds and Pex inhibitors for *Toxoplasma gondii*

In this chapter we explore the use of another natural compound Aureobasidin A (AbA), and its derivatives against *T. gondii* Type I and Type II. From previously published work, Wuts *et al* 2015. showed that the activity of Aureobasidin A-derivatives on fungal pathogens gave similiar efficacy values (typically < 0.5 μM) [13]. These compounds have also previously been shown to be active against yeast and asks the question of whether they, would be active against protozoa. Here we report the EC_{50} of AbA and its derivatives against *T. gondii* Type I and Type II, showing that one of the AbA derivative is active against Type II *T. gondii* the encysted form of *Toxoplasma,* and could potentially be used in treatment of chronic toxoplasmosis when the parasite is in the bradyzoite form.

The research contained in this chapter has been previously published in a peer reviewed paper:

- Alqaisi, A Q I and Mbekeani, A J and Llorens, M Bassas and Elhammer, A P and Denny, P W, "The antifungal Aureobasidin A and an analogue are active against the protozoan parasite *Toxoplasma gondii* but do not inhibit

sphingolipid biosynthesis", Parasitology 145 (2018), pp. 148--155.

5.1 Preliminary work on Aureobasidin A

AbA is a well known depsipeptide produced by *Aureobasidium pullulans* strain BP-1938 and targets the fungal inositol phosphorylceramide (IPC) synthase, an enzyme in the sphingolipid biosynthesis pathway. In addition, AbA has been shown to be active against various species of *Leishmania* and other protozoa [82, 100].Wuts *et al* 2015, synthesised a library of approximately 30 compounds based on the parent AbA structure and Dr Ake P. Elhammer at AureoGen Biosciences carried out testing on *Candida albicans*. From these results we selected the four compounds shown in Figure 5.1 [13] that showed the highest potency against *C. albicans* and *Aspergillus fumigatus* for testing against *Toxoplasma.*

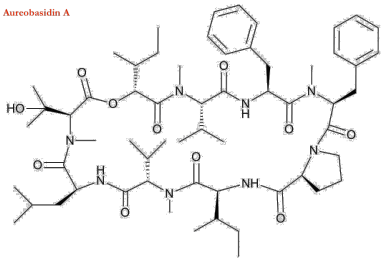

(a) Aureobasidin A (AbA)

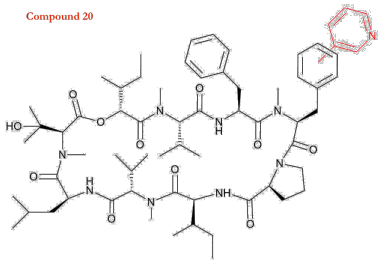

(b) Compound 20 (AbA-3-pyridyl)

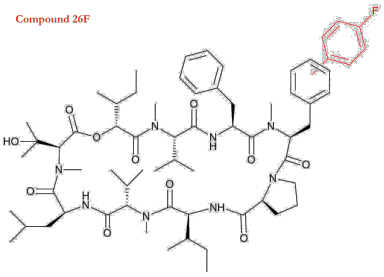

(c) Compound 26F (AbA-fluorophenyl)

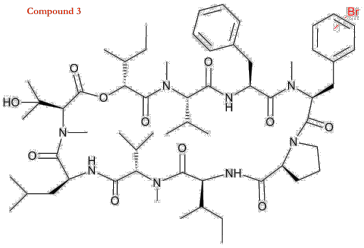

(d) Compound 3 (AbA + Br)

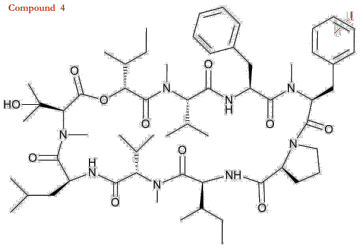

(e) Compound 4 (ABA+I)

Figure 5.1: Aureobasidin A and derivatives synthesised by Wuts *et al* 2015.

Compounds	*C. albicans* EC_{50}[μg/mL]
Compound 3	0.03
Compound 4	2.50
Compound 20	0.05
Compound 26F	0.05

Table 5.1: *C. albicans* data showing that compound 26F has the lowest EC_{50} [13]

5.2 EC_{50} of Aureobasidin A and derivatives against Type I *Toxoplasma gondii*

In order to test the activity of these natural compounds against Type I *Toxoplasma gondii*, four AbA derivatives and AbA were screened against YFP tagged RH *Toxoplasma* tachyzoites [101]. The methodology, is described in detail in Chapter 2, breifly, HFF cells were infected with Type I parasites and after 20 hours, compounds were added and fluorescence analyzed using a macro-data spreadsheet (Appendix A) The data output was used to generate an EC_{50} and produce a sigmoidal dose-response curve in Prism V7. Results were plotted using percentage growth versus log concentration (Figure 5.2). Positive (AbA) and negative controls gave expected results on each occasion.

As shown in Table 5.2, all four compounds showed activity against Type I *T. gondii* and gave varied EC_{50} values, with the lowest coming from AbA. Since compound 20 was the more potent at 48 hrs 0.75 μg/mL than compound 3 0.89 μg/mL , it was decided that this compound would be suitable for testing against encysted form of *T. gondii.*

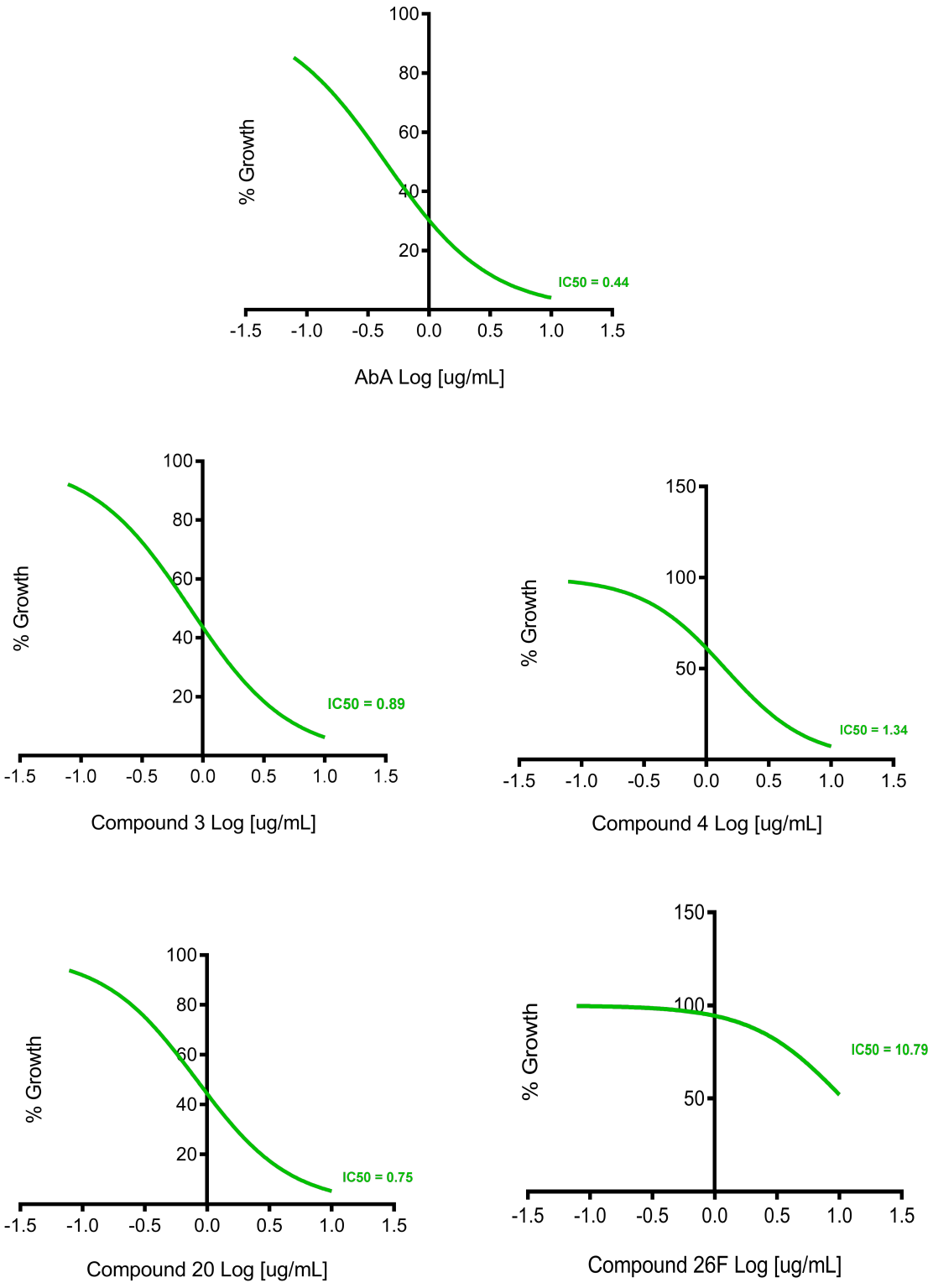

Figure 5.2: EEfficacy of Aureobasidin A, Compound 3, 4, 20 and 26F against *Toxoplasma* Type I. Compound 3 and Compound 20 gave the highest activities at 48 hours, similar to Aureobasidin A.

Compound	EC_{50}[μg/mL]	95%CI	SD
AbA	0.44	1.25	4.40
Compound 3	0.89	2.52	4.73
Compound 4	1.34	1.63	5.24
Compound 20	0.75	1.34	4.53
Compound 26F	10.79	1.20	1.86

Table 5.2: Efficacy of Aureobasidin A, Compound 3, 4, 20 and 26F against *Toxoplasma* Type I.

5.3 Testing Aureobasidin A and derivatives against Type II *Toxoplasma gondii*

As AbA and Compound 20 were the most potent in the 48 hour drug screen against Type I *T. gondii,* both were selected for testing against the GFP-tagged *Toxoplasma* Type II Pru strain [92]. As described in Chapter 2, breifly, HFF cells grown on 96 well plates were infected with the Type II parasites before transformation to bradyzoites. Encysted bradyzoites were then treated with compounds and incubated for 3 days after which fluorescence was measured and analyzed using a macro-data spreadsheet (Appendix B). The data output was used to calculate an EC_{50} in Prism V7 and results were plotted as inhibition versus log concentration. Both AbA and Compound 20 (Figure 5.3) showed activity against encysted Type II *Toxoplasma gondii* and gave EC_{50}values of 2.51 μg/mL and 3.74 μg/mL respectively. These two compounds proved to be potent inhibitors of encysted Type II *Toxoplasma gondii* showing low mammalian cytotoxicity. In addition to promising pharmacokinetic properties of Compound 20 [13], this class of cyclic depsipeptides could be used in future experimentation, *in vivo* and potentially on clinical trials, to treat chronic toxoplasmosis and some psychiatric disorders. [82] .

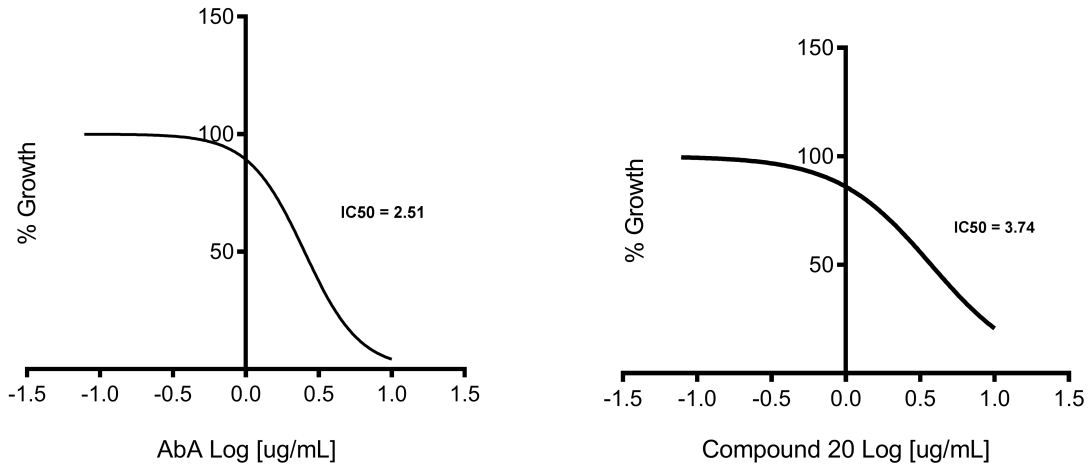

Figure 5.3: $EC_{50}$of Aureobasidin A and Compound 20 against *T.gondii* Type II

5.4 Screening Pex5-Pex14 inhibitors against intra-cellular RH *Toxoplasma gondii*

The Pex5-Pex14 interaction is crucial for lipid transport in protozoa [41,102]. Compounds 5MA, CMPD 11 NH2, 5MA NH2, 6MA, DOL 320, MAB NH2, PR DD 43, PR DD 51 provided by Prof. Ralf Ederman at Ruhr University, Germany are Pex5-Pex14 inhibitors that disrupt glycosomal protein import and killing trypanosomes by affecting the Pex5-interaction site specifically in *T. brucei*. In addition, these compounds are active against Pex14 in other protozoa such as *T. cruzi* and *Leishmania* Pex14 [102]. To investigate this class of compounds further, we utilized the availability of these eighteen Pex5-Pex14 inhibitors to test their efficacy against *Toxoplasma*.

For these experiments, *T. gondii* tachyzoites *RH Type I* with YFP [101] were inoculated into HFF cells and compounds added after 18 hrs at concentrations from 0.21μM to 50 μM; pyrimethamine was used as a positive control and DMSO the negative control. Florescence was mesasured in plates and data analysed as before. Eleven hit compounds were identified in this screen. All with an EC_{50} of < 10 μM

Table 5.3. Interestingly, all of the hit compounds exhibited host toxicity at higher concentrations 16.67 μM and/or 50 μM. The assay was robust and gave a Z factor of > 0.80.

Compounds	EC_{50}	95%CI
5M	33.77	15.56 - 73.32
5MA	6.83	5.35 - 8.71
5M III	21.68	very wide
5 III MAB	N/A	N/A
DOL 008	13.80	very wide
DOL 145	110.40	very wide
CMPD 11	46.43	very wide
CMPD 11 NH2	0.96	0.80 - 1.14
5MA NH2	6.57	1.94 -22.23
6MA	4.33	4.15 - 4.52
DOL 320	6.96	4.09 - 11.82
DOL40-4	49.21	very wide
MABAM POL	6.13	very wide
MAB NH2	1.16	1.50 - 1.75
PR DD 43	4.00	3.28 - 4.88
PR DD 51	6.64	3.53 - 12.47
5G	48.09	very wide

Table 5.3: *T. gondii* Pex5-Pex14 EC_{50} assay with 17 test compounds. Very wide (< 60)

5.5 *Toxoplasma* compound screen conclusion

In conclusion the work described in this chapter involved the screening of 4 Aureobasidin A-derivatives in *T. gondii* and *C. albicans* drug assays. Compound 3 and Compound 20 showed the highest activity in the *C. albicans* assays. In the *T. gondii* assays compound 20 showed highest potency in both tachyzoite and bradyzoite forms. Additional testing of 18 compounds that target peroxins showed that eleven compounds had a low EC_{50} against *T. gondii* but also displayed high mammalian cytoxicity. Further exploration of their potential as Pex5 or Pex14 inhibitors was not warranted due to their toxicity against mammalian cells. Optimisation of these compounds to reduce their toxicity to mammalian cells could potentially be pursued and lead to the development of a non-toxic Pex protein inhibitor as achieved

with other protozoan research [1, 2, 7]. However, in order to discover target specific inhibitors, there needs to be a closer examination and analysis of the Pex5 protein at a bioinformatic level that could help in determining a mode of action. Additionally, identifying key regions in the peroxins that are unique to the parasite could lead to subsequent medicinal chemistry optimisation of the eleven potent inhibitors identified here. Binding sites such as the TPR domains found in Pex5 described in the next chapter, could be exploited in the discovery of a specific Pex5 inhibitor.

Chapter 6

Results: Evaluation of peroxisomal proteins *Tg*SCP2 and *Tg*Pex5

Having identified eleven inhibitors of Pex5 and Pex14 in *Toxoplasma*, attention turned to reviewing the biological properties of Pex proteins, in particular Pex5 and its associated protein ligands SCP2. To begin the functional analysis of *Tg*Pex5, and *Tg*SCP2 a sequence comparison of Pex5 proteins from *S. cerevisiae*, *T. gondii* and *H. sapiens*, was compiled. Expression data on peroxisomal proteins was also undertaken. In addition, the results of functional complementation studies between yeast *Toxoplasma* and humans was also reported. The possible location of peroxisomes within the tachyzoite forms of *Toxoplasma* was also explored, as was the interaction between the peroxisomal proteins $Tg\text{SCP2}_{\text{PTS1}}$ and $Tg\text{Pex5}_{\text{C-TERMINAL}}$.

The research contained in this chapter has been previously published in a peer reviewed paper:

Alison J. Mbekeani, W Stanley, V Kalel, N Dahan, E Zalckvar, L Sheiner. "Functional Analyses of a Putative, Membrane-Bound, Peroxisomal Protein Import Mechanism from the Apicomplexan Protozoan Toxoplasma gondii", Genes 9, 9 (2018), pp. 434.

6.1 Exploring Pex5

6.1.1 Gene Expression of *Tg*Pex5 and *Tg*SCP2

A clear difference in the amount of *Tg*SCP2 expressed at different stages of the parasites life-cycle is evident, showing highest levels in the oocyst stage (Figure 6.1). One explanation for this is that the increase in expression of *Tg*SCP2 is linked to the parasites requirement for sterol just prior to the entry into the dormant, sporulated oocyst stage. This could involve, the addition of further lipid bilayers within membranes increasing the transport of lipids into the peroxisome just before oocyst formation.

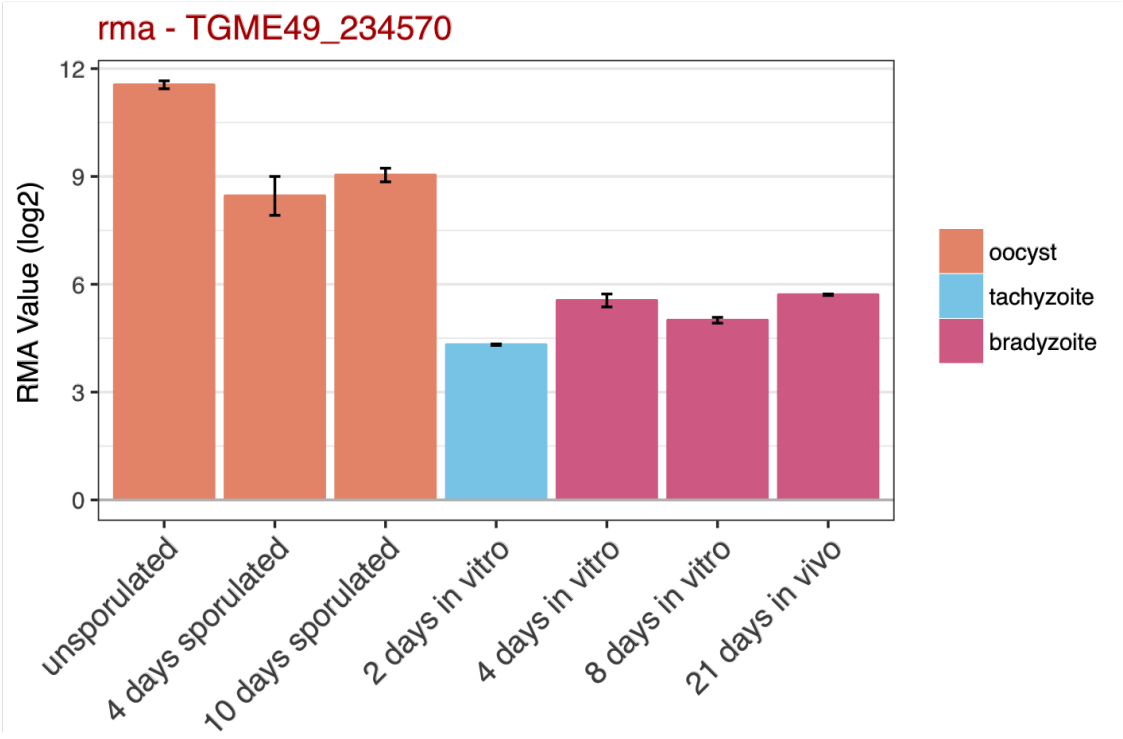

Figure 6.1: Expression level of *Tg*SCP2 at different stages in *T.gondii* life-cycle. Data obtained from toxodb.org [103]

As would be expected, *Tg*Pex5 expression parallels the expression pattern of *Tg*SCP2 and as shown in Figure 6.2. As with *Tg*SCP2, *Tg*Pex5 is highly expressed in the oocyst stages and moderately expressed in the bradyzoite and tachyzoite stages. The higher expression of *Tg*Pex5 in the oocyst, like *Tg*SCP2, could be attributed to

preparation for the next stage of the parasites life-cycle, where a sporulated oocysts may potentially require the function of the peroxisome.

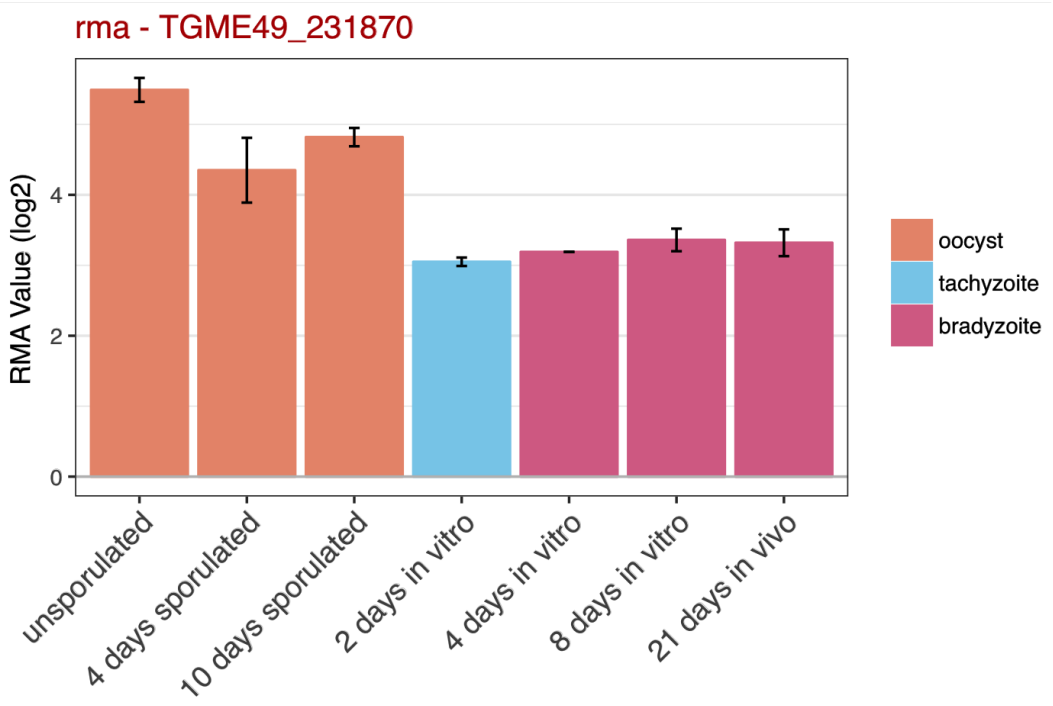

Figure 6.2: Expression level of *Tg*Pex5 at different stages in *T.gondii* life-cycle. Data taken from toxodb.org [103]

6.1.2 Sequence alignments of Pex5

The Pex5 receptor is conserved in many species (Figure 6.3) is mainly characterised by two domains: the N-terminal domain, which has copies of a unique pentapeptide motif, WXXX(F/Y) and the C-terminus which contains tetratricopeptide repeats (TPR) [40,42,43,45,80,104]. The number of N-terminal pentapeptide motifs varies, where *S. cerevisiae* Pex5 has two, *Leishmania donovani* and *Trypanosoma brucei* have three and *Homo sapiens* have seven. These seven pentapeptide motifts has been shown to bind to Pex14 in mammal [41]. In contrast, the C-terminal TPR region of Pex5 has seven degenerate 34 amino acid motifs present in all species and

is involved in PTS1 binding [105] . Deletion of the TPR domain at the Pex5 C-terminus is not sufficient to disrupt functionality, indicating a distinct functionality for the N-terminal region of Pex5 [106].

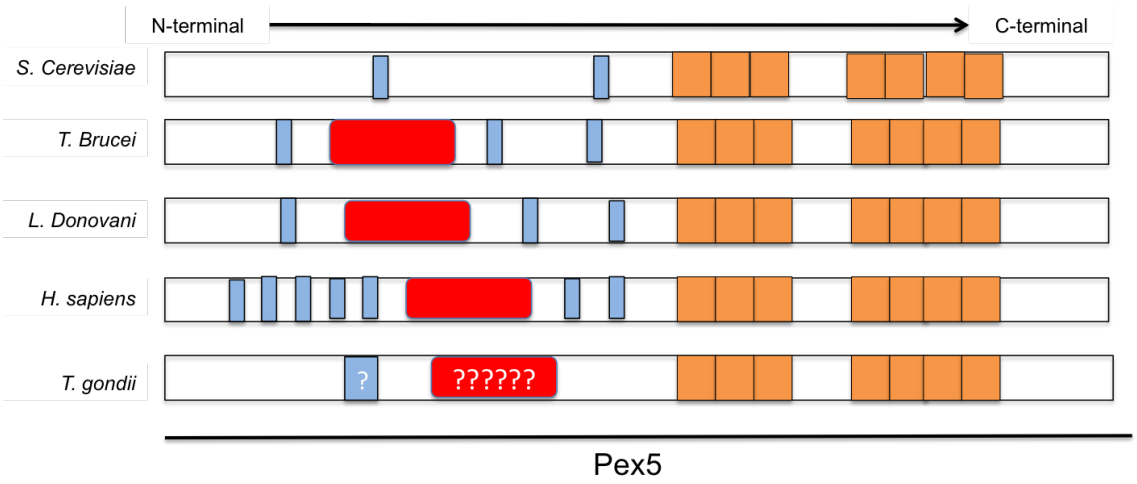

Figure 6.3: Schematic representation of the Pex5 protein from 5 different species, including *Tg*Pex5. All show characteristic TPR domains (orange) at the C-terminal end, pentapeptide motifs (blue) and the Pex7 binding domain (red). In *Toxoplasma*, The Pex7 recognition domain is not known. Adapted from [104].

The N-terminal domain of Pex5 is known to bind to Pex7 [41, 104]. This Pex5 receptor, mainly cytosolic, is believed to have six WD domains in most species as depicted in Figure 6.3 . The WD domains are approximately 50 amino acids long and end with a tryptophan-aspartic acid pair. These WD repeats were reported to fold into anti-parallel β-sheets and the structure of human Pex7 has been shown to have a PTS2 binding site as well as binding sites for chaperones [41,104]. Pex7 in *L. major*, *T. brucei* and *H. sapiens* use Pex5 as a chaperone while *S. cerevisiae* Pex7 relies on other peroxins such as Pex13 and Pex14 [41]. *Tg*Pex7 could be similar to either yeast or *L. major*, *T. brucei* and *H. sapiens*. [40]. Figure 6.4 provides a comparision of the N-terminal and C-terminal domains, highlighting the regions to which PTS1 and Pex7 bind, but also key residues required for Fox1 interaction, which appear to be conserved. The Fox1 binding regions reside in the N-terminal half of *Sc*Pex5 asequence homology here is consitant with *Tg*Pex5 having a similar site [80, 107].

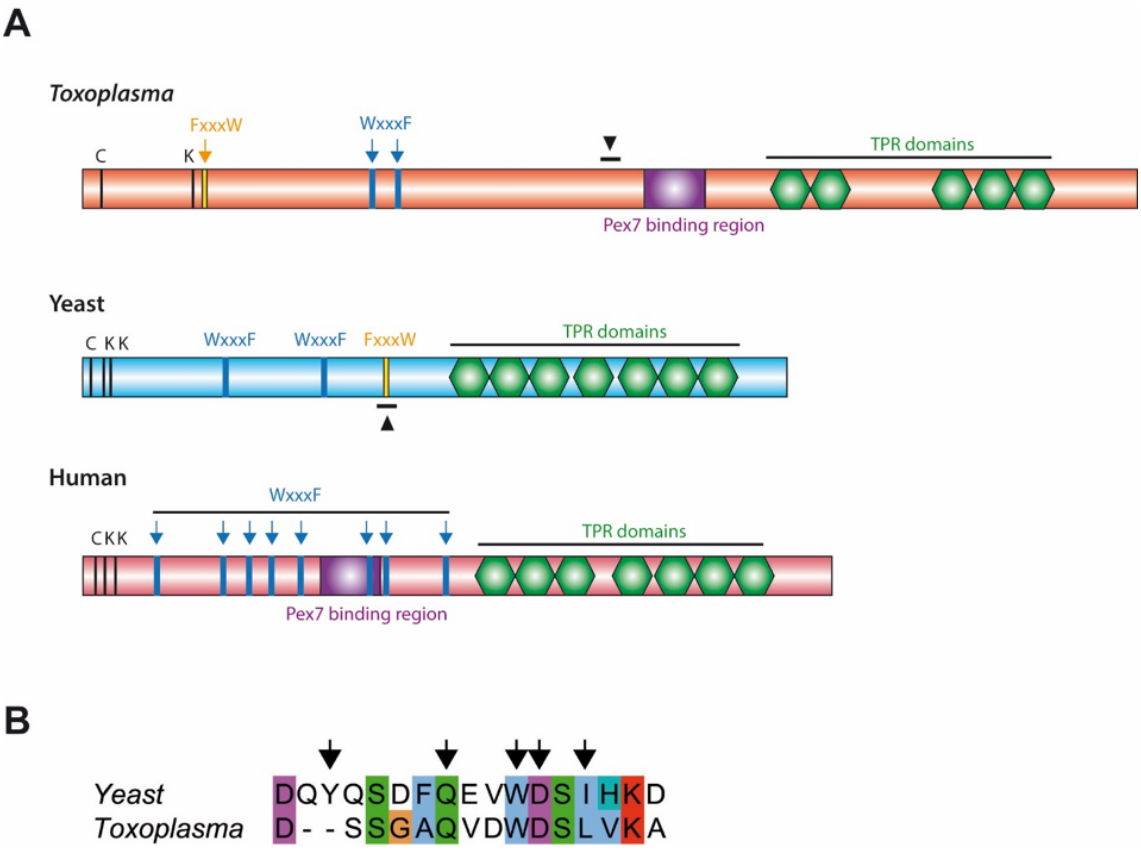

Figure 6.4: *Toxoplasma Toxoplasma* Peroxin 5 (Pex5) contains structures with yeast and human Pex5. Comparison of *Toxoplasma* Pex5 protein with yeast and human counterparts indicated the presence of critical cysteine and lysine residues (C, K), pentapeptide motifs (WxxxF/FxxxW) and structural domains (Pex7-binding region and TPRdomains which bind peroxisomal-targeting signal 1 [PTS1] ligands). Additionally, a region homologous to the Fox1 binding site in yeast Pex5 is also found in *Toxoplasma* Pex5 and is indicated by black arrowheads. (B) Sequence alignment of the Fox1 binding site in yeast Pex5 (ScPex5251-267) with the predicted equivalent in *Toxoplasma* Pex5 (TgPex5442-456), arrows indicate positions in ScPex5. [80]

Having seen the similarity between Pex5 proteins from *S. cerevisiae*, *T.gondii* and *H. sapiens* further *in vitro* investigations were carried out to better understand the function of *T.gondii* Pex5 and SCP2 proteins.

6.2 Exploring the function of *Tg*Pex5 in yeast

Investigating the function of *Tg*Pex5 in yeast cells involved both a qualitative and quantitative approach. The qualitative analysis involved a spot test and an immuno-

precipitation assay, while the quantitative analysis used optical density to monitor growth.

6.2.1 Qualitative analysis

6.2.1.1 *TgPex5* in yeast complementation spot test

Complementation of *Tg*Pex5 in yeast Pex mutants was tested after transformation of pRS416-*Tg*Pex5 into WT (UTL7) and ΔPex5 yeast as detailed in methods Chapter 2. As can be seen in the spot test (Figure 6.5) - URA glucose and - URA oleate plates, showed growth of both mutants and wild-type (empty vector) on the glucose plate. On the oleate plate however, ΔPex5 empty vector yeast cells showed stunted growth as there was a lack of glucose and inability to utilise oleate as an energy source. This was represented by fewer yeast colonies and slower growth for the mutant and is explained by the lack of the Pex5 within the yeast peroxisome. As can be seen, this functionality of the peroxisome is restored when either *Sc*Pex5 and *Tg*Pex5 are transfected back into the yeast mutants. Such that, in the yeast ΔPex5 + *Sc*Pex5 and ΔPex5 + *Tg*Pex5 growth was well established and represented by a halo around the yeast colonies which is typical of oleate substrate utilisation (*). This spot test indicated that *Tg*Pex5 did complement ,yeast ΔPex5 and clearly shows that functionality of Pex5 in these mutants can be restored by either *Tg*Pex5 or *Sc*Pex5. Additional analysis of these yeast colonies was carried out in an immunoflorecence assay [80].

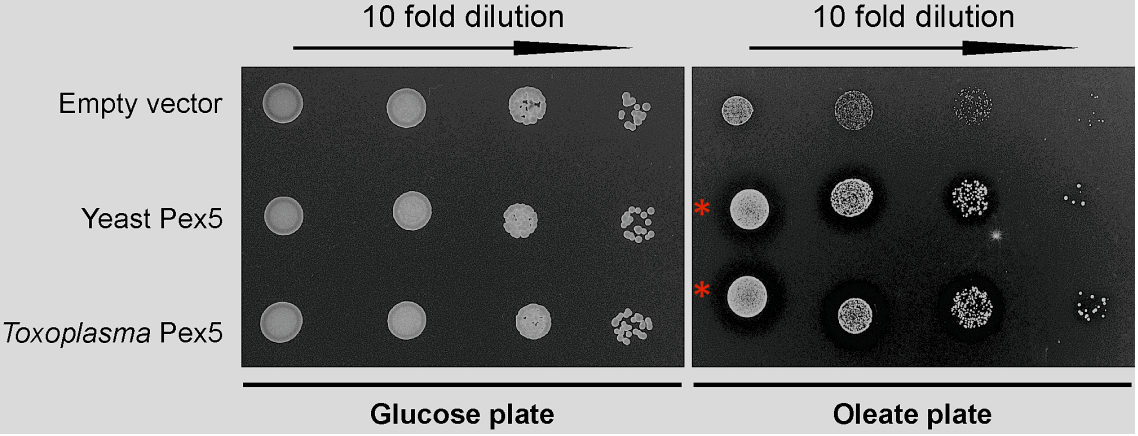

Figure 6.5: *Tg*Pex5 yeast complementation spot test on -URA glucose and -URA oleate plates. Mutants and wild-type (empty vector) show no growth difference on the glucose plates, while on the oleate plate, only mutants with functional Pex5 showed robust growth, indicated by yeast colonies surrounded by a halo (*).

6.2.1.2 *Tg*Pex5 yeast complementation immunoflorecence assay

Having identified that *Tg*Pex5 can restore functionality to ΔPex5 yeast cells in a spot test, *Tg*Pex5 we visualised peroxisomes in mutant and transformed yeast colonies. As in the spot test, the *Tg*Pex5 in yeast UTL7 Pex mutants was further confirmed after pRS416-*Tg*Pex5 plasmids were transfected into wild-type UTL7 and mutant ΔPex5 were grown in oleate and glucose substituted yeast media as detailed in Chapter 2. After 24 hour incubation the IFA images in both glucose and oleate were obtained Figure 6.6. In the negative control (top row) of both the glucose and oleate media images as expected, the empty plasmid transfected into ΔPex5 yeast cells, did not show localisation as indicated by GFP signal throughout the cytoplasm. However, agreement with the spot test results, puncta in the cytoplasm indicate localisation of *TgPex5* and *ScPex5* to peroxisomes in the ΔPex5 yeast cells.

This spot test and immunoflorecence assay provide a good qualitative representation of *TgPex5* restoring the functionality of mutant Pex5 yeast. In order to quantify the functionality of *TgPex5* in the yeast mutant, a growth assay was carried out. The experiments with *S. cerevisiae* demonstrated that TgPex5 could clearly restore GFP-PTS1 targeting to peroxisomes in a cellular context in the immunoflorecence

assay. These results suggest that *Tg*Pex5, like *Sc*Pex5 restores peroxisomal function and β-oxidation as characterised by increased growth and the utilisation of fatty acid oleate, as indicated by the halo formation around the colonies on oleate plates [80].

6.2.2 Quantitative analysis

6.2.3 *TgPex5* yeast complementation in oleate growth media.

Having clearly established the complementation of *TgPex5* in yeast UTL7 Pex5 mutants, transfected *Tg*Pex5-pRS416-WT wild-type UTL7 and mutant ΔPex5 were grown in - URA oleate and - URA glucose media for 24 hrs as detailed in Chapter 2. Growth of yeast cells was measured using optical density (OD) at 600 nM (Figure 6.7). As expected there was no significant difference in yeast cell growth between the different strains in media containing glucose. However, when the food source was substituted for oleate, there was a significant difference in growth between the negative control, the yeast mutant and wild-type strains over 24 hrs. The ΔPex5 mutant expressing *ScPex5* showed improved growth over the ΔPex5 mutant. Showing a 4 fold improvement in growth. The ΔPex5 mutant expressing *Tg*Pex5 also showed improved growth 3 fold difference better than mutant one. These results, further support the conclusion that *Tg*Pex5 is able to restore growth to a Pex5 mutant in the absence of glucose, using oleate as an energy source.

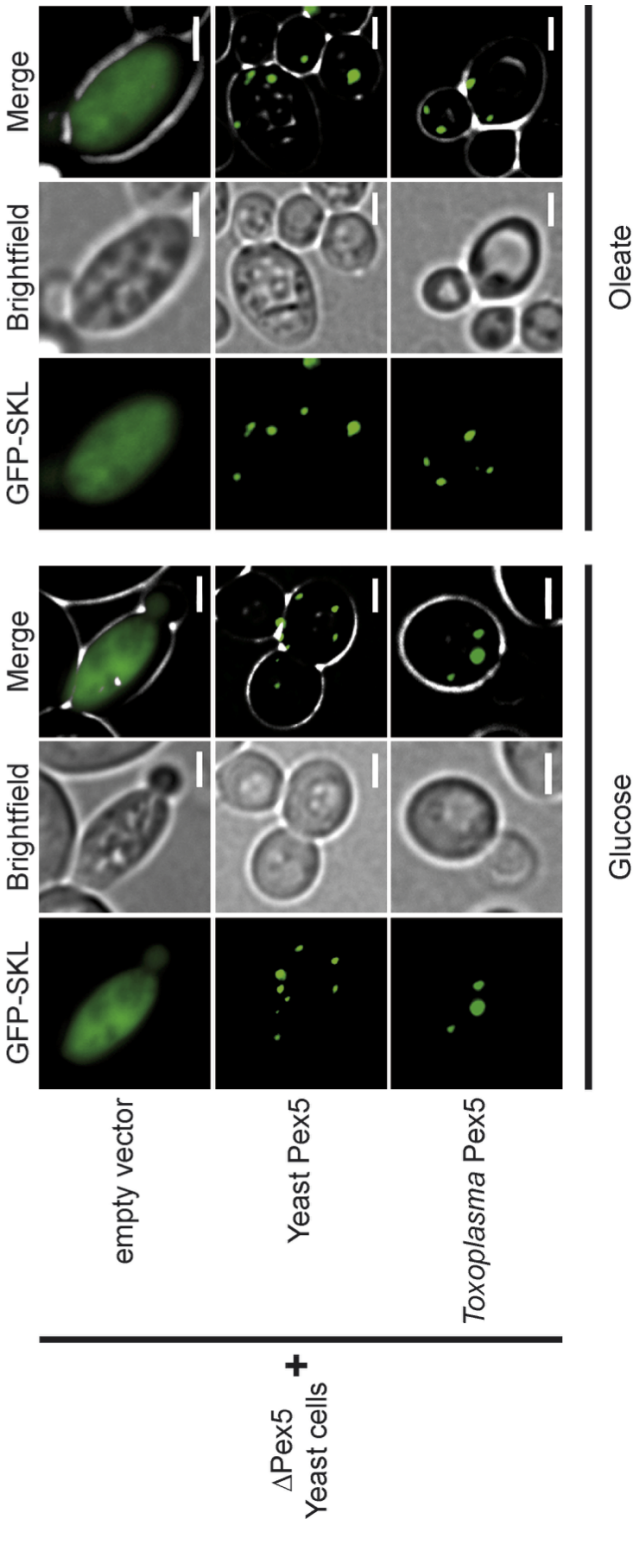

Figure 6.6: *Tg*Pex5 yeast complementation immunoflorecence assay which shows that plasmid *Tg*Pex5-pRS416-WT and *Sc*Pex5-pRS416-WT both localise to peroxisomes when transfected into ΔPex5 yeast cells grown in glucose and oleate. The scale bar is 1 µM.

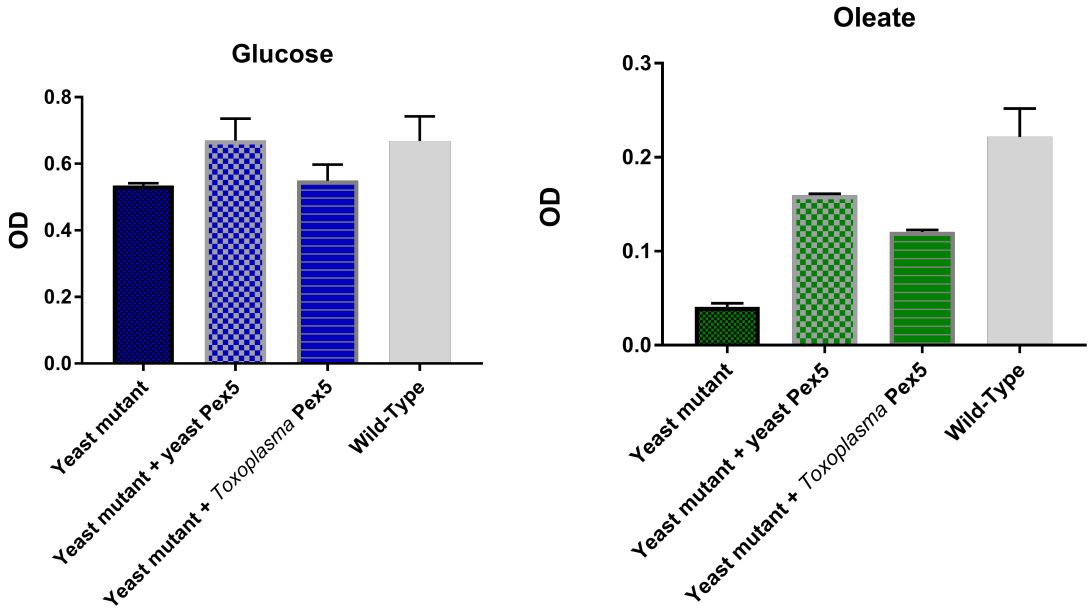

Figure 6.7: Complementation of yeast Pex5 mutant using *Tg*Pex5 during growth in oleate and glucose media. Four replicates of each sample were performed . A *t*-test indicated a significant ($P < 0.05$) difference between ΔPex5, and ΔPex5 carrying yeast Pex5 yeast and *Toxoplasma* Pex5.

Both the qualitative and quantitative analysis of the *Tg*Pex5 in yeast show that *Tg*Pex5 can replace Pex5 function in yeast and indicating that peroxisome functionality has also been restored. Hence *Sc*Pex5 and *Tg*Pex5 seem to be functionally interchangeable, playing a similar role in their respective organisms. The next stage was to establish wether the same was true of human and *Toxoplasma* Pex5 proteins.

6.3 *Tg*Pex5 complementation in human fibroblasts

6.3.1 *Tg*Pex5 human fibroblast complementation immunofloresence assay

After establishing sucessful complementation of *Tg*Pex5 in yeast, *Tg*Pex5 complementation in human Pex5 mutant fibroblasts was carried out, through the transfection of pIRES2-EGFP-SKL-*Tg*Pex5 in wild-type fibroblast and ΔPex5 human

fibroblasts as detailed in Chapter 2. After 72 hours the immunoflorecent images in (Figure 6.8) indicate that, the empty vector in wild-type fibroblasts and the ΔPex5 fibroblasts carrying human Pex5 both show puncta within their cytoplasm's. In contrast, the empty vector in a Pex5 mutant fibroblast and the ΔPex5 fibroblasts carrying *Toxoplasma* Pex5 did not show any puncta. The Pex5 mutant fibroblast carrying the empty vector showed non-localised cytosolic GFP signal throughout the cytoplasm. The lack of puncta strongly suggests that *Toxoplasma* Pex5 cannot restore Pex5 functionality to ΔPex5 mutant human fibroblasts. This result supports the bioinformatics analysis reported in the previous sections, in that the *Toxoplasma* Pex5 gene does not carry all the some motifs present in the human Pex5 so it is not too surprising that it was incapable of restoring functionality [80].

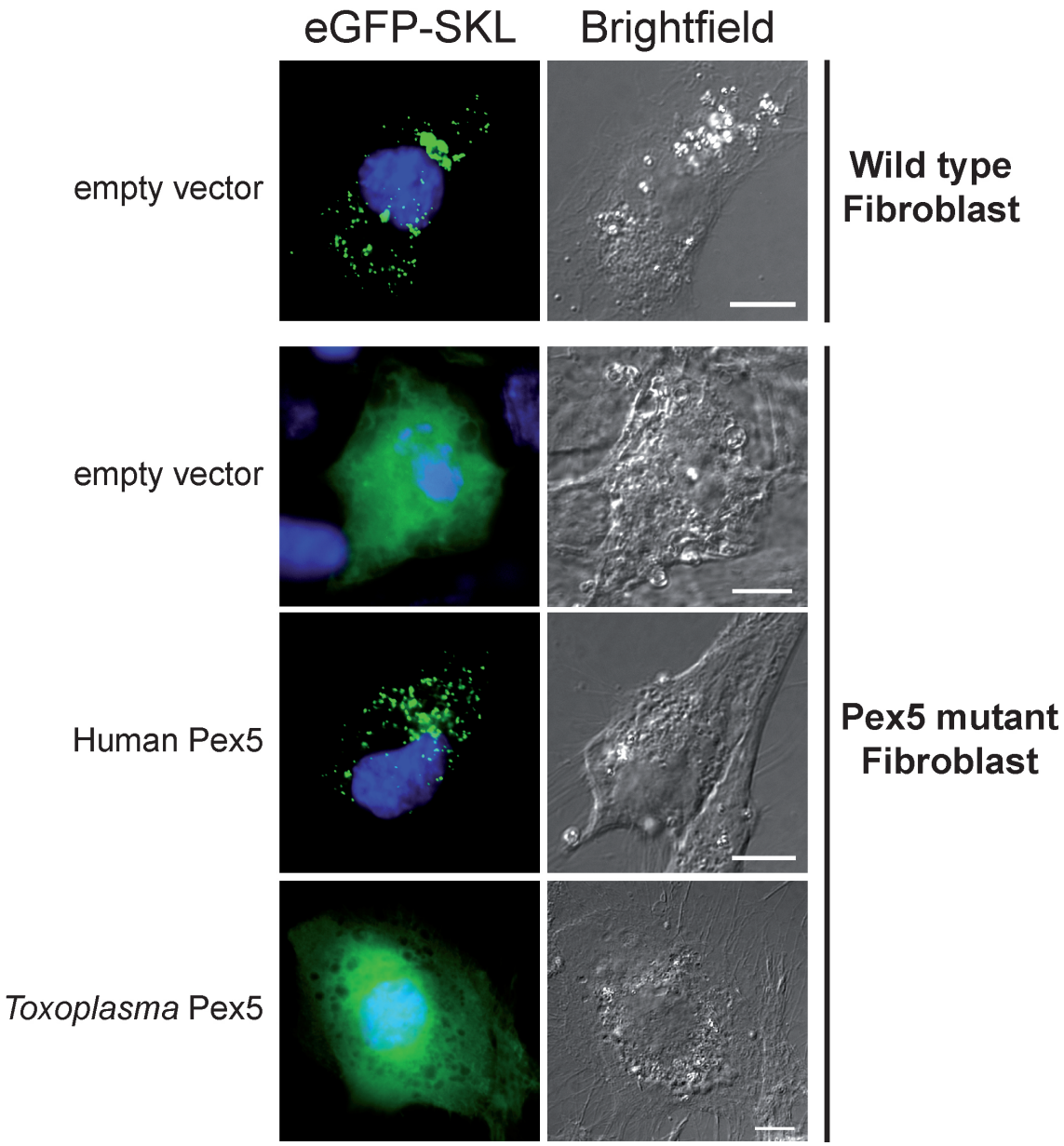

Figure 6.8: *Tg*Pex5 human fibroblast complementation immunoflorecence assay shows that *Toxoplasma* Pex5 does not complement Pex5 in Pex5 mutant fibroblasts. *Toxoplasma* Pex5 and empty vector both show GFP signal throughout the cytoplasm where as the positive control, human Pex5 with Pex5 mutant fibroblast do show localised peroxisomes. The scale bar is 10 µM.

In summary, these complementation studies indicate that the heterologous *Tg*Pex5 targets not only the artificial cargo GFP-PTS1, but also the endogenous yeast enzymes, into peroxisomes. Interestingly, this restored translocation of *Tg*Pex5 into the organellar lumen of not only the β-oxidation enzymes with typical PTS1, but also of the non-PTS acyl-CoA oxidase Fox1. Fox1 is the initial enzyme required for

the fatty acid catabolic pathway. This also fits with the Fox1 binding regions have being assigned to the N-terminal half of *Sc*Pex5 [107].

In conclusion, the functionality of mutant Pex5 yeast cells was restored when *Toxoplasma* Pex5 was introduced, showing that it is a functional equivalent. Additionally, the analysis also indicates that *Tg*Pex5 is cannot functionally replace the human version of Pex5. Ideally we would show that *Toxoplasma* Pex5 localise directly to the peroxisomes of *Toxoplasma* [80].

6.4 Localising peroxisomes in *T .gondii*

6.4.1 *In vitro* localisation of GFP-*Tg*SCP2 in wild-type *T. gondii*

After the transfection of parasites with *Tg*SCP2-TUB8-myc-GFP-myo-ATy-HX (Chapter 2) the transfected parasites were fixed and subsequently stained with DAPI, anti-IMC inner membrane complex (IMC) and anti-GFP antibody. Figure 6.9 shows a merged image of all three of these stains after 24 hours incubation. The nuclei of both the parasite and HFF cells can be visualised using DAPI, as all four parasites nuclei are stained blue. The IMC which is only present in the parasite, is stained red in all four *T. gondii*. GFP-tagged *Tg*SCP2 localises at the basal end of wild-type *T. gondii*, suggesting that *Tg*SCP2, with its PTS1 site, is co-localising with *Tg*Pex5 or *Tg*Pex5 like molecule at basal end of the parasite. This localisation of GFP-tagged *Tg*SCP2 to the basal end of wild-type *T. gondii* is similar to that found previously [24] Overexpression of GFP-tagged protein has been shown to localise at the basal end of the parasite before, so in order to clarify this specificity we employed GFP-ePTS1.

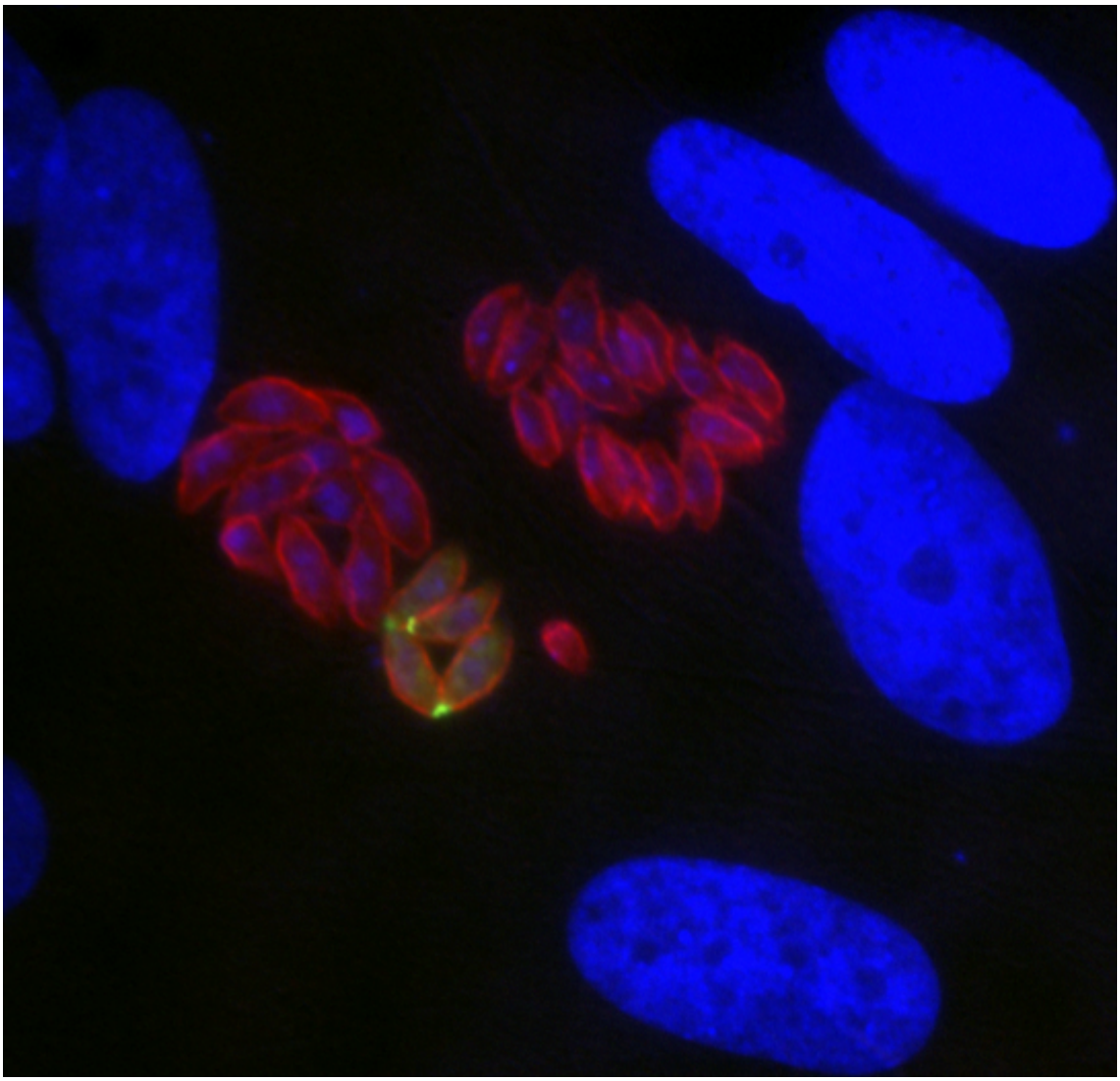

Figure 6.9: GFP--tagged *Tg*SCP2 localises at basal end of parasite when transiently expressed in *Toxoplasma.* GFP-SCP2 is stained with anti-GFP antibody (green) and the parasite pellicle stained with anti-IMC1 antibody (red) and nuclei stained with DAPI (blue). The scale bar is 1 µM.

6.4.2 *In vitro* localisation of GFP–ePTS1 in wild-type *T. gondii*

In collaboration with Dr. Lilach Sheiner at Glasgow University.

In order to provide clearer quantitative analysis of the localisation of peroxisomes within toxoplasma tachyzoites, enhanced (e)PTS1 was used. The GFP–ePTS1 which had been identified and used in yeast is a more efficient way of localising PTS1 proteins when florencently tagged [75]. Therefore, when GFP-ePTS1 was ex-

pressed in *Toxoplasma,* clear round bodies with diameters ranging from129-311 nm were visible (Figure 6.10) This is similar to the sizes reported for peroxisomes with a region of 100–200 nm and previous observations in this parasite [50] [52].

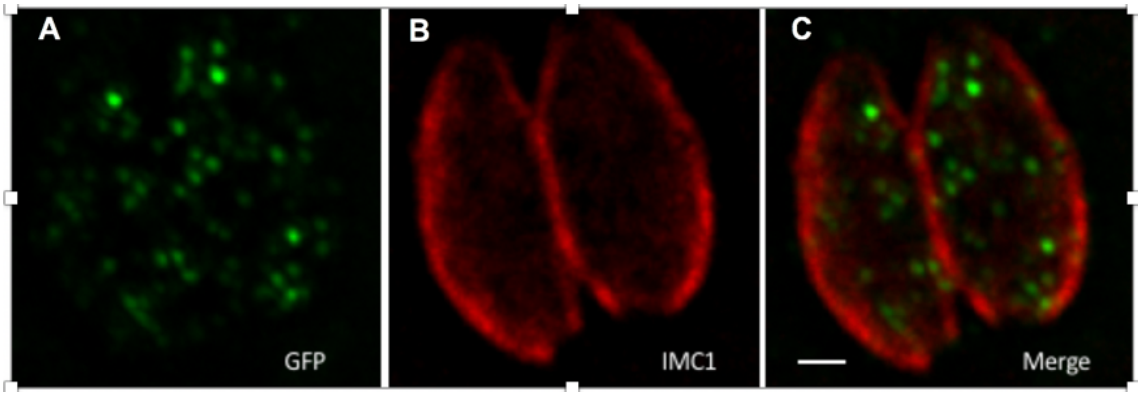

Figure 6.10: GFP tagged with ePTS1 localised to peroxisome-like bodies when transiently expressed in *Toxoplasma.* Two parasites within a HHF vacuole are seen with, GFP-ePTS1 stained with anti-GFP antibody (A, green), the parasite pellicle stained with anti-IMC1 antibody (B, red), and a merge of A and B (C). The scale bar is 1 µM.

This finial observation of punctate structures after localisation indicates that PTS1 co-localises with Pex5 within *Toxoplasma* and supports the interactions between theses two proteins observed previously in *S. cerevisiae.* The determination of a gennuine interaction between PTS1 and the C-terminal end of these Pex proteins was further investigated by examining recombinant protein interactions *in vitro*

6.5 *Tg*SCP2 and *Tg*Pex5 protein expression and purification

6.5.1 Protein expression of HIS-GST-TEV-*Tg*SCP2$_{\text{PTS1}}$ and HIS-GST-TEV-*Tg*Pex5$_{\text{C-TERMINAL}}$

Having identified peroxisome like structures in *Toxoplasma,* recombinant Pex proteins were expressed and purified in order to establish an interaction between *Tg*SCP2

and *Tg*Pex5. Individual expression of the *T.gondii* fusion proteins , HIS-GST-TEV-*Tg*Pex5$_{\text{C-TERMINAL}}$ and HIS-GST-TEV-*Tg*SCP2$_{\text{PTS1}}$ was successful in *E. coli* BL21 cells.

6.5.2 HIS-GST-TEV-*Tg*SCP2$_{\text{PTS1}}$ protein purification

Expression of HIS-GST-TEV-*Tg*SCP2$_{\text{PTS1}}$ was followed by several purification steps. The first stage of the purification was to pass the filtered sample containing protein from the soluble lysate through a GSTrap column. The eluted protein from this column was visualised by SDS-PSGE as shown in Figure 6.11 (A) The band at approximately 43.4 kDa representing HIS-GST-TEV-*Tg*SCP2$_{\text{PTS1}}$fusion protein and overexpressed HIS$_6$-GST at approximately 29 KDa. Following TEV protease digestion in (B), three bands noted: un-cleaved HIS-GST-TEV-*Tg*SCP2$_{\text{PTS1}}$, HIS$_6$-GST and *Tg*SCP2$_{\text{PTS1}}$. After passingthis sample through the nickel affinity column (NI-NTA) purified *Tg*SCP2$_{\text{PTS1}}$can be observed (C) at approximately 14.6 KDa. In summary *Tg*SCP2$_{\text{PTS1}}$ protein was successfully overexpressed and purified.

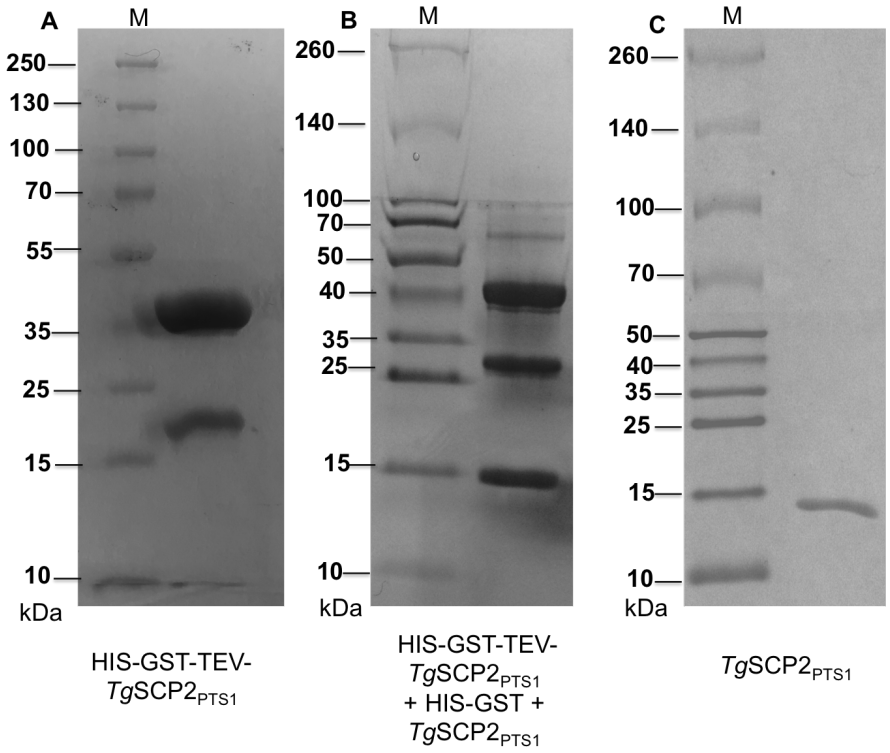

Figure 6.11: Purification steps of $Tg\text{SCP2}_{\text{PTS1}}$analysed by SDS-PAGE. 12.5% SDS-PAGE gels of purified HIS-GST-TEV-$Tg\text{SCP2}_{\text{PTS1}}$ & $Tg\text{SCP2}_{\text{PTS1}}$ shown alongside a 100 kDa ladder. Expected bands at 43.4 kDa (A) for fusion protein HIS-GST-TEV-$Tg\text{SCP2}_{\text{PTS1}}$, and after TEV protease digestion in gel (B) $Tg\text{SCP2}_{\text{PTS1}}$(14.6 kDa) HIS-GST-tag (29 kDa) and undigested fusion protein HIS-GST-TEV-$Tg\text{SCP2}_{\text{PTS1}}$. In (C) Sample after the Ni-NTA column, showing purified $Tg\text{SCP2}_{\text{PTS1}}$(14.6 kDa).

6.5.3 HIS-GST-TEV-*Tg*Pex5$_{\text{C-TERMINAL}}$ protein purification

As with HIS-GST-TEV-$Tg\text{SCP2}_{\text{PTS1}}$, the first stage in purification of the $Tg\text{PEX5}_{\text{C-TERMINAL}}$ protein was to pass the cell lyste through a GSTrap column. Eluted protein form this column contained the full-length fusion protein as shown in Figure 6.12 (A). The single band at approximately 62.5 kDa represents the HIS-GST-TEV-$Tg\text{PEX5}_{\text{C-TERMINAL}}$fusion. TEV protease digestion produced, two bands. SDS-PAGE consisting of the cleaved $Tg\text{Pex5}_{\text{C-TERMINAL}}$ (35.4 kDa) and the HIS_6-GST tag (29 kDa) Figure 6.12 (B). Nickel affinity chromatography of this mixture yielded pure $Tg\text{Pex5}_{\text{C-TERMINAL}}$ at approximately 34.5 kDa Figure 6.12 (C). Hence the $Tg\text{Pex5}_{\text{C-TERMINAL}}$ protein was successfully expressed and purified.

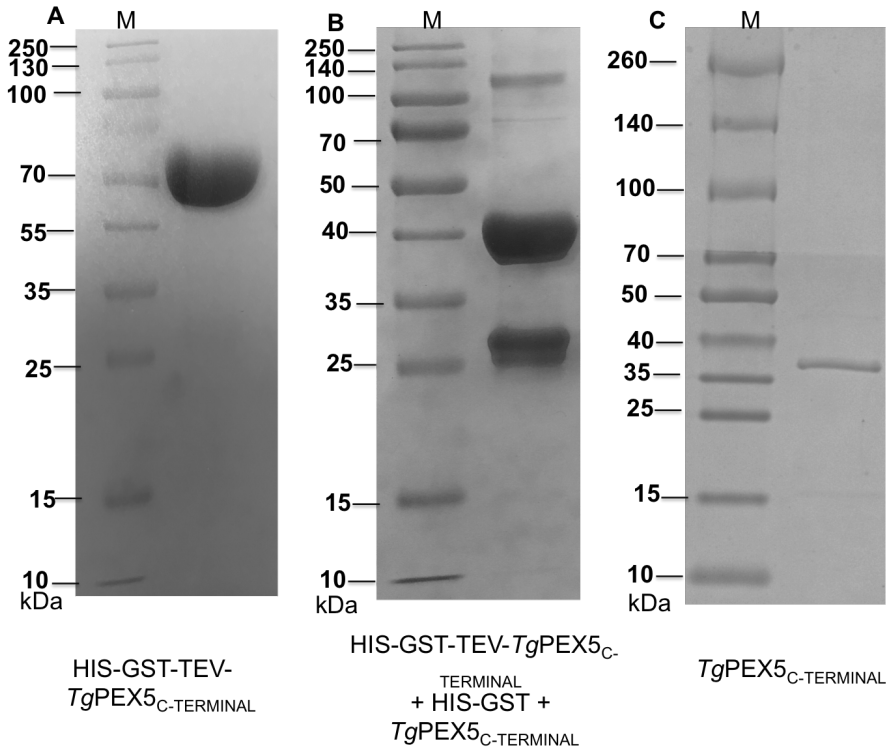

Figure 6.12: Purification of TgPex5$_{\text{C-TERMINAL}}$followed by SDS-PAGE . A 100 kDa ladder washed as a marker on SDS-PAGE gels stained purified HIS-GST-TEV-TgPEX5$_{\text{C-TERMINAL}}$ gave a single band of the expected size of 62.5 kDa (A). Fusion protein HIS-GST-TEV-TgPex5$_{\text{C-TERMINAL}}$, after TEV protease digestion (B) produces TgPex5$_{\text{C-TERMINAL}}$at 35.4 kDa and HIS-GST tag at 29 KDa. Purified TgPex5$_{\text{C-TERMINAL}}$ was eluted after passing through a Ni-NTA column (C)

6.6 Pull-Down Assay

Having successfully expressed and purified recombinant TgSCP2 and TgPex5, a series of experiments were undertaken to investigate the interaction between the PTS1 end of SCP2 and the C-terminal end of Pex5. A small scale affinity pull down assay was used to detecti protein-protein interactions. The GST-$_{\text{Trap}}$column was used to immobilise the fusion tagged TgSCP2$_{\text{PTS1}}$protein which acted as "bait." Bound HIS-GST-TEV-TgSCP2$_{\text{PTS1}}$was then used to trap and bind predicted binding partner, TgPex5$_{\text{C-TERMINAL}}$which is untagged. After incubation of this "prey" protein on the GST-$_{\text{Trap}}$column, and several wash steps, the resulting mixture was analyzed by SDS-PAGE.

6.6.1 HIS-GST-TEV-*Tg*SCP2$_{\text{PTS1}}$ with purified *Tg*Pex5$_{\text{C-TERMINAL}}$

Previous pull-down assays performed by Dr W. A Stanely, (Figure 6.14) showed that immobilise *bait* protein HIS-GST-TEV-*Tg*SCP2$_{\text{PTS1}}$ bind to purified *Tg*Pex5$_{\text{C-TERMINAL}}$ on a GST-$_{\text{Trap}}$ column. HIS-GST-TEV-*Tg*SCP2$_{\text{PTS1}}$ at 43.4 kDa bound to column and showed a protein-protein interaction with *prey* protein *Tg*Pex5$_{\text{C-TERMINAL}}$ (34.5 kDa)

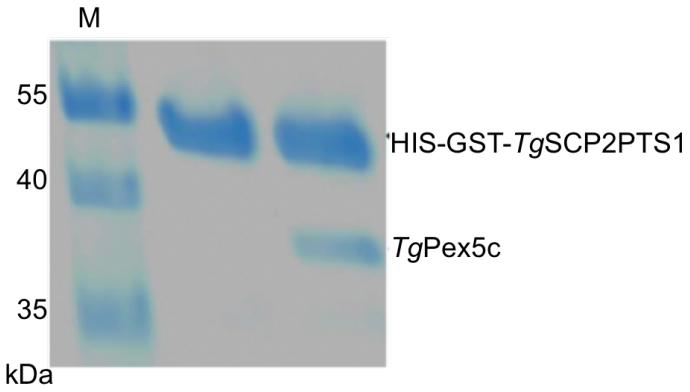

Figure 6.13: Interaction of *Tg*SCP2$_{\text{PTS1}}$ and purified *Tg*Pex5$_{\text{C-TERMINAL}}$ *in vitro*. The pull-down assay was performed using *bait* HIS-GST-TEV-*Tg*SCP2$_{\text{PTS1}}$. Eluates of the pull-down without prey protein (Lane 1, negative control) and *Tg*Pex5C (Lane 2)

6.6.2 HIS-GST-TEV-*Tg*Pex5$_{\text{C-TERMINAL}}$ with purified *Tg*SCP2$_{\text{PTS1}}$

Having confirmed a successful interaction between the *Tg*SCP2$_{\text{PTS1}}$ with purified *Tg*Pex5$_{\text{C-TERMINAL}}$, a further pull down assay was carried out to confirm the same interaction using a different bait protein. For this the HIS-GST-TEV-*Tg*Pex5$_{\text{C-TERMINAL}}$ was used with purified *Tg*SCP2$_{\text{PTS1}}$ (Figure 6.14). A fresh GST-$_{\text{Trap}}$ column was used to immobilise the HIS-GST-TEV-*Tg*Pex5$_{\text{C-TERMINAL}}$ and the column washed to remove any unbound bait protein (visable in fractions 1-5) (Figure 6.14 A), showing unbound HIS-GST-TEV-*Tg*Pex5$_{\text{C-TERMINAL}}$ at ~62.5 kDa and traces of GST-tag at ~29 kDa. After the application of purified *Tg*SCP2$_{\text{PTS1}}$ to the immobilised fusion protein (Figure 6.14 B) bands at ~29 kDa for the GST-tag and at ~14.6 kDa for unbound *Tg*SCP2$_{\text{PTS1}}$ were detected in fractions 3-8.

Any protein-protein interaction between bait and prey proteins was revealed by column in fractions 1-3 (*) which shows both HIS-GST-TEV-*Tg*Pex5$_{\text{C-TERMINAL}}$ (62.5

kDa) and *Tg*SCP2$_{\text{PTS1}}$(14.6 kDa) coeluting. A protein-protein interaction between HIS-GST-TEV-*Tg*Pex5$_{\text{C-TERMINAL}}$and purified *Tg*SCP2$_{\text{PTS1}}$can be seen in the pull-down assay (Figure 6.14 C).

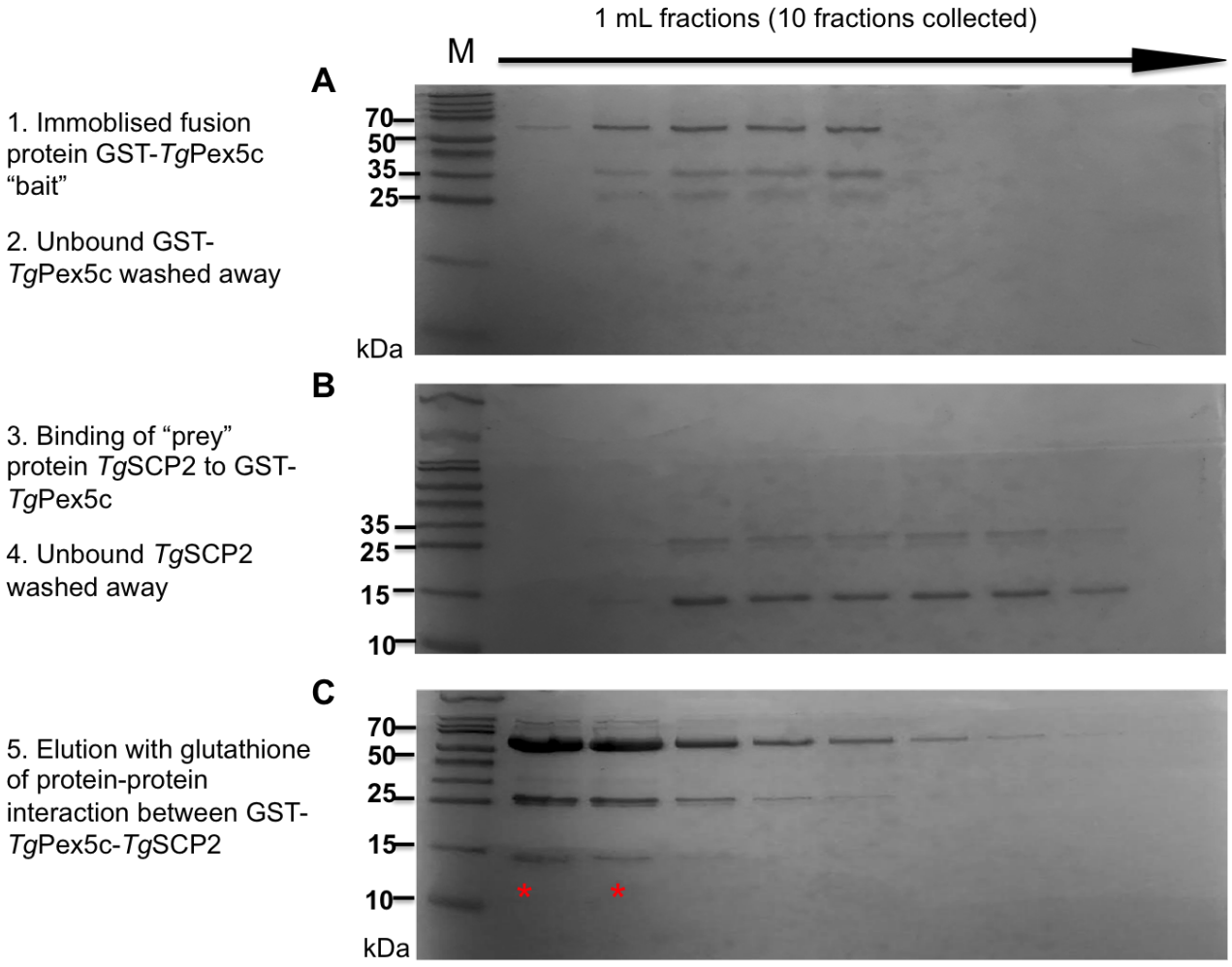

Figure 6.14: Interaction of HIS-GST-TEV-*Tg*PEX5$_{\text{C-TERMINAL}}$with purified *Tg*SCP2$_{\text{PTS1}}$. *in vitro*. Steps 1 and 2 involved loading GST column with fusion protein HIS-GST-TEV-*Tg*PEX5$_{\text{C-TERMINAL}}$and washing off any unbound bait. Unbound fusion protein is evident on (A) SDS gel. (B) SDS gel steps 3 and 4 involved loading prey protein *Tg*SCP2$_{\text{PTS1}}$. and washing away any unbound purified protein. (C) SDS page shows the GST-tag at 29 KDa and the protein-protein (*)interaction between HIS-GST-TEV-*Tg*PEX5$_{\text{C-TERMINAL}}$and *Tg*SCP2$_{\text{PTS1}}$.

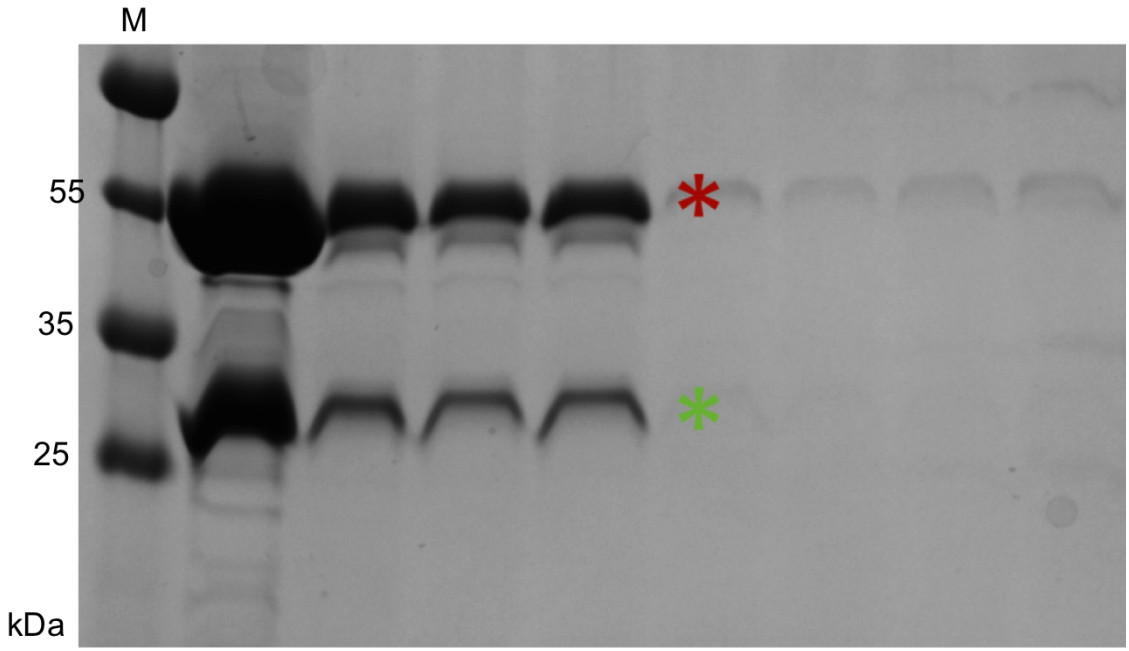

Figure 6.15: Interaction of HIS-GST-TEV-*Tg*SCP2$_{\text{PTS1.}}$with lysate *in vitro*. Pull down assay was performed using HIS-GST-TEV-*Tg*SCP2$_{\text{PTS1.}}$*bait* (*Red). Loading GST column with fusion protein HIS-GST-TEV-*Tg*SCP2$_{\text{PTS1.}}$followed by lysate addition and several washes. Unbound fusion protein is evident SDS gel with no trapped prey protein form lysate. SDS also shows the GST-tag (* Green)

6.6.3 HIS-GST-TEV-*Tg*SCP2$_{\text{PTS1}}$pull down with *Toxoplasma gondii* lysate

Having verified a successful interaction with HIS-GST-TEV-*Tg*Pex5$_{\text{C-TERMINAL}}$and purified *Tg*SCP2$_{\text{PTS1}}$ and HIS-GST-TEV-*Tg*SCP2$_{\text{PTS1}}$with purified *Tg*Pex5$_{\text{C-TERMINAL}}$. we decided to use a *T. gondii* lysate using this pull down method. For *bait* protein HIS-GST-TEV-*Tg*SCP2$_{\text{PTS1}}$was immoblised onto a GST-$_{\text{Trap}}$ column and freshly lysed tachyzoite *T. gondii*, was loaded onto the column. Interestingly, after several washes, and SDS gel analysis there were no protein-protein interactions with any of the lysate proteins (Figure *6.15*). It is likely that there are insufficient quantities from the tachyzoites to be detectable in this assay.

In summary, the *in vitro* analyses of the interaction between *Tg*SCP2$_{\text{PTS1}}$ and *Tg*Pex5$_{\text{C-TERMINAL}}$ showed that recombinant proteins expressed in *E. coli* , can be successfully isolated. When subjected to pull-down assays, protein-protein inter-

action were confirmed orientations in both *Tg*Pex5 binding to *Tg*SCP2 when the HIS-GST-TEV-*Tg*Pex5$_{\text{C-TERMINAL}}$ end was used as the bait and then vice-versa when HIS-GST-TEV-*Tg*SCP2$_{\text{PTS1}}$was used as bait. These two interchangeable experiments demonstrated that the *Tg*Pex5 can bind to the parasite PTS1. However, the tachyzoite lysate pull-down assay failed to rescue any peroxins when the bait fusion protein HIS-GST-TEV-*Tg*SCP2$_{\text{PTS1}}$in the tachyzoite form. We therefore explored this further to examine peroxins produced at the tachyzoite stage using LOPIT (Localization of organelle proteins by isotope tagging).

6.7 Exploration of Pex proteomics using LOPIT assignments

Data provided by Ross Waller University of Cambridge

Proteomic analysis by LOPIT used the method described by [108] to determine protein distributions. The results (Table 6.1) show un-detectable Pex assignments, re-affirming that expression of Pex proteins is absent or at least significantly lower in the tachyzoite stage of the parasite. Pex5, identified by the TDR domain, shows an ND (non-detectable) level. The proteomic analysis supports the experiments with the HIS-GST-TEV-*Tg*SCP2$_{\text{PTS1}}$pull down with *T. gondii*, suggesting that the level of Pex proteins is too low to be detectable from a the tachyzoite lysate.

6.8 Peroxisomal protein conclusion

*Tg*SCP2$_{\text{PTS1}}$ (-SRL) clearly binds to *Tg*Pex5$_{\text{C-TERMINAL}}$ parasite binding domain *in vitro* as shown by the two binding pull down assays and supports the hypothesis that the observed co-localisation of ePTS1-tagged GFP is due to direct interaction within peroxisome-like bodies in *Toxoplasma*. In addition, expression of heterologous *Tg*Pex5 in a Pex5 knock-out in yeast, highlights the importance of Pex5 within the

Protein	LOPIT assignment	Hit_ID	Annotation	BlastP nr	Comment
Pex1	ND	>TGME49_308960 ATPase, AAA family protein	putative peroxisome biogenesis factor 1	ATPase, AAA family protein [Toxoplasma gondii ME49]	
Pex4	ER	>TGME49_280440 ubiquitin conjugating enzyme E2, putative	peroxin-4	ubiquitin conjugating enzyme E2, putative [Toxoplasma gondii ME49]	
Pex5	ND	>TGME49_231870 tetratricopeptide repeat-containing protein	peroxisome biogenesis protein 5	tetratricopeptide repeat-containing protein [Toxoplasma gondii ME49]	
Pex6	ND	>TGME49_255210 ATPase, AAA family protein	peroxisomal biogenesis factor 6	ATPase, AAA family protein [Toxoplasma gondii ME49]	
Pex7	ND	>TGME49_201850 WD domain, G-beta repeat-containing protein	putative peroxisome biogenesis factor 7	WD domain, G-beta repeat-containing protein [Toxoplasma gondii ME49]	
Pex10	ND	>TGME49_248330 zinc finger, C3HC4 type (RING finger) domain-containing protein	Pex10	zinc finger, C3HC4 type (RING finger) domain-containing protein [Toxoplasma gondii ME49]	Pex 10, but only RING domain
Pex11	ND	>TGME49_243720 peroxisomal biogenesis factor PEX11	Pex11	peroxisomal biogenesis factor PEX11 [Toxoplasma gondii ME49]	
Pex14	ND	>TGME49_248170 hypothetical protein	peroxisomal membrane anchor	hypothetical protein TGME49_248170 [Toxoplasma gondii ME49]	Pex14 domain (incomplete) and PUB domain
Pex22	ER	>TGME49_266810 hypothetical protein	peroxisome biogenesis protein 22	hypothetical protein TGME49_266810 [Toxoplasma gondii ME49]	

Table 6.1: LOPIT data showing that Pex proteins cannot be detected (ND) in the tachyzoite stage of the parasite.

peroxisomal complex by showing that the endogenous fatty acid-degrading enzymes with or without the PTS1 site involved in the peroxisomal process were activated and used in the breakdown and utilisation of oleate. In contrast, *Toxoplasma* Pex5 was unable to direct eGFP-SKL to human fibroblast peroxisomes making it impossible to restore the functionality of their mammalian equivalent Pex5-deficient cells. Together, the two complementation experiments in yeast and human fibroblasts showed that *Tg*Pex5 is a functional orthologue and that differences in functionality between the parasite and human Pex5 could be exploited in drug target studies.

Chapter 7

Discussion and conclusions

Despite numerous efforts into the research and development of treatments towards protozoa, in particular toxoplasmosis and leishmaniasis, there are still many gaps in the development of new treatment regimes and drug targets. Further information about the mode of action and exploration of natural products as potential sources of treatment is essential for treating these debilitating diseases. The work carried out in this thesis describes the screening of natural compounds against *Leishmania* and *Toxoplasma*, as well as the identification of peroxisomes as a potential drug target within *T. gondii*. This chapter summaries and discusses the results outlined in this study, as well as highlighting the important benefits of using natural products as potential drugs against *Toxoplasma* and *Leishmania*.

7.1 Discussion

7.1.1 *Toxoplasma gondii*

The *T. gondii* parasite causes various forms of toxoplasmosis and is treatable in the acute form of the disease but more difficult to treat in the chronic stages or in pregnant women [19]. Although there are a range of treatment regimes for *T. gondii*, the current front-line drugs are limited due to a rise in drug resistant strains and

also reports of severe side effects [13, 20, 29, 30]. These issues have, created a need to discover new drug targets and demand for new compounds that are non-toxic and can be used on the encysted form of the parasite. By exploiting the biology of *T. gondii,* we were able to identify peroxisomes as a potential novel drug target within this obligate parasite. This, alongside the screening of natural compounds and peroxisome specific inhibitors against *T. gondii,* may lead to a new repertoire of compounds.

7.1.1.1 Identifying peroxisomes in *Toxoplasma gondii*

Chapter 6 of this thesis investigated the existence of peroxisomes in *Toxoplasma.* The recent bioinformatic analyses that demonstrated the presence of a family of Pex proteins in coccidian apicomplexans, but not in other subclasses [109–111], merited further functional analysis. In previous studies, the existence of *Toxoplasma* peroxisomes has proven to be controversial. *Toxoplasma* catalase (an identifier of peroxisomes) was localised to peroxisome-like vesicles in one study [52], and in the same year it was reported that the putative catalase PTS1 failed to direct GFP to these membrane-bound microbodies [51]. Another PTS1 protein, the sterol carrier protein (SCP2), has also been shown to localise to peroxisome-like bodies in *Toxoplasma* [50]. To improve the molecular understanding of the putative peroxisomal bodies in *T. gondii*, we conducted a series of cellular and biochemical experiments using the Pex5 orthologue of the parasite. We first established that *Tg*Pex5 showed significant similarity with yeast Pex5, especially in the C-terminal domain, supporting work carried out by others [24, 40, 41, 43, 45]. Furthermore, analyses of *Toxoplasma* Pex5 in a ΔPex5 yeast strain using a sequence of qualitative and quantitative methods [42, 43, 45] confirmed that the Pex5 orthologue was functional *in vitro*. Heterologous expression of *Tg*Pex5 restored the utilisation of oleate in Pex5-deficient yeast clearly demonstrating that a complete set of endogenous fatty

acid-degrading enzymes with, and without, typical PTS1 sequences are recognized and targeted to peroxisomes by the parasite peroxin. This shared cargo selectivity of the yeast and *Toxoplasma* receptor, which included Fox1, was recognized by the PTS1-independent binding domain and N-terminal of the yeast Pex5 PTS1-binding region. Importantly, unlike the mammalian orthologue, *Tg*Pex5 maintains a Fox1-binding region (a region involved in peroxisomal β-oxidation). *Tg*Pex5 was unable to direct eGFP-SKL to human fibroblast peroxisomes and thus rescue the import defect of an equivalent mammalian Pex5-deficient cell line. Taken together, this data indicates that *Tg*Pex5 is a functional orthologue of the yeast protein but not its human peroxin counterpart. This difference between the Pex proteins of these two species could be exploited when considering the *Tg*Pex5-PTS1 interaction as a drug target.

In the other, *in vitro,* studies we investigated protein-protein interactions between the *Tg*Pex5 receptor and its associated protein ligand *Tg*SCP2 in pull down binding assays. Successful purification of $Tg\text{Pex5}_{\text{C-terminal}}$ and $Tg\text{SCP2}_{\text{PTS1}}$ proteins allowed us to show protein-protein interaction between *Toxoplasma* peroxisomal proteins $Tg\text{Pex5}_{\text{C-terminal}}$ and $Tg\text{SCP2}_{\text{PTS1C-terminal}}$ and vice versa with $Tg\text{SCP2}_{\text{PTS1}}$ and $Tg\text{Pex5}_{\text{C-terminal}}$. The interaction with $Tg\text{SCP2}_{\text{PTS1}}$, showed that the *Toxoplasma* Pex5 can bind to the parasite PTS1. However, a similar pull-down assay designed to fish for further Pex proteins in tachyzoite lysates was unsuccessful. These findings were later confirmed by LOPIT data which indicates that the level of Pex proteins is too low to be detected at this stage of the parasite life cycle.

Localization studies of yeast-derived ePTS1 were sufficient to localise GFP to peroxisome-like bodies in *Toxoplasma* and like [50, 52], other PTS1 proteins the SRL domain clearly binds to the parasite *Tg*Pex5 PTS1-binding domain *in vitro.*

In summary, the investigations carried out here, strongly suggest that this apicomplexan parasite has peroxisomes. The relative lack of structural evidence may be due to lifecycle-dependent expression, with the peroxins characterised by upregula-

tion during the extracellular stages of the lifecycle, oocysts and sporozoites. Future studies should be directed here, rather than at the more tractable, intracellular, tachyzoite forms [111].

7.1.1.2 Natural products and Pex inhibitor screen

Frontline drugs in the treatment of toxoplasmosis have a higher cure rate in tachyzoites, however, current drug therapies are problematic and have extended treatment periods with long lasting toxic side effects when targeting encysted forms of *T. gondii* [13,30]. The result is that, available drugs that fail to be effective against *T.gondii* tissue cysts, create a challenge when trying to develop compounds with short treatment courses. Current problems facing toxoplasmosis drug discovery today include finding a novel compound effective against the encysted parasite [8,30]. Previous research has shown that the repurposing of medicines for protozoa is one way of tackling treatment [1,7]. Pex5-Pex14 inhibitors (Chapter 5) have previously been identified as disrupting glycosomal protein import and killing trypanosomes by affecting the Pex5-interaction in *T. brucei* and have been shown to be active against Pex14 in other related protozoa, such as *T. cruzi* and *Leishmania* [102]. Here we decided to screen these inhibitors against *T. gondii* intracellular tachyzoites, and were able to identify 11 Pex5-Pex14 inhibitors that gave an $EC_{50} < 10$ μM. However, despite the significant inhibition rate the majority of the compounds demonstrated high mammalian toxicity. Optimization of these compounds to make them non-toxic to mammalian cells could be pursued and lead to the development of a new class of specific Pex protein inhibitor for *T.gondii.* In addition to the repurposing of the Pex5-Pex14 inhibitors we also tested a natural compound Aureobasidin A (AbA) and several derivatives against *Toxoplasma.* For this an existing bradyzoite *in vitro* drug assay [78,92] was optimized to test AbA and derivatives against encysted forms of *T.gondii.* AbA, Compound 3, and Compound 20 demonstrated

good efficacy against these forms, suggesting that the cyclic depsipeptides represent promising candidates for therapies to treat both acute and chronic toxoplasmosis.

7.1.2 *Leishmania mexicana*

Cutaneous Leishmaniasis is caused by New World species *L. mexicana,* and with recent publications showing the rise in the cases of leishmaniasis at a global level, investigations into the use of natural compounds for the treatment of various forms of leishmaniasis has become crucial [15, 28, 56]. As for toxoplasmosis, the current treatments are both toxic, and have increasing reports of resistance. To improve and increase the number potential antileishmanials, researchers have screened naturally-derived compounds in *in vitro* assays [60, 62, 66, 69].

7.1.2.1 Natural product screen

In Chapter 3 using an iterative screening and fractionation approach we 'mined' the HDLSX Hypha compound library of 313 fungal extracts which contain a large number of small molecule secondary metabolites. Using well established *Leishmania in vitro* assays [54, 87] we were able to identify four compounds with anti-leishmanial properties (EC_{50} of less than 10 μM) in the axenic assay and *L. mexicana* intra-macrophage and two compounds showing low mammalian cytotoxicity. HD871-2 and the pure secondary fractionation component, HD871-1 with a molecular weight of 262, were identified as potent antileishmanials. HD871-1 was characterised as a novel bisabolane sesquiterpene with a high degree of oxygenation and unsaturation and structural similarities to cheimonophyllons A-E. These bisabolane sesquiterpenes isolated from fermentations of the basidiomycete *Cheimonophyllum candidissimum*, are known to possess nematicidal properties [112]. The similarity of HD871-1 to cheimonophyllons puts this molecule in the same class of compounds, which

potentially representent a new class of broad-spectrum anti-parasitics. In order to moveforward and develop antileishmanials, the identification of the mode of action was key, and here we carried out a metabolomic study on both HD871-1 and HD871-2.

7.1.2.2 Metabolomic analyses of HD871-1 and HD871-2

To begin deconvolution of the target of HD871-1 and HD871-2, in Chapter 4, metabolomics was used to identify changes to the metabolic network of *L. mexicana* amastigotes exposed to these compounds. Using a 36 hour time point and a compound dose 2-fold higher than the EC_{50}, a number of clear changes to metabolism occurred. These included changes in the deoxynucleotide pool and therefore represent possible effects on nucleotide metabolism, although whether this was the cause of cell death, or a secondary effect due to other changes, is not clear. A reduction in the levels of the chief redox reactive thiol trypanothione and accumulation of cystine pointed to oxidative stress being induced by HD871-1 and HD871-2. Since both reduced and oxidised trypanothione was diminished, as was glutathione, a possible role is drug binding prior to efflux from the cell, as apparent with the parasite response to antimony [113]. Trypanothione enzymes potentially targeted by these compounds would be worthy of future investigation as has been shown when eflornithine is used against *T. brucei* [4]. In *Leishmania donovani* for example, Sb(III) interferes with thiol metabolism, leading to decreased thiol-buffering capacity, but is also involved in the inhibition of trypanothione reductase which results in a lethal imbalance in thiol homeostasis [114]. This similarity of HD871-1 and HD871-2 to Sb(III) is of particular interest as the effects of the biological activity of our tested compounds seem to show similar the mode of action of Sb(III), which is related to clinically prescribed Sb(V) [114].

7.2 Conclusions

The results described in this thesis illustrate the discovery of two novel natural compounds that are active against *L. mexicana,* are non-toxic to mammalian cells, and have a low EC_{50}, with a suggested mode of action. This new knowledge allowed the identification of a novel class of compounds which could be used in the future treatment of leishmaniasis. The other breakthrough investigation was the confirmation of peroxisomes in *Toxoplasma* and we were able to identify these as organelles for further drug target studies.

7.3 Proposed Future work

From the work carried out in this thesis, the following key areas are identified as potential avenues for future work:

Further confirmation on the mode of action of compounds HD871-1 and HD871-2; they could both be screened in trypanothione reductase and synthase assays to revel the mode of action, similar to the kinetic analysis experiments of these enzymes carried out in *Trypansoma brucei* [5]

Breakthrough knowledge of peroxisomes in *Toxoplasma* could be exploited by considering the *Tg*Pex5-PTS1 interaction as a potential drug target, as there is a clear difference between the Pex proteins from humans and this apicomplexan parasite. The Pex5-PTS1 complex has been examined in *Trypansoma brucei* as a potential drug target [115].

Exploration into peroxisomes in the extracellular stages of *T. gondii* is essential to fully understand the role of peroxisomes in *Toxoplasma* oocysts. In addition, further investigation into other Pex proteins such as *Tg*Pex7 and *Tg*Pex14 and functional analyses using technologies such as CRISPR-Cas9 are essential for fuller understanding [116].

Bibliography

[1] G. A. Biagini, N. Fisher, A. E. Shone, M. A. Mubaraki, A. Srivastava, A. Hill, T. Antoine, A. J. Warman, J. Davies, C. Pidathala, R. K. Amewu, S. C. Leung, R. Sharma, P. Gibbons, D. W. Hong, B. Pacorel, A. S. Lawrenson, S. Charoensutthivarakul, L. Taylor, O. Berger, A. Mbekeani, P. A. Stocks, G. L. Nixon, J. Chadwick, J. Hemingway, M. J. Delves, R. E. Sinden, A.-M. Zeeman, C. H. M. Kocken, N. G. Berry, P. M. O'Neill, and S. A. Ward, "Generation of quinolone antimalarials targeting the Plasmodium falciparum mitochondrial respiratory chain for the treatment and prophylaxis of malaria.," *Proceedings of the National Academy of Sciences of the United States of America*, vol. 109, pp. 8298–303, may 2012.

[2] R. Sharma, A. S. Lawrenson, N. E. Fisher, A. J. Warman, A. E. Shone, A. Hill, A. Mbekeani, C. Pidathala, R. K. Amewu, S. Leung, P. Gibbons, D. W. Hong, P. Stocks, G. L. Nixon, J. Chadwick, J. Shearer, I. Gowers, D. Cronk, S. P. Parel, P. M. O'Neill, S. A. Ward, G. A. Biagini, and N. G. Berry, "Identification of novel antimalarial chemotypes via chemoinformatic compound selection methods for a high-throughput screening program against the novel malarial target, PfNDH2: increasing hit rate via virtual screening methods.," *Journal of medicinal chemistry*, vol. 55, pp. 3144–54, apr 2012.

[3] A. Olotu, P. Moris, J. Mwacharo, J. Vekemans, D. Kimani, M. Janssens, O. Kai, E. Jongert, M. Lievens, A. Leach, T. Villafana, B. Savarese, K. Marsh, J. Cohen, and P. Bejon, "Circumsporozoite-specific T cell responses in children vaccinated with RTS,S/AS01E and protection against P falciparum clinical malaria.," *PloS one*, vol. 6, p. e25786, jan 2011.

[4] I. M. Vincent, D. J. Creek, K. Burgess, D. J. Woods, R. J. S. Burchmore, and M. P. Barrett, "Untargeted Metabolomics Reveals a Lack Of Synergy between Nifurtimox and Eflornithine against Trypanosoma brucei," *PLoS Neglected Tropical Diseases*, vol. 6, p. e1618, may 2012.

[5] M. Beig, F. Oellien, L. Garoff, S. Noack, R. L. Krauth-Siegel, and P. M. Selzer, "Trypanothione reductase: a target protein for a combined in vitro and in silico screening approach.," *PLoS neglected tropical diseases*, vol. 9, no. 6, p. e0003773, 2015.

[6] WHO, "WHO | Leishmaniasis," 2017.

[7] S. C. Leung, P. Gibbons, R. Amewu, G. L. Nixon, C. Pidathala, W. D. Hong, B. Pacorel, N. G. Berry, R. Sharma, P. A. Stocks, A. Srivastava, A. E. Shone, S. Charoensutthivarakul, L. Taylor, O. Berger, A. Mbekeani, A. Hill, N. E. Fisher, A. J. Warman, G. A. Biagini, S. A. Ward, and P. M. O'Neill, "Identification, design and biological evaluation of heterocyclic quinolones targeting Plasmodium falciparum type II NADH:quinone oxidoreductase (PfNDH2).," *Journal of medicinal chemistry*, vol. 55, pp. 1844–57, mar 2012.

[8] M. Antczak, K. Dzitko, and H. Długońska, "Human toxoplasmosis - Searching for novel chemotherapeutics," *Biomedicine & Pharmacotherapy*, vol. 82, pp. 677–684, aug 2016.

[9] B. Tiwari, R. Pahuja, P. Kumar, S. K. Rath, K. C. Gupta, and N. Goyal, "Nanotized Curcumin and Miltefosine, a Potential Combination for Treatment of Experimental Visceral Leishmaniasis," *Antimicrobial agents and chemotherapy*, vol. 61, no. 3, 2016.

[10] M. J. Delves, F. Angrisano, and A. M. Blagborough, "Antimalarial Transmission-Blocking Interventions: Past, Present, and Future.," *Trends in parasitology*, vol. 34, pp. 735–746, sep 2018.

[11] T. S. S.-A. Katherine, T. Andrews, Gillian Fisher, "Drug repurposing and human parasitic protozoan diseases," *International Journal for Parasitology: Drugs and Drug Resistance*, vol. 4, no. March 2016, pp. 95–111, 2011.

[12] S. Sonda, G. Sala, R. Ghidoni, A. Hemphill, and J. Pieters, "Inhibitory Effect of Aureobasidin A on Toxoplasma gondii," *Antimicrobial Agents and Chemotherapy*, vol. 49, pp. 1794–1801, may 2005.

[13] P. G. Wuts, L. J. Simons, B. P. Metzger, R. C. Sterling, J. L. Slightom, and A. P. Elhammer, "Generation of Broad-Spectrum Antifungal Drug Candidates from the Natural Product Compound Aureobasidin A," *ACS Medicinal Chemistry Letters*, vol. 6, no. 6, pp. 645–649, 2015.

[14] P. Mubashir Hussain, S. Munir, T. Ali Khan, A. Khan, S. Ayaz, M. Ameen Jamal, I. Ahmed, S. Aziz, N. Watany, M. Kasbari, M. Hussain, S. Munir, T. Khan, A. Khan, A. Wali Khan University, and M. Jamal, "Emerging Infectious Diseases," *Emerging Infectious Diseases*, vol. 24, no. 1, 2018.

[15] N. Salam, W. M. Al-Shaqha, and A. Azzi, "Leishmaniasis in the Middle East: Incidence and Epidemiology," *PLoS Neglected Tropical Diseases*, vol. 8, no. 10, pp. 1–8, 2014.

[16] R. Du, P. J. Hotez, W. S. Al-Salem, and A. Acosta-Serrano, "Old World Cutaneous Leishmaniasis and Refugee Crises in the Middle East and North Africa," *PLoS Neglected Tropical Diseases*, vol. 10, no. 1371, pp. 1–11, 2016.

[17] K. Hayani, A. Dandashli, and E. Weisshaar, "Cutaneous Leishmaniasis in Syria: Clinical Features, Current Status and the Effects of War," *Acta Dermato Venereologica*, vol. 95, no. 1, pp. 62–66, 2015.

[18] Z.-D. Wang, S.-C. Wang, H.-H. Liu, H.-Y. Ma, Z.-Y. Li, F. Wei, X.-Q. Zhu, and Q. Liu, "Prevalence and burden of Toxoplasma gondii infection in HIV-infected people: a systematic review and meta-analysis.," *The lancet. HIV*, vol. 4, pp. e177–e188, apr 2017.

[19] J. B. McAuley, "Congenital toxoplasmosis," *Journal of the Pediatric Infectious Diseases Society*, vol. 3, no. SUPPL1, pp. 30–35, 2014.

[20] A. Palencia, A. Bougdour, M.-P. Brenier-Pinchart, B. Touquet, R. Bertini, C. Sensi, G. Gay, J. Vollaire, V. Josserand, E. Easom, Y. R. Freund, H. Pel-

loux, P. J. Rosenthal, S. Cusack, and M. Hakimi, "Targeting Toxoplasma gondii CPSF3 as a new approach to control toxoplasmosis," *EMBO Molecular Medicine*, vol. 9, pp. 385–394, mar 2017.

[21] Y. Nishikawa, F. Quittnat, T. T. Stedman, D. R. Voelker, J. Y. Choi, M. Zahn, M. Yang, M. Pypaert, K. A. Joiner, and I. Coppens, "Host cell lipids control cholesteryl ester synthesis and storage in intracellular Toxoplasma," *Cellular Microbiology*, vol. 7, no. 6, pp. 849–867, 2005.

[22] C. Jin, K. Kaewintajuk, J. Jiang, W. Jeong, M. Kamata, H.-S. KIM, Y. Wataya, and H. Park, "Toxoplasma gondii: A simple high-throughput assay for drug screening in vitro," *Experimental Parasitology*, vol. 121, pp. 132–136, feb 2009.

[23] C.-F. Xin, H.-S. Kim, A. Sato, H.-J. Lee, Y.-W. Lee, K.-H. Pyo, and E.-H. Shin, "In vitro inhibition of Toxoplasma gondii by the anti-malarial candidate, 6-(1,2,6,7-tetraoxaspiro[7.11]nonadec-4-yl)hexan-1-ol," *Parasitology International*, vol. 65, pp. 494–499, oct 2016.

[24] I. Coppens and K. A. Joiner, "Host but Not Parasite Cholesterol Controls Toxoplasma Cell Entry by Modulating Organelle Discharge," *Molecular Biology of the Cell*, vol. 14, pp. 3804–3820, 2003.

[25] G. Friedman, "The next 100 years," *New Statesman*, vol. 138, no. 4964, pp. 16–20, 2009.

[26] J. P. Dubey, D. S. Lindsay, and C. A. Speer, "Structures of Toxoplasma gondii tachyzoites, bradyzoites, and sporozoites and biology and development of tissue cysts," *Clinical Microbiology Reviews*, vol. 11, no. 2, pp. 267–299, 1998.

[27] F. Robert-Gangneux and M.-L. Darde, "Epidemiology of and Diagnostic Strategies for Toxoplasmosis," *Clinical Microbiology Reviews*, vol. 25, pp. 264–296, apr 2012.

[28] K. J. Esch and C. A. Petersen, "Transmission and Epidemiology of Zoonotic Protozoal Diseases of Companion Animals," *Clinical Microbiology Reviews*, vol. 26, no. 1, pp. 58–85, 2013.

[29] S. B. Porter and M. A. Sande, "Toxoplasmosis of the Central Nervous System in the Acquired Immunodeficiency Syndrome," *New England Journal of Medicine*, vol. 327, pp. 1643–1648, dec 1992.

[30] P. Holland Alday and J. Stone Doggett, "Drug Design, Development and Therapy Dovepress Drugs in development for toxoplasmosis: advances, challenges, and current status," *Drug Design, Development and therapy*, vol. 11, pp. 273–293, 2017.

[31] F. Seeber and S. Steinfelder, "Recent advances in understanding apicomplexan parasites," *F1000Research*, vol. 5, no. 0, p. 1369, 2016.

[32] C. Duve, "Evolution of the peroxisome," *Annals of the New York Academy of Sciences*, vol. 168, pp. 369–381, dec 1969.

[33] M. L. Ginger, G. I. Mcfadden, and P. A. M. Michels, "Rewiring and regulation of cross-compartmentalized metabolism in protists," *Phil. Trans. R. Soc. B*, vol. 365, pp. 831–845, 2010.

[34] V. Zarsky and J. Tachezy, "Evolutionary loss of peroxisomes - not limited to parasites," *Biology Direct*, vol. 10, no. 1, p. 74, 2015.

[35] M. Schrader and H. D. Fahimi, "The peroxisome: Still a mysterious organelle," *Histochemistry and Cell Biology*, vol. 129, no. 4, pp. 421–440, 2008.

[36] Ida J van der Klei and Marten Veenhuis, "Peroxisomes: flexible and dynamic organelles," *Current Opinion in Cell Biology*, vol. 14, no. 4, pp. 500–505m, 2002.

[37] R. Rucktäschel, W. Girzalsky, and R. Erdmann, "Protein import machineries of peroxisomes," *Biochimica et Biophysica Acta - Biomembranes*, vol. 1808, no. 3, pp. 892–900, 2011.

[38] C. P. Williams and W. a. Stanley, "Peroxin 5: A cycling receptor for protein translocation into peroxisomes," *International Journal of Biochemistry and Cell Biology*, vol. 42, no. 11, pp. 1771–1774, 2010.

[39] D. Soldati and J. C. Boothroyd, "Transient transfection and expression in the obligate intracellular parasite Toxoplasma gondii," *Science*, vol. 260, pp. 349–352, apr 1993.

[40] W. A. Stanley and M. Wilmanns, "Dynamic architecture of the peroxisomal import receptor Pex5p," *Biochimica et Biophysica Acta - Molecular Cell Research*, vol. 1763, no. 12, pp. 1592–1598, 2006.

[41] W. a. Stanley, K. Fodor, M. a. Marti-Renom, W. Schliebs, and M. Wilmanns, "Protein translocation into peroxisomes by ring-shaped import receptors," *FEBS Letters*, vol. 581, no. 25, pp. 4795–4802, 2007.

[42] R. Erdmann and G. Blobel, "Identification of Pex13p, a peroxisomal membrane receptor for the PTS1 recognition factor ," 1996.

[43] R. Erdmann and W. Schliebs, "Peroxisomal matrix protein import: the transient pore model," *Nature Reviews Molecular Cell Biology*, vol. 6, pp. 738–742, sep 2005.

[44] C. de Duve, "The origin of eukaryotes: a reappraisal," *Nature Reviews Genetics*, vol. 8, p. 395, apr 2007.

[45] R. Erdmann and W.-H. Kunau, "A genetic approach to the biogenesis of peroxisomes in the yeastSaccharomyces cerevisiae," *Cell Biochemistry and Function*, vol. 10, pp. 167–174, sep 1992.

[46] T. Gabaldón and M. A. Huynen, "From Endosymbiont to Host-Controlled Organelle: The Hijacking of Mitochondrial Protein Synthesis and Metabolism," *PLoS Computational Biology*, vol. 3, no. 11, p. e219, 2007.

[47] T. Gabaldon, "Peroxisome diversity and evolution," *Philosophical Transactions of the Royal Society B: Biological Sciences*, vol. 365, no. 1541, pp. 765–773, 2010.

[48] A. Schlüter, S. Fourcade, R. Ripp, J. L. Mandel, O. Poch, and A. Pujol, "The evolutionary origin of peroxisomes: An ER-peroxisome connection," *Molecular Biology and Evolution*, vol. 23, no. 4, pp. 838–845, 2006.

[49] F. Opperdoes and P. Michels, "The glycosomes of the Kinetoplastida," *Biochimie*, vol. 75, pp. 231–234, jan 1993.

[50] B. Lige, B. Jayabalasingham, H. Zhang, M. Pypaert, and I. Coppens, "Role of an Ancestral D-Bifunctional Protein Containing Two Sterol-Carrier Protein-2 Domains in Lipid Uptake and Trafficking in Toxoplasma," *Molecular Biology of the Cell*, vol. 20, pp. 658–672, nov 2008.

[51] M. Ding, C. Clayton, and D. Soldati, "Toxoplasma gondii catalase: are there peroxisomes in toxoplasma?," *Journal of cell science*, vol. 113 (Pt 1, pp. 2409–2419, 2000.

[52] A. J. Kaasch and K. A. Joiner, "Targeting and Subcellular Localization of," *The Journal of biological chemistry*, vol. 275, no. 2, pp. 1112–1118, 2000.

[53] F. E. G. Cox, "History of Human Parasitology," *Clinical microbiology reviews*, vol. 15, no. 4, pp. 595–612, 2002.

[54] G. A. Eggimann, H. L. Bolt, P. W. Denny, and S. L. Cobb, "Investigating the Anti-leishmanial Effects of Linear Peptoids," *ChemMedChem*, vol. 10, pp. 233–237, feb 2015.

[55] I. Kevric, M. A. Cappel, and J. H. Keeling, "New World and Old World Leishmania Infections: A Practical Review," *Dermatologic Clinics*, vol. 33, pp. 579–593, jul 2015.

[56] N. D. Das Antu, Manash C. Das and S. Bhattacharjee, "Evaluation of the antileishmanial potency, toxicity and phytochemical constituents of methanol bark extract of Sterculia villosa," *Pharmaceutical Biology*, vol. 55, no. 1, pp. 998–1009, 2017.

[57] L. Monzote, "Current Treatment of Leishmaniasis : A Review," *The Open Antimicrobial Agents Journal*, vol. 1, no. January 2009, pp. 9–19, 2016.

[58] J. Chakravarty and S. Sundar, "Drug resistance in leishmaniasis.," *Journal of global infectious diseases*, vol. 2, pp. 167–76, may 2010.

[59] WHO Leishmaniases and Geneva, "WHO Technical Report Series CONTROL OF THE LEISHMANIASES," *II.World Health Organization. III.Series. ISBN*, vol. 978, pp. 22–26, 2010.

[60] R. R. P. da Silva, B. J. M. da Silva, A. P. D. Rodrigues, L. H. S. Farias, M. N. da Silva, D. T. V. Alves, G. N. T. Bastos, J. L. M. do Nascimento, and E. O. Silva, "In vitro biological action of aqueous extract from roots of Physalis angulata against Leishmania (Leishmania) amazonensis," *BMC Complementary and Alternative Medicine*, vol. 15, p. 249, dec 2015.

[61] B. Muller Cardoso, T. França Perles de Mello, S. Negrão Lopes, I. Galhardo Demarchi, D. Stefani Lopes Lera, R. Bocchi Pedroso, D. Aparício Cortez, Z. Cristiani Gazim, S. Mara Alessi Aristides, T. Gomes Verzignassi Silveira, and M. Valdrinez Campana Lonardoni, "Antileishmanial activity of the essential oil from Tetradenia riparia obtained in different seasons," *Mem Inst Oswaldo Cruz, Rio de Janeiro*, vol. 110, no. 8, pp. 1024–1034, 2015.

[62] L. C. Santana, S. M. P. Carneiro, L. B. Caland-Neto, D. D. Arcanjo, J. M. Moita-Neto, A. M. Citó, and F. A. A. Carvalho, "Brazilian brown propolis elicits antileishmanial effect against promastigote and amastigote forms of Leishmania amazonensis," *Natural Product Research*, vol. 28, no. 5, pp. 340–343, 2014.

[63] M. Aparecida Andrade, C. dos Santos Azevedo, F. Nader Motta, M. Lucília dos Santos, C. Lasse Silva, J. Martins de Santana, and I. M. D Bastos, "Essential oils: in vitro activity against Leishmania amazonensis, cytotoxicity and chemical composition," *BMC Complementary and Alternative Medicine*, vol. 16, no. 444, 2016.

[64] T. M. Abdallah, K. a. Elmardi, A. H. Elhassan, M. B. Omer, M. S. Elhag, M. a. Desogi, M. F. Siddig, and I. Adam, "Comparison of artesunate and quinine in the treatment of severe Plasmodium falciparum malaria at Kassala hospital,

Sudan.," *Journal of infection in developing countries*, vol. 8, pp. 611–5, may 2014.

[65] Á. I. Calderón, L. I. Romero, E. Ortega-Barría, P. N. Solís, S. Zacchino, A. Gimenez, R. Pinzón, A. Cáceres, G. Tamayo, C. Guerra, A. Espinosa, M. Correa, and M. P. Gupta, "Screening of Latin American plants for antiparasitic activities against malaria, Chagas disease, and leishmaniasis," *Pharmaceutical Biology*, vol. 48, pp. 545–553, may 2010.

[66] M. Olivier, D. J. Gregory, and G. Forget, "Subversion Mechanisms by Which Leishmania Parasites Can Escape the Host Immune Response: a Signaling Point of View," *Clinical Microbiology Reviews*, vol. 18, no. 2, pp. 293–305, 2005.

[67] A. A. Zahir, I. S. Chauhan, A. Bagavan, C. Kamaraj, G. Elango, J. Shankar, N. Arjaria, S. M. Roopan, A. A. Rahuman, and N. Singh, "Green Synthesis of Silver and Titanium Dioxide Nanoparticles Using Euphorbia prostrata Extract Shows Shift from Apoptosis to G0/G1 Arrest followed by Necrotic Cell Death in Leishmania donovani.," *Antimicrobial agents and chemotherapy*, vol. 59, pp. 4782–99, aug 2015.

[68] M. Abreumiranda, R. F. J. Tiossi, M. R. Dasilva, K. C. Rodrigues, C. C. Kuehn, L. G. Rodriguesoliveira, S. Albuquerque, J. D. McChesney, C. M. Lezama-Davila, A. P. Isaac-Marquez, and J. Kenuppbastos, "In vitro leishmanicidal and cytotoxic activities of the glycoalkaloids from solanum lycocarpum (solanaceae) fruits," *Chemistry and Biodiversity*, vol. 10, no. 4, pp. 642–648, 2013.

[69] M. C. Duarte, "Antileishmanial activity and mechanism of action from a purified fraction of Zingiber officinalis Roscoe against Leishmania amazonensis," *Experimental Parasitology*, vol. 166, pp. 21–28, jul 2016.

[70] J. M. da Silva, L. M. R. Antinarelli, N. d. C. C. Pinto, E. S. Coimbra, E. M. de Souza-Fagundes, A. Ribeiro, and E. Scio, "HPLC-DAD analysis, antileishmanial, antiproliferative, and antibacterial activities of Lacistema pubescens:

an Amazonian medicinal plant.," *BioMed research international*, vol. 14, aug 2014.

[71] H. L. Bolt, G. A. Eggimann, P. W. Denny, and S. L. Cobb, "Enlarging the chemical space of anti-leishmanials: a structure - activity relationship study of peptoids against Leishmania mexicana, a causative agent of cutaneous leishmaniasis," *MedChemComm*, vol. 7, pp. 799–805, may 2016.

[72] R. G. Taylor, D. C. Walker+, and R. R. Mclnnes, "E.coli host strains significantly affect the quality of small scale plasmid DNA preparations used for sequencing," Tech. Rep. 7, 1993.

[73] P. Daegelen, F. W. Studier, R. E. Lenski, S. Cure, and J. F. Kim, "Tracing Ancestors and Relatives of Escherichia coli B, and the Derivation of B Strains REL606 and BL21(DE3)," *Journal of Molecular Biology*, vol. 394, pp. 634–643, dec 2009.

[74] D. Truan, A. Vasil, M. Stonehouse, M. L. Vasil, and E. Pohl, "High-level over-expression, purification, and crystallization of a novel phospholipase C/sphingomyelinase from Pseudomonas aeruginosa," *Protein expression and purification*, vol. 90, pp. 40–46, 2013.

[75] W. C. Deloache, Z. N. Russ, and J. E. Dueber, "Towards repurposing the yeast peroxisome for compartmentalizing heterologous metabolic pathways," *Nature Communications*, vol. 7, p. 11152, dec 2016.

[76] D. S. Roos, R. G. Donald, N. S. Morrissette, and A. L. Moulton, "Molecular tools for genetic dissection of the protozoan parasite Toxoplasma gondii.," *Methods in cell biology*, vol. 45, pp. 27–63, 1994.

[77] A. Herm-Götz, C. Agop-Nersesian, S. Münter, J. S. Grimley, T. J. Wandless, F. Frischknecht, and M. Meissner, "Rapid control of protein level in the apicomplexan Toxoplasma gondii," *Nature Methods*, vol. 4, pp. 1003–1005, 2007.

[78] M. Soête, D. Camus, and J. F. Dubremetz, "Experimental induction of bradyzoite-specific antigen expression and cyst formation by the RH strain

of Toxoplasma gondii in vitro.," *Experimental parasitology*, vol. 78, pp. 361–70, jun 1994.

[79] M. J. Wichroski, J. A. Melton, C. G. Donahue, R. K. Tweten, and G. E. Ward, "Clostridium septicum Alpha-Toxin Is Active against the Parasitic Protozoan Toxoplasma gondii and Targets Members of the SAG Family of Glycosylphosphatidylinositol-Anchored Surface Proteins," *Infection and immunity*, vol. 70, no. 8, pp. 4353–4361, 2002.

[80] A. J. A. Mbekeani, W. W. A. Stanley, V. V. V. C. Kalel, N. Dahan, E. Zalckvar, L. Sheiner, W. Schliebs, R. Erdmann, E. Pohl, P. W. P. P. Denny, A. J. A. Mbekeani, W. W. A. Stanley, V. V. V. C. Kalel, N. Dahan, E. Zalckvar, L. Sheiner, W. Schliebs, R. Erdmann, E. Pohl, and P. W. P. P. Denny, "Functional Analyses of a Putative, Membrane-Bound, Peroxisomal Protein Import Mechanism from the Apicomplexan Protozoan Toxoplasma gondii," *Genes*, vol. 9, p. 434, aug 2018.

[81] J. Schindelin, I. Arganda-Carreras, E. Frise, V. Kaynig, M. Longair, T. Pietzsch, S. Preibisch, C. Rueden, S. Saalfeld, B. Schmid, J.-Y. Tinevez, D. J. White, V. Hartenstein, K. Eliceiri, P. Tomancak, and A. Cardona, "Fiji: an open-source platform for biological-image analysis," *Nature Methods*, vol. 9, pp. 676–682, jul 2012.

[82] A. Q. I. Alqaisi, A. J. Mbekeani, M. B. Llorens, A. P. Elhammer, and P. W. Denny, "The antifungal Aureobasidin A and an analogue are active against the protozoan parasite Toxoplasma gondii but do not inhibit sphingolipid biosynthesis," *Parasitology*, vol. 145, no. 2, pp. 148–155, 2018.

[83] A. Schäfer, D. Kerssen, M. Veenhuis, W.-H. Kunau, and W. Schliebs, "Functional Similarity between the Peroxisomal PTS2 Receptor Binding Protein Pex18p and the N-Terminal Half of the PTS1 Receptor Pex5p," *Molecular and cellular biology*, vol. 24, no. 20, pp. 8895–8906, 2004.

[84] B. Schwartzkopff, H. W. Platta, S. Hasan, W. Girzalsky, and R. Erdmann, "Cite this article as," *Bioscience Reports*, vol. 35, 2015.

[85] P. A. Bates, "Complete developmental cycle of Leishmania mexicana in axenic culture.," *Parasitology*, vol. 108 (Pt 1, pp. 1–9, jan 1994.

[86] M. De Rycker, I. Hallyburton, J. Thomas, L. Campbell, S. Wyllie, D. Joshi, S. Cameron, I. H. Gilbert, P. G. Wyatt, J. A. Frearson, A. H. Fairlamb, and D. W. Gray, "Comparison of a High-Throughput High-Content Intracellular Leishmania donovani Assay with an Axenic Amastigote Assay," *Antimicrobial Agents and Chemotherapy*, vol. 57, no. 7, pp. 2913–2922, 2013.

[87] J. L. Norcliffe, J. G. Mina, E. Alvarez, J. Cantizani, F. de Dios-Anton, G. Colmenarejo, S. G.-D. Valle, M. Marco, J. M. Fiandor, J. J. Martin, P. G. Steel, and P. W. Denny, "Identifying inhibitors of the Leishmania inositol phosphorylceramide synthase with antiprotozoal activity using a yeast-based assay and ultra-high throughput screening platform," *Scientific Reports*, vol. 8, p. 3938, dec 2018.

[88] E. G. E. Armitage, A. A. Q. I. Alqaisi, J. Godzien, I. Peña, A. J. A. Mbekeani, V. Alonso-Herranz, Á. López-Gonzálvez, J. Martín, R. Gabarro, P. P. W. Denny, M. P. M. Barrett, and C. Barbas, "Complex Interplay between Sphingolipid and Sterol Metabolism Revealed by Perturbations to the Leishmania Metabolome Caused by Miltefosine," *Antimicrobial agents and chemotherapy*, vol. 62, no. 5, pp. 1–12, 2018.

[89] R. A. Scheltema, A. Jankevics, R. C. Jansen, M. A. Swertz, and R. Breitling, "PeakML/mzMatch: A File Format, Java Library, R Library, and Tool-Chain for Mass Spectrometry Data Analysis," *Analytical Chemistry*, vol. 83, pp. 2786–2793, apr 2011.

[90] D. J. Creek, A. Jankevics, K. E. V. Burgess, R. Breitling, and M. P. Barrett, "IDEOM: an Excel interface for analysis of LC - MS-based metabolomics data," *Bioinformatics*, vol. 28, pp. 1048–1049, apr 2012.

[91] L. W. Sumner, A. Amberg, D. Barrett, M. H. Beale, R. Beger, C. A. Daykin, T. W.-M. Fan, O. Fiehn, R. Goodacre, J. L. Griffin, T. Hankemeier, N. Hardy, J. Harnly, R. Higashi, J. Kopka, A. N. Lane, J. C. Lindon, P. Marriott, A. W.

Nicholls, M. D. Reily, J. J. Thaden, and M. R. Viant, "Proposed minimum reporting standards for chemical analysis," *Metabolomics*, vol. 3, pp. 211–221, sep 2007.

[92] S.-K. Kim, A. E. Fouts, and J. C. Boothroyd, "Toxoplasma gondii dysregulates IFN-gamma-inducible gene expression in human fibroblasts: insights from a genome-wide transcriptional profiling.," *Journal of immunology (Baltimore, Md. : 1950)*, vol. 178, pp. 5154–65, apr 2007.

[93] L. S. Moraes, M. R. Donza, A. P. D. Rodrigues, B. J. Silva, D. S. Brasil, M. D. G. B. Zoghbi, E. H. Andrade, G. M. Guilhon, E. O. Silva, and T. J. Schmidt, "Leishmanicidal activity of (+)-Phyllanthidine and the phytochemical profile of margaritaria nobilis (Phyllanthaceae)," *Molecules*, vol. 20, no. 12, pp. 22157–22169, 2015.

[94] C. B. Moraes, G. Witt, M. Kuzikov, B. Ellinger, T. Calogeropoulou, K. C. Prousis, S. Mangani, F. Di Pisa, G. Landi, L. D. Iacono, C. Pozzi, L. H. Freitas-Junior, B. dos Santos Pascoalino, C. P. Bertolacini, B. Behrens, O. Keminer, J. Leu, M. Wolf, J. Reinshagen, A. Cordeiro-da Silva, N. Santarem, A. Venturelli, S. Wrigley, D. Karunakaran, B. Kebede, I. Pöhner, W. Müller, J. Panecka-Hofman, R. C. Wade, M. Fenske, J. Clos, J. M. Alunda, M. J. Corral, E. Uliassi, M. L. Bolognesi, P. Linciano, A. Quotadamo, S. Ferrari, M. Santucci, C. Borsari, M. P. Costi, and S. Gul, "Accelerating Drug Discovery Efforts for Trypanosomatidic Infections Using an Integrated Transnational Academic Drug Discovery Platform," *SLAS DISCOVERY: Advancing Life Sciences R&D*, vol. 24, pp. 346–361, mar 2019.

[95] F. L. Chadbourne, C. Raleigh, H. Z. Ali, P. W. Denny, and S. L. Cobb, "Studies on the antileishmanial properties of the antimicrobial peptides temporin A, B and 1Sa," *Journal of Peptide Science*, vol. 17, pp. 751–755, nov 2011.

[96] A. Inchausti', G. Yaluff', A. Rojas De Arias', S. Torres', M. E. Ferreira', H. Nakayama', A. Schinini', K. Lorenzen', T. Anke', and A. Fournet3, "Leish-

manicidal and Trypanocidal Activity of Extracts and Secondary Metabolites from-" * Basidiomycetes," tech. rep., 1997.

[97] A. Gehrt, G. Erkel, T. Anke, and O. Sterner, "Nitidon, a new bioactive metabolite from the basidiomycete Junghuhnia nitida (Pers.: Fr.) Ryv.," *Zeitschrift fur Naturforschung. C, Journal of biosciences*, vol. 53, no. 1-2, pp. 89–92, 1998.

[98] K. J. Alzahrani, J. A. Ali, A. A. Eze, W. L. Looi, D. N. Tagoe, D. J. Creek, M. P. Barrett, and H. P. de Koning, "Functional and genetic evidence that nucleoside transport is highly conserved in Leishmania species: Implications for pyrimidine-based chemotherapy," *International Journal for Parasitology: Drugs and Drug Resistance*, vol. 7, pp. 206–226, aug 2017.

[99] D. Ramu, S. Garg, R. Ayana, A. Keerthana, V. Sharma, C. Saini, S. Sen, S. Pati, and S. Singh, "Novel β-carboline-quinazolinone hybrids disrupt Leishmania donovani redox homeostasis and show promising antileishmanial activity," *Biochemical Pharmacology*, vol. 129, pp. 26–42, apr 2017.

[100] P. W. Denny, H. Shams-Eldin, H. P. Price, D. F. Smith, and R. T. Schwarz, "The Protozoan Inositol Phosphorylceramide Synthase a novel drug target that defines a new class of sphingolipid synthase," *Journal of Biological Chemistry*, vol. 281, no. 38, pp. 28200 – 28209, 2006.

[101] M.-J. Gubbels, C. Li, and B. Striepen, "High-throughput growth assay for Toxoplasma gondii using yellow fluorescent protein.," *Antimicrobial agents and chemotherapy*, vol. 47, pp. 309–16, jan 2003.

[102] M. Dawidowski, L. Emmanouilidis, V. C. Kalel, K. Tripsianes, K. Schorpp, K. Hadian, M. Kaiser, P. Mäser, M. Kolonko, S. Tanghe, A. Rodriguez, W. Schliebs, R. Erdmann, M. Sattler, and G. M. Popowicz, "Inhibitors of PEX14 disrupt protein import into glycosomes and kill Trypanosoma parasites.," *Science (New York, N.Y.)*, vol. 355, pp. 1416–1420, mar 2017.

[103] H. M. Fritz, K. R. Buchholz, X. Chen, B. Durbin-Johnson, D. M. Rocke, P. A. Conrad, and J. C. Boothroyd, "Transcriptomic analysis of toxoplasma development reveals many novel functions and structures specific to sporozoites and oocysts.," *PloS one*, vol. 7, no. 2, p. e29998, 2012.

[104] N. Galland and P. A. M. Michels, "Comparison of the peroxisomal matrix protein import system of different organisms. Exploration of possibilities for developing inhibitors of the import system of trypanosomatids for anti-parasite chemotherapy," *European Journal of Cell Biology*, vol. 89, no. 9, pp. 621–637, 2010.

[105] A. Gurvitz, L. Wabnegger, S. Langer, B. Hamilton, H. Ruis, and A. Hartig, "The tetratricopeptide repeat domains of human, tobacco, and nematode PEX5 proteins are functionally interchangeable with the analogous native domain for peroxisomal import of PTS1-terminated proteins in yeast," *Molecular genetics and genomics : MGG*, vol. 265, pp. 276–286, apr 2001.

[106] R. K. Szilard and R. A. Rachubinski, "Tetratricopeptide repeat domain of Yarrowia lipolytica Pex5p is essential for recognition of the type 1 peroxisomal targeting signal but does not confer full biological activity on Pex5p," *Biochem. J*, vol. 346, no. 1, pp. 177–184, 2000.

[107] A. T. J. A. T. J. Klein, M. Van Den Berg, G. Bottger, H. F. Tabak, and B. Distel, "Saccharomyces cerevisiae acyl-CoA oxidase follows a novel, non-PTS1, import pathway into peroxisomes that is dependent on Pex5p.," *The Journal of biological chemistry*, vol. 277, pp. 25011–9, jul 2002.

[108] T. P. J. Dunkley, R. Watson, J. L. Griffin, P. Dupree, and K. S. Lilley, "Localization of Organelle Proteins by Isotope Tagging (LOPIT)," *Molecular & Cellular Proteomics*, vol. 3, pp. 1128–1134, nov 2004.

[109] T. Gabaldón, M. L. Ginger, and P. A. Michels, "Peroxisomes in parasitic protists," *Molecular and Biochemical Parasitology*, vol. 209, no. 1-2, pp. 35–45, 2016.

[110] A.-K. Ludewig-Klingner, V. Michael, M. Jarek, H. Brinkmann, and J. Petersen, "Distribution and Evolution of Peroxisomes in Alveolates (Apicomplexa, Dinoflagellates, Ciliates)," *Genome Biology and Evolution*, vol. 10, pp. 1–13, jan 2018.

[111] D. Moog, J. M. Przyborski, and U. G. Maier, "Genomic and Proteomic Evidence for the Presence of a Peroxisome in the Apicomplexan Parasite Toxoplasma gondii and Other Coccidia," *Genome Biology and Evolution*, vol. 9, no. 11, pp. 3108–3121, 2017.

[112] M. Stadler and H. Anke, "New nematicidal and antimicrobial compounds from the basidiomycete Cheimonophyllum candidissimum (Berk & Curt.) sing. I. Producing organism, fermentation, isolation, and biological activities.," *The Journal of antibiotics*, vol. 47, pp. 1284–9, nov 1994.

[113] S. Wyllie, S. Patterson, L. Stojanovski, F. R. C. Simeons, S. Norval, R. Kime, K. D. Read, and A. H. Fairlamb, "The Anti-Trypanosome Drug Fexinidazole Shows Potential for Treating Visceral Leishmaniasis," *ScienceTranslationalMedicine*, vol. 4, no. 119, 2012.

[114] S. Wyllie, M. L. Cunningham, and A. H. Fairlamb, "Dual Action of Antimonial Drugs on Thiol Redox Metabolism in the Human Pathogen Leishmania donovani," *Journal of Biological Chemistry*, vol. 279, pp. 39925–39932, sep 2004.

[115] P. Sampathkumar, C. Roach, P. A. Michels, and W. G. Hol, "Structural Insights into the Recognition of Peroxisomal Targeting Signal 1 by Trypanosoma brucei Peroxin 5," *Journal of Molecular Biology*, vol. 381, pp. 867–880, sep 2008.

[116] S. M. Sidik, D. Huet, and S. Lourido, "CRISPR-Cas9-based genome-wide screening of Toxoplasma gondii," *Nature Protocols*, vol. 13, pp. 307–323, jan 2018.

Appendix A

Basic and Auxiliary Results

A.0.1 Restriction site mapping of *TgSCP2*TUB8mycGFPmyoATy-HX colon

Insertion of *Tg*SCP2 were confirmed by two methods; restriction site mapping using *BamHI* for *TgSCP2*TUB8mycGFPmyoATy-HX as shown in Figure A.1 Lane 1 = 10 000 bp ladder, Lane 2 = as expected band (A) cut by *EcoRI* gave a band at 8494 bp, Lane 3 = As expected band (B) and (C) cut by *BamHI* gave bands at 7761 bp and 733 bp respectively. This confirmed successful cloning of *Tg*SCP2 into plasmid (TUB8mycGFPmyoATy-HX)

A.1 Restriction site mapping of *Tg*Pex5-pIRES2-EGFP-SKL and *Tg*Pex7-pIRES2-EGFP-SKL colons

Insertion of *Tg*Pex5 and *Tg*Pex7 were confirmed by two methods; restriction site mapping using *BamHI* for *Tg*Pex5-pIRES2-EGFP-SKL and *BstBI* *Tg*Pex7-pIRES2-EGFP-SKL shown in Figure A.2 . In gel image (A) Lane 1 = 10 000 bp ladder. Lane 2 is *Tg*Pex5-pIRES2-EGFP-SKL digestion with *BamHI* gave as expected 2 bands one at 5431 bp and the other at 2568 bp. In gel image (B) Lane 1 = 10 000 bp ladder. Lane 2 is *Tg*Pex7-pIRES2-EGFP-SKL digestion with *BstBI* gave 3 expected bands at 4378 bp, 1921 bp and 362 bp. This mapping confirmed successful cloning of *Tg*Pex5 and *Tg*Pex7 into plasmid (pIRES2-EGFP-SKL)

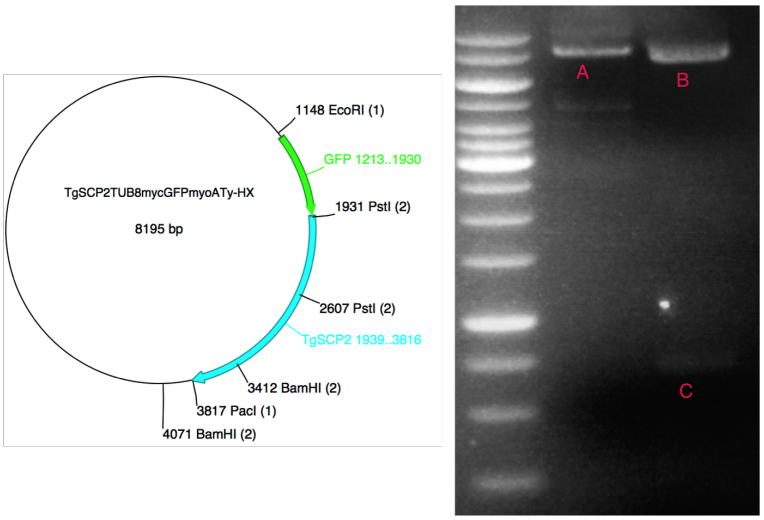

Figure A.1: Restriction Site Mapping *Tg*SCP2 in Plasmid; Lane 1 = 10 000 bp ladder, Lane 2 = (A) cut by *EcoRI* gave a band at 8494 bp, Lane 3 = band (B) and (C) cut by *BamHI* gave bands at 7761 bp and 733 bp respectively.

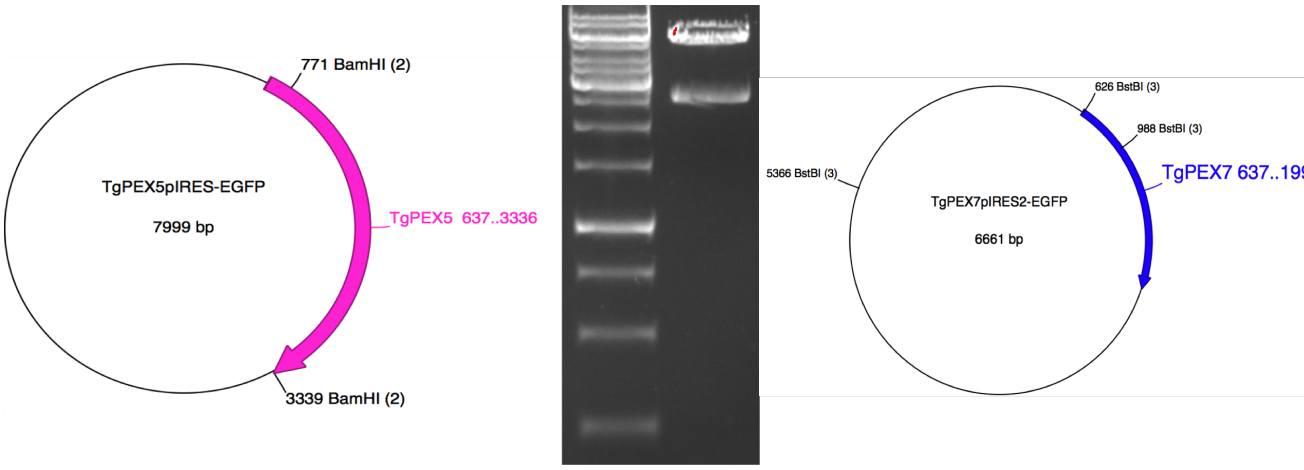

Figure A.2: Restriction Site Mapping *Tg*Pex5 and *Tg*Pex7 in Yeast Plasmid; (A) Lane 1 = 10 000 bp ladder. Lane 2 is *Tg*Pex5-pIRES2-EGFP-SKL digestion with *BamHI* gave 2 bands at 5431 bp and 2568 bp. (B) Lane 1 = 10 000 bp ladder. Lane 2 is *Tg*Pex7-pIRES2-EGFP-SKL *BstBI* digestion gave bands at 4378 bp, 1921 bp and 362 bp.

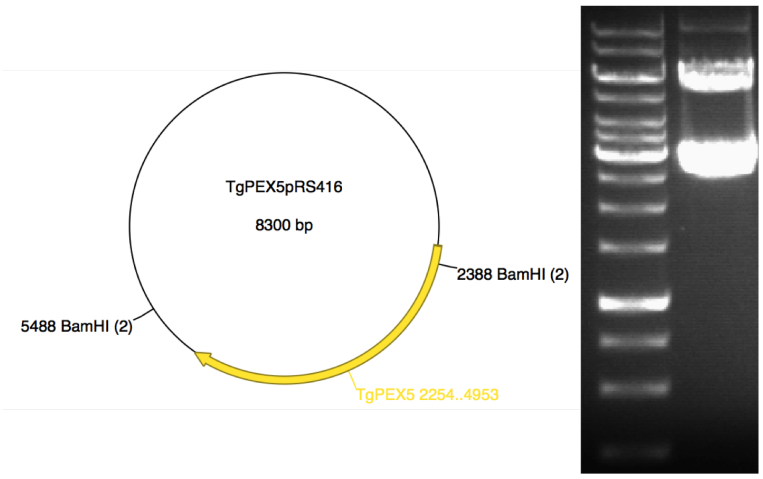

Figure A.3: Restriction Site Mapping *Tg*Pex5 and *Tg*Pex7 in Human Plasmid; (A) Lane 1 = 10 000 bp ladder. Lane 2 is *Tg*Pex5-pIRES2-EGFP-SKL digestion with *BamHI* gave 2 bands at 5431 bp and 2568 bp. (B) Lane 1 = 10 000 bp ladder. Lane 2 is *Tg*Pex7-pIRES2-EGFP-SKL *BstBI* digestion gave bands at 4378 bp, 1921 bp and 362 bp.

A.1.1 Restriction site mapping of *Tg*Pex5-pRS416-WT and *Tg*Pex7-pRS416-WT colons

Insertion of amplicons *Tg*Pex5 and *Tg*Pex7 were confirmed by two methods; restriction site mapping using *BamHI* for *Tg*Pex5-pRS416-WT and *SacII* for *Tg*Pex7-pRS416-WT as shown in Figure A.3. In gel(A) Lane 1 = 10 000 bp ladder. Lane 2 with *Tg*Pex5-pRS416-WT plasmid after digestion with *BamHI* gave 2 expected bands one at 5200 bp and the other at 3100 bp. In gel (B) Lane 1 = 10 000 bp ladder. Lane 2 is *Tg*Pex7-pRS416-WT digestion with *SacII* gave 3 expected bands at 5589 bp, 874 bp and 499 bp. This confirmed successful cloning into the human pRS416-WT plasmid vector.

A.2 Macro data sheet

In Vitro Growth Inhibition Assay **Compound Name**

Organism

Compound: **Rep:** 1 **Start** **Finish**

Op:AJMbekeani **Date**

Run File:

	AMP	TEST Compound				CONTROL	TEST Compound				CONTROL
uM	**50 uM**	**100.00**	**33.33**	**11.11**	**3.71**		**1.24**	**0.41**	**0.14**	**0.05**	**neg**
Av:	#DIV/0!	#DIV/0!	#DIV/0!	#DIV/0!	#DIV/0!	#DIV/0!	#DIV/0!	#DIV/0!	#DIV/0!	#DIV/0!	#DIV/0!
										Ctrl:	#DIV/0!
%:	**#DIV/0!**	**#DIV/0!**	**#DIV/0!**	**#DIV/0!**	**#DIV/0!**	**0.000**	**#DIV/0!**	**#DIV/0!**	**#DIV/0!**	**#DIV/0!**	**#DIV/0!**
Sub. Neg. Control:	#DIV/0!	#DIV/0!	#DIV/0!	#DIV/0!	#DIV/0!		#DIV/0!	#DIV/0!	#DIV/0!	#DIV/0!	#DIV/0!
Div. Control	#DIV/0!	#DIV/0!	#DIV/0!	#DIV/0!	#DIV/0!		#DIV/0!	#DIV/0!	#DIV/0!	#DIV/0!	#DIV/0!

Concentration	Log10	Growth
100	2.00	
33.000	1.52	
11.000	1.04	
3.710	0.57	
1.240	0.09	
0.410	-0.39	
0.140	-0.85	
0.050	-1.30	

Figure A.4: Macro data sheet used for IC50 calculations in Chapter 3 and Chapter 4